


# 國立交通大學

電子工程學系 電子研究所碩士班

碩 士 論 文

旋塗式有機主動層薄膜電晶體的製程改  
善與可靠度分析



**The Analysis of Process Improvement  
and Reliability Characteristic  
of Spin-On Organic TFT**

研 究 生：林榮祥

指導教授：葉清發 教授

羅正忠 教授

中 華 民 國 九 十 三 年 六 月

# 旋塗式有機主動層薄膜電晶體的製程改善與可靠度分析

研究生:林榮祥

指導教授: 葉清發、羅正忠 博士

國立交通大學 電子工程學系 電子研究所碩士班

## 摘要

近年來，有機顯示器成為市場上的前瞻技術，利用有機發光二極體和有機薄膜電晶體已經可以製作出低成本、可彎曲、全彩的平面顯示器。本論文以“bottom contact”的結構，SiO<sub>2</sub> 為絕緣層，利用旋塗的方式成長有機薄膜，成功地製作出以 poly(3-hexylthiophene)、簡稱 P3HT 為有機材料的有機薄膜電晶體。

在第二章當中，我們利用二甲苯和氯仿這兩種不同的溶劑來溶解 P3HT，可發現當 P3HT 的重量百分濃度高於 0.3%時，就無法完全溶解於二甲苯中，並留下許多微小顆粒，而氯仿則能夠溶解高濃度的 P3HT (> 2 wt%)，顯示氯仿對於 P3HT 而言是一種極佳的溶劑。此外，我們發現以氯仿為溶劑所製作出來的有機薄膜電晶體能夠有效地抑制異常的閘極漏電流，當 P3HT 的重量百分濃度超過 0.8%時，會有明顯的 bulk 漏電流現象產生，以 0.3%之 P3HT 製成的薄膜電晶體則可以獲得最低的表面粗糙度以及較佳的元件特性。

在第三章當中，有機薄膜電晶體分別經由不同時間的真空處理、氧氣處理、氮氣處理、泡水處理或閘極偏壓 stress；由於氧氣是 P3HT 的摻雜物之一，經由氧氣處理之有機薄膜電晶體的臨限電壓值與漏電流會隨著氧氣處理時間而大幅增加，氮氣和真空處理都可以降低 P3HT 薄膜內的氧含量，故可有效改善元件特性；至於泡水處理則對於有機薄膜電晶體的特性不會產生明顯的影響。在閘極施加正的偏壓 stress 會使 P3HT 內部的耦極重新排列，並造成臨限電壓的正偏移，閘極負偏壓 stress 則會使臨限電壓往負方向偏

移。

在第四章當中，我們利用鉑、金、鎳和鈦來當作有機薄膜電晶體之源極和汲極的電極材料，由於鉑跟金的功函數大於 P3HT，兩者都能夠和 P3HT 形成較佳的歐姆接觸，以鎳為源極/汲極電極材料的電晶體，則在低汲極電壓下產生 crowding effect。我們亦改變附著層金屬和接觸層金屬的厚度比例來觀察其對電性的影響，但是實驗發現接觸電阻受其影響的程度非常小。



# **The Analysis of Process Improvement and Reliability Characteristic of Spin-On Organic TFT**

Student: Jung-hsiang Lin

Advisor: **Dr. Jen-Chung. Lou**

**Dr. Ching-Fa Yeh**

Department of Electronics Engineering &

Institute of Electronics

National Chiao Tung University

## **Abstract**

Recently, active matrix organic diode displays (AMOLEDs) become the most advanced technology in the market; organic light-emitting diodes (OLEDs) and organic thin film transistors (OTFTs) enable the fabrication of low-coat, flexible, full color flat panel displays. In this paper, organic thin film transistors based on poly (3-hexylthiophene) (P3HT) with the “bottom contact” structure, SiO<sub>2</sub> as insulating layer, organic active layer grown with spin-coating have successfully been demonstrated.

In chapter 2, we used two kinds of solvents, xylene and chloroform, to dissolve P3HT. While weight percentage is as high as 0.3%, the P3HT cannot completely be dissolved in xylene and then many clusters of undissolved P3HT powder is observed. However, chloroform can dissolve high weight percentage of P3HT (> 2 wt%). Therefore, it is proved that chloroform is a good solvent for P3HT. Furthermore, we observed that the anomalous gate leakage current was suppressed by fabricating OTFTs with chloroform solution. As the weight percentage of P3HT is above 0.8%, it would cause obvious bulk leakage current. In summary, the P3HT OTFTs fabricated by 0.3% chloroform solution can acquire the lowest surface roughness and the better performance of devices than others.

In chapter 3, the OTFTs are treated with vacuum treatment, O<sub>2</sub> treatment, N<sub>2</sub> treatment, immersed in water or gate bias stress for different time. Since oxygen is a kind of dopant for P3HT, threshold voltage and leakage current of the OTFTs drastically increase with O<sub>2</sub> treatment time. Vacuum and N<sub>2</sub> treatments can be used to recover some of the lost performance through vacuum-induced expulsion of absorbed oxygen. As regards the OTFTs being immersed in water, the performance of electrical characteristics would not be affected. When a positive bias was applied to the gate electrode, it would lead to the dipole moment arranging in the P3HT polymer and positive threshold voltage shift. Negative gate bias stress causes negative threshold voltage shift.

In chapter 4, we use Pt, Au, Ni or Ti as S/D contact materials of OTFTs. Because the work function of Pt and Au are larger than the work function of P3HT, they can form better ohmic contact with P3HT than others. Nevertheless, it was observed that the crowding effect was occurred at the small drain bias for Ni as S/D contact material of OTFTs. Secondly, we adjusted the thickness ratio of adhesion/contact metals, such as Ti/Pt and Ti/Au. From experiment results, it was observed that contact resistance is weakly dependent on the thickness ratio of adhesion/contact metals.

## 誌 謝

葉清發、羅正忠教授：

感謝葉清發老師在我碩士生涯的一開始給予我精神上的支持和鼓勵，讓我重新調整自己面對問題和解決問題的方法及態度，並且調整自己的求學態度。感謝羅正忠老師在實驗方面的規劃和指導，才能夠順利的將實驗完成。

我的家人：

感謝我的父親林崑山、我的母親林碧華和我的弟弟林榮泰，因為他們的栽培，我才能夠在求學的路程上順利的完成我的學業；因為他們的支持和鼓勵，我才能夠突破我人生中的每一項關卡。

實驗室學長：

感謝實驗室學長陳添富、蕭智文和王碩晟。尤其要感謝王碩晟學長，在我做實驗沮喪時，給我安慰；在我做實驗茫然時，指引我方向；在我做實驗灰心時，給予我信心。也感謝陳添富和蕭智文學長在各方面的關心和指導。

實驗室學弟：

感謝實驗室學弟鍾漢邠、蔣陳偉、陳昶維、施俊宏、洪啟哲和吳伯慶。尤其要感謝鍾漢邠，在我實驗最忙身體又不適的時候，給予最為即時的幫助。也感謝蔣陳偉和陳昶維接下實驗室管理方面的工作，表現的非常認真和努力。也要感謝施俊宏幫我解決電腦軟體上的一些問題。

實驗室同學：

感謝實驗室同學劉俊彥和薛國欽。在課業上的切磋及討論，能夠順利渡過每一堂課。

我的女友：

感謝我的女友賴錦怡，在這一年多來陪我走過碩二最辛苦、最忙碌的時期；也能體諒我做實驗的忙碌，不能常常陪伴她；也能包容我的許多小疏忽。

大學同學：

感謝我的大學同學莊嘉平、王聖元、宋英超、劉哲宏、余俊德、謝怡慧、蔡仁祥、宋英超、楊士昌和陳慶勳。由於彼此互相的關心和鼓勵，使在新竹讀書的每個人都能順利的取得了碩士學位。

曾信榮學長：

感謝曾信榮學長，在我覺得孤單和無助時，陪我聊天，讓我能夠重新振作起來。

教會的朋友：

感謝教會朋友政忠、世學、哲維、佳垣、皇興以及其他未提到的朋友。因為有你們的建議和幫忙，在面臨許多選擇的同時，在面對挫折及迷惘時，給予了相當的思考空間及改變。

最後我要將我的碩士論文獻給我最愛的人-我的母親，希望她能夠在世界的另外一方看到我的成長。



## Contents

Abstract (in Chinese).....	i
Abstract (in English).....	iii
Acknowledgement.....	v
Contents.....	vii
Figure Captions.....	x
Table Captions.....	xi

### Chapter 1 Introduction

1.1 General Background and Motivation.....	1
1.2 Charge Transport in Organic Semiconductor.....	2
1.3 Operation of Organic Thin Film Transistors.....	3
1.4 Thesis Organization.....	4

### Chapter 2 Property of P3HT and Spin-Coating technique

2.1 Introduction.....	11
2.2 The Molecular Structure of P3HT.....	12
2.3 Fabrication of Organic Thin Film Transistors	
2.3.1 Process Flow of P3HT OTFTs Fabrication.....	13
2.3.2 Modification of Oxide surface.....	14
2.3.3 The Layout of Bottom-Contact OTFT.....	15
2.4 Electrical Characteristics of P3HT OTFTs	
2.4.1 Measurement.....	15
2.4.2 Threshold Voltage and OFF Current Definition.....	15
2.4.3 The Extraction Method of Mobility.....	16
2.5 OTFTs Fabrication by Different Solvents	
2.5.1 Experimental Detail.....	17
2.5.2 Result and Discussion	
2.5.2.1 Physical properties of spin-on P3HT film.....	17
2.5.2.2 The anomalous gate leakage current effect from xylene solution.....	19
2.5.2.3 The correlation between mobility of P3HT OTFT and solvents.....	20



## **2.6 OTFTs Fabrication by Different Weight Percentages of P3HT**

2.6.1 Experimental Detail.....	19
2.6.2 Result and Discussion	
2.6.2.1 Physical properties of spin-on P3HT film.....	20
2.6.2.2 The bulk current effect from high weight percentage of P3HT.....	20
2.6.2.3 The correlation between the performances of P3HT OTFT and weight percentage of P3HT.....	21
2.7 Summary.....	22

## **Chapter 3 Reliability Characteristics of P3HT OTFTs**

3.1 Introduction.....	57
3.2 The Effect of P3HT Stored in Vacuum	
3.2.1 Experimental Detail.....	58
3.2.2 Result and Discussion.....	58
3.3 The Variation of Threshold Voltage and Mobility during Electrical Measurement	
3.2.1 Experimental Detail.....	59
3.2.2 Result and Discussion.....	59
3.4 The Effect of P3HT OTFT under O <sub>2</sub> , N <sub>2</sub> and H <sub>2</sub> O Treatment	
3.2.1 Experimental Detail.....	60
3.2.2 Result and Discussion.....	61
3.5 Stress Measurement of P3HT OTFTs	
3.2.1 Experimental Detail.....	62
3.2.2 Result and Discussion.....	63
3.6 Summary.....	64

## **Chapter 4 Contact Resistance of P3HT OTFTs**

<b>4.1 Introduction.....</b>	<b>80</b>
<b>4.2 Experimental Detail.....</b>	<b>81</b>
<b>4.3 Result and Discussion</b>	
<b>4.3.1 Channel Length Effect on P3HT OTFT Performance.....</b>	<b>81</b>
<b>4.3.2 Dependence between the Electrode Materials and P3HT OTFT Performance..</b>	<b>82</b>
<b>4.3.3 Composition of adhesion/contact materials effect on P3HT contact resistance...</b>	<b>83</b>
<b>4.4 Summary.....</b>	<b>84</b>

## **Chapter 5 Conclusions and Future Work**

### **5.1 Conclusions**

<b>5.1.1 OTFTs Fabricated by Different Solvents and Weight Percentages of P3HT...</b>	<b>100</b>
<b>5.1.2 Reliability Characteristics of P3HT OTFTs.....</b>	<b>100</b>
<b>5.1.3 Contact Resistance of P3HT OTFTs.....</b>	<b>101</b>
<b>5.2 Future Work.....</b>	<b>102</b>

<b>Reference.....</b>	<b>104</b>
-----------------------	------------

<b>Vita.....</b>	<b>107</b>
------------------	------------

## Figure Captions

### Chapter 1

**Figure1-1** Semilogarithmic plot of the highest field-effect mobility( $\mu$ ) reported for OTFTs fabricated from the most promising polymeric and oligomeric semiconductors versus year from 1986 to 2000.[1]

**Figure1-2** Schematic of operation of organic thin film transistor, showing a lightly p-doped semiconductor: + indicates a positive charge in semiconductor ; (-) indicates a negatively charge counterion (a) no-bias (b) accumulation mode (c) depletion mode (d) non-uniform charge density (e) channel pinch-off [3]

### Chapter 2

**Figure 2-1** Chemical diagram of the polymer poly (3-hexylthiophene).R represents the alkyl chain

**Figure2-2** Bottom-contact structure of P3HT OTFTs

**Figure2-3** Process flow of bottom-contact OTFTs

**Figure2-4** Two different orientations of ordered P3HT domains with respect to the FET substrate [9]

**Figure2-5** Layouts of bottom-contact OTFTs (a) linear type (b) finger type

**Figure2-6** Normalized drain-source current vs gate voltage

**Figure2-7** AFM micrograph of P3HT 0.3% in (a) xylene (b) chloroform

**Figure2-8** Source and gate leakage current versus gate bias

**Figure2-9** Influence of gate leakage current on output characteristics  $I_S$  vs  $V_D$ :(a) xylene 0.3% (b) chloroform 0.3%

- Figure2-10** On-Off ratio versus W/L
- Figure2-11** Transfer characteristics  $I_S$  vs  $V_G$  and field-effect mobility of samples prepared from different solvent (a) W/L=10000/10  $\mu\text{m}$  (b) W/L=5000/10  $\mu\text{m}$  (c) W/L=1000/10  $\mu\text{m}$  (d) W/L=1000/50  $\mu\text{m}$
- Figure2-12** AFM micrograph of P3HT 0.1% in chloroform (a) top-view (b) high angle view
- Figure2-13** AFM micrograph of P3HT 0.3% in chloroform (a) top-view (b) high angle view
- Figure2-14** AFM micrograph of P3HT 0.8% in chloroform (a) top-view (b) high angle view
- Figure2-15** AFM micrograph of P3HT 2.0% in chloroform (a) top-view (b) high angle view
- Figure2-16**  $I_S$  versus  $V_D$  curve at different gate voltages (a) in the accumulation mode (b) in the depletion mode (W/L=1000/25 $\mu\text{m}$ )
- Figure2-17**  $I_S$  versus  $V_D$  curve at different gate voltages (a) in the accumulation mode (b) in the depletion mode (W/L=1000/35 $\mu\text{m}$ )
- Figure2-18**  $I_S$  versus  $V_D$  curve in the depletion mode as a function of weight concentration of P3HT in chloroform (a) W/L=1000/25 $\mu\text{m}$  (b) W/L=1000/35 $\mu\text{m}$
- Figure2-19** Transfer characteristics  $I_S$  vs  $V_G$  as a function of weight concentration of P3HT in chloroform: (a) W/L=10000/10 $\mu\text{m}$  (b) W/L=1000/35 $\mu\text{m}$  (c) W/L=500/15 $\mu\text{m}$  (d) W/L=500/25 $\mu\text{m}$
- Figure2-20** Transfer characteristics  $I_S$  vs  $V_G$  as a function of weight concentration of P3HT in chloroform : (a) W/L=10000/10 $\mu\text{m}$  (b) W/L=1000/15 $\mu\text{m}$  (c) W/L=1000/35 $\mu\text{m}$  (d) W/L=500/15 $\mu\text{m}$  (e) W/L=500/25 $\mu\text{m}$
- Figure2-21** Threshold voltage as a function of weight concentration of P3HT in chloroform

- Figure2-22** Threshold voltage as a function of weight concentration of P3HT in chloroform: (a) inter-digital type (b) linear type
- Figure2-23** Field-effect mobility in the linear regime as a function of weight concentration of P3HT in chloroform: (a) inter-digital type (b) linear type
- Figure2-24** On-off ratio as a function of weight concentration of P3HT in chloroform: (a) inter-digital type (b) linear type
- Figure2-25** Field-effect mobility in the linear regime as a function of weight concentration of P3HT in chloroform
- Figure2-26** On-off ratio as a function of weight concentration of P3HT in chloroform

### Chapter 3

- Figure 3-1** Transfer characteristics  $I_S$  vs  $V_G$  and field-effect mobility of samples measured after 0 or 2 days in vacuum (a)  $W/L=5000/10\mu m$  (b)  $W/L=1000/35\mu m$  (c)  $W/L=500/35\mu m$
- Figure3-2** The variation of field-effect mobility and threshold voltage within 120min of measurement
- Figure3-3** (a) The threshold voltage shift and (b) the variation of field-effect mobility under different treatment.
- Figure3-4** Transfer characteristics  $I_S$  vs  $V_G$  of OTFT after 0sec, 10sec, 20sec, 50sec, 100sec, 200sec, 500sec, 1000sec, 2000sec and 5000sec
- Figure3-5** Transfer characteristics  $I_S$  vs  $V_G$  of OTFT after 0sec, 10sec, 20sec, 50sec, 100sec, 200sec, 500sec, 1000sec, 2000sec and 5000sec -25V gate bias stress
- Figure3-6** Transfer characteristics  $I_S$  vs  $V_G$  of OTFT after 0sec, 10sec, 20sec, 50sec, 100sec, 200sec, 500sec, 1000sec, 2000sec and 5000sec +25V gate bias stress

**Figure3-7** The variation of threshold voltage under No gate stress, +25V gate stress and -25V gate stress

**Figure3-8** Alternative gate bias stress (-25V/+25V) for 10sec, 20sec, 50sec, 100sec, 200sec, 500sec, 1000sec and 2000sec. The threshold voltage were measured at the end of each stress time.

**Figure3-9** The polarization effect in the P3HT polymer with negative gate bias.

**Figure3-10** The polarization effect in the P3HT polymer with positive gate bias.

## Chapter 4

**Figure4-1** The variation of threshold voltage and mobility in the linear regime as a function of the channel length (a) S/D metal is Ti/Au (b) S/D metal is Ti/Pt

**Figure4-2** Output characteristics  $I_S$  vs  $V_D$  for OTFTs with different channel lengths of 50, 25, 15  $\mu\text{m}$ .  $W/L=20$

**Figure4-3** Output characteristics  $I_S$  vs  $V_D$  of OTFT with (a) Ti (b) Ti/Ni (c) Ti/Au (d) Ti/Pt Source and Drain contact

**Figure4-4** Current-voltage characteristics of OTFT with (a) Ti/Au (b) Ti/Pt electrodes at small drain voltage

**Figure4-5** Transfer characteristics  $I_S$  vs  $V_G$  of OTFT in the linear regime with different S/D contact metal ( $W/L=1000/50\mu\text{m}$ )

**Figure4-6** Width-normalized ON resistance as a function of channel length at different gate voltage and at (a)  $V_{DS}=-1\text{V}$  (b)  $V_{DS}=-5\text{V}$ . The solid lines represent the linear least square fit of the data. (Ti/Au=1000/200Å)

**Figure4-7** Width-normalized ON resistance as a function of channel length at different gate voltage and at (a)  $V_{DS}=-1\text{V}$  (b)  $V_{DS}=-5\text{V}$ . The solid lines

represent the linear least square fit of the data. (Ti/Au=200/1000Å)

**Figure4-8** Width-normalized ON resistance as a function of channel length at different gate voltage and at (a)  $V_{DS}=-1V$  (b)  $V_{DS}=-5V$  .The solid lines represent the linear least square fit of the data. (Ti/Pt=200/1000Å)

**Figure4-9** Width-normalized ON resistance as a function of channel length at different gate voltage and at (a)  $V_{DS}=-1V$  (b)  $V_{DS}=-5V$  .The solid lines represent the linear least square fit of the data. (Ti/Pt=1000/200Å)

**Figure4-10** I-V characteristics of contacts between metal and semiconductor in integrated circuits (a) ideal ohmic contact (b) nonlinear ohmic contact

**Figure4-11** OTFT channel sheet conductance as a function of gate voltage (S/D contact metal is Ti/Au)

**Figure4-12** OTFT channel sheet conductance as a function of gate voltage (S/D contact metal is Ti/Pt)



## Table Captions

### Chapter 1

**Table1-1** Highest field-effect mobility( $\mu$ ) values measured from OTFTs as reported in the literature annually from 1986 through 2000.[1]

### Chapter 2

**Table2-1** The magnitude of off current with different channel length and different channel width.

**Table2-2** Field-effect mobility and ON/OFF ratios of samples prepared from different conditions Condition 1: cast, vacuum pumped for 24 h; condition 2: spin-coated; condition 3: treated with NH<sub>3</sub> for 10 h; condition 4: heated to 100 °C under N<sub>2</sub> for 5 min; condition 5: heated to 150 °C under N<sub>2</sub> for 35 min.

**Table2-3** Room mean square of P3HT film as a function of weight concentration of P3HT in chloroform.

### Chapter 3

**Table3-1** Field-effect mobility of samples measured after 0 or 2 days in vacuum with different W/L ratio.

**Table3-2** Threshold voltage of samples measured after 0 or 2 days in vacuum with different W/L ratio.

**Table3-3** ON-OFF ratio of samples measured after 0 or 2 days in vacuum with different W/L ratio.

### Chapter 4

**Table4-1** The contact resistance between source/drain electrodes and P3HT with different composition of adhesion/contact materials.



# Chapter 1

## Introduction

### 1.1 General Background and Motivation

For more than a decade now, organic thin film transistors (OTFTs) based on conjugated polymers, oligomers or other molecules have been envisioned as a viable alternative to more traditional, mainstream thin film transistors (TFTs) based on inorganic materials. **Figure1-1** presented a semilogarithmic plot of the highest yearly reported field-effect mobility value measured from thin-film transistor based on specific organic semiconductor, beginning 1986. An update of that plot is shown in Figure1-1, which is based on **table1-1**[1]. Because of the relatively low mobility of organic semiconductor layers, OTFTs cannot rival the performance of field-effect transistors based on single-crystalline inorganic semiconductors, such as Si and Ge, which have charge carrier mobility( $\mu$ ) about three orders of magnitude higher. However, the unique processing characteristics and demonstrated performance of OTFTs suggest that they can be competitive candidates for novel thin film transistor applications. Firstly, the techniques for depositing films of the semiconductor allow large area to be coated. Small oligomer can be vacuum-deposited at moderate temperatures in the region of 200°C. Perhaps more appealing, many of the polymers and oligomers are soluble and can be processed by spin coating or casting and possibly in the future could be printed. Thus, the transistor could be used in large-area electronic applications. A second advantage is that polymers are mechanically tough and thin film are flexible, presenting the possibility for non-planar flexible electronics. Such application include switching devices for active-matrix flat-panel displays(AMFPDs)based on either liquid crystal pixels(AMLCDs) or organic light-emitting diode(AMOLEDDs).

Among a lot of organic semiconductor materials, we use Poly (3-hexylthiophene ) P3HT as the semiconducting layer. Poly (3-hexylthiophene) P3HT has many potential advantages for use the semiconducting layer in field-effect transistors. (1) Poly (3-hexylthiophene) P3HT is a well-known polymer as an organic semiconductor and has shown the field-effect mobility from  $10^{-4} \text{ cm}^2/\text{Vs}$  in 1988 to  $0.2 \text{ cm}^2/\text{Vs}$  in 2003. (2) Poly (3-hexylthiophene) P3HT has high solvent selectiveness, can dissolve in toluene, xylene , chloroform and so on. (3) Poly (3-hexylthiophene) P3HT is solution processed, therefore can be processed by spin coating.

## 1.2 Charge Transport in Organic Semiconductor

Charge Transport in Organic Semiconductor is refer to [2] and described below. In inorganic semiconductor crystals like silicon or germanium, the strong coupling between the constituting atoms and the long-range order lead to the delocalization of the electronic states and the formation of allowed valence and conduction bands, separated by a forbidden energy gap. By thermal activation or photo-excitation, free electrons are generated in the conduction band, leaving behind positively charged holes in the valence band. The transport of these free charge carriers is described in the quantum-mechanical language of Bloch functions, k-space, and dispersion relations familiar to solid-state physicists. Structural or chemical defects in the crystal introduce states in the forbidden energy gap, spatially localized at the defect. A mobile carrier from the transport bands may get trapped at such a defect state, and no longer contribute to the conductivity until it is released again.

However, in organic solids, intramolecular interactions are mainly covalent, but intermolecular interactions are due to much weaker van der Waals and London forces. As a result, the transport bands in organic crystals are much narrower than those of their inorganic counterparts and the band structure is easily disrupted by introducing disorder in the system. Thus,

even in molecular crystals, the concept of allowed energy bands is of limited validity and excitations and interactions localized on individual molecules play a predominant role. The common electronic feature of many organic pigments is the p-conjugated system, which is formed by the overlap of carbon pz orbitals. Due to the orbital overlap, the p electrons are delocalized within a molecule and the energy gap between the highest occupied molecular orbital (HOMO) and the lowest unoccupied molecular orbital (LUMO) is relatively small, i.e. with transition frequencies within the visible range. The low coupling between the molecules in the solid state ensures that the carriers in these materials are strongly localized on a molecule. Transport occurs via a sequence of charge transfer steps from one molecule to another, similar to the hopping between defect states in inorganic semiconductors.

### 1.3 Operation of Organic Thin Film Transistor

The operation of OTFT is refer to [3] and described below. Organic Thin film transistors are primarily operated as accumulation-mode enhancement type transistor, which are opposed to the usual inversion mode operation of silicon MOSFETs. Ideally the source and drain contacts should behave as ohmic contacts for the majority carrier in the organic semiconductor.

In the further discussion of device operation the example of p-type semiconductor will be used. In **Fig. 1-2 (a)**, a schematic diagram is shown, in which zero bias was applied to all three contacts of an OTFT. If a small drain bias,  $V_D$ , is applied then the source-drain current,  $I_{DS}$ , will be small and ohmic.

If a negative bias,  $V_G$ , is applied to the gate electrode (**Fig. 1-2 (b)**), the voltage is dropped over the insulator and over the semiconductor near insulator/semiconductor interface, giving rise to band bending in the semiconductor, the accumulation region. The additional positive charge accumulated in this region is supplied by the ohmic source and drain contacts. The semiconductor

now contains positive charges both from doping and from the ‘field effect’ which created the accumulation layer. When a small bias is applied on the drain contact, a current larger than the ohmic current will be measured.

If a positive gate bias is applied, then the opposite band bending occurs in the semiconductor at the insulator interface, leading to depletion of charge (**Fig. 1-2(c)**). Inversion mode cannot be observed in the organic TFTs since the metal contacts are ohmic contacts for electron injection into the organic semiconductors.

As the drain bias becomes increasingly negative, the accumulation charge density will decrease from source to drain contact (**Fig. 1-2 (d)**). If the drain becomes more negative than the gate then a depletion zone will begin to appear and grow from the drain contact (**Fig. 1-2 (e)**).

#### 1.4 Thesis Organization

In chapter 1, we describe our background and motivation of this study.



In chapter 2, we used different solvents, xylene and chloroform, to dissolve P3HT, and then used spin-coating technique to form organic semiconductor layer. Afterwards, we investigated electrical characteristics of P3HT OTFTs. In addition to studying different solvents, we prepared different weight percentages of P3HT in chloroform, 0.1% , 0.3%, 0.8% and 2.0%. Afterwards, we investigated electrical characteristics of P3HT OTFTs.

In chapter 3, we treated OTFTs with O<sub>2</sub>, N<sub>2</sub> and H<sub>2</sub>O deliberately to clarify the correlation between electrical characteristics of P3HT OTFTs and the exposed ambient. Additionally, we investigate the behavior of P3HT OTFTs during stress measurements.

In chapter 4, we employ different electrode materials, such as Ti, Ni, Pt and Au, to check it can form ohmic contact between source/drain electrodes and the organic semiconductor or not. Next, we adjust adhesion/contact thickness ratio to check it can affect the contact resistance between source/drain electrodes and the organic semiconductor or not.

In chapter 5, we will describe the conclusions and the future work.



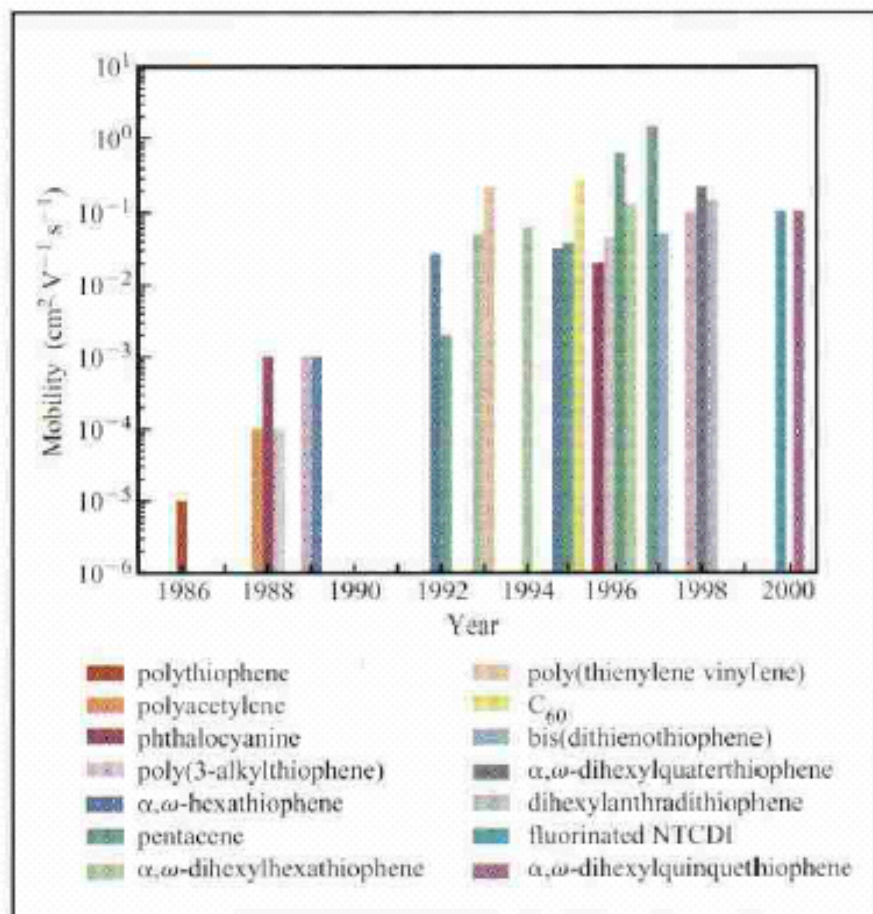
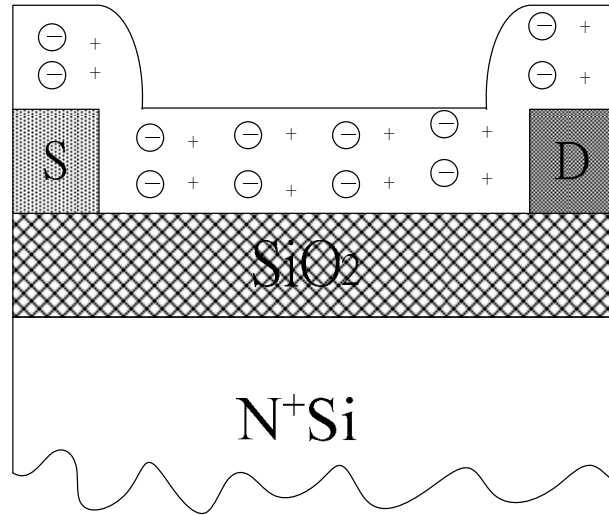


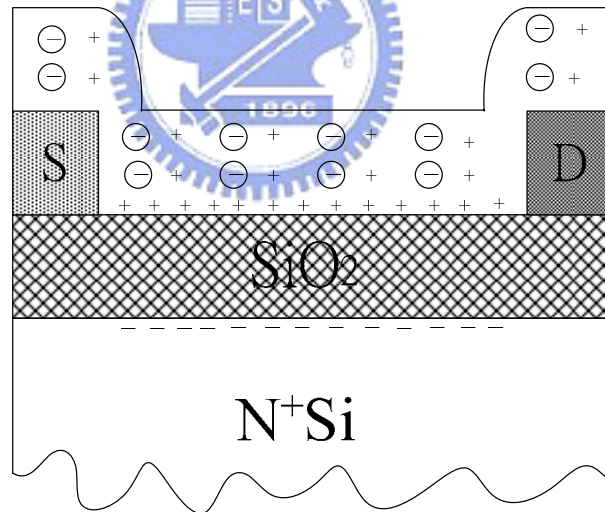
**Figure 1-1:** Semilogarithmic plot of the highest field-effect mobility( $\mu$ ) reported for OTFTs fabricated from the most promising polymeric and oligomeric semiconductors versus year from 1986 to 2000.[1]

$$V_G = V_S = V_D = 0$$



(a)

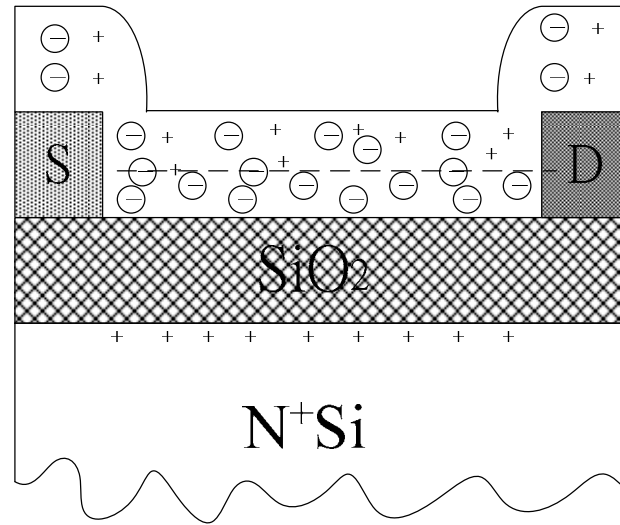
$$V_S = V_D = 0, V_G < 0$$



(b)

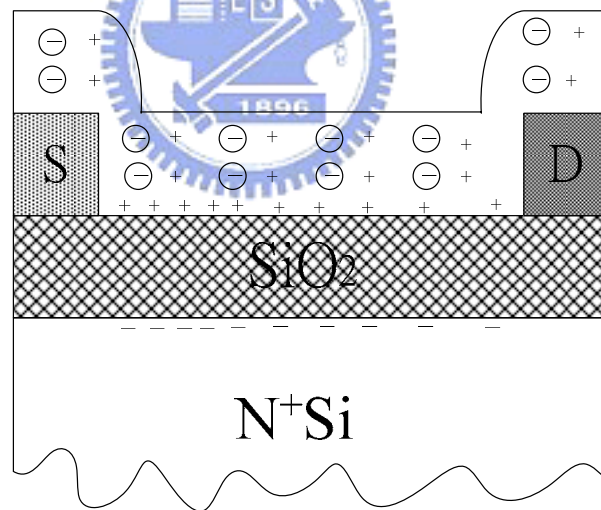
**Figure1-2:** Schematic of operation of organic thin film transistor, showing a lightly p-doped semiconductor: + indicates a positive charge in semiconductor ; (-) indicates a negatively charge counterion (a) no-bias (b) accumulation mode (c) depletion mode (d) non-uniform charge density (e) channel pinch-off [3] (continue)

$$V_S = V_D = 0, V_G > 0$$



(c)

$$V_S = 0, V_G < V_D < 0$$

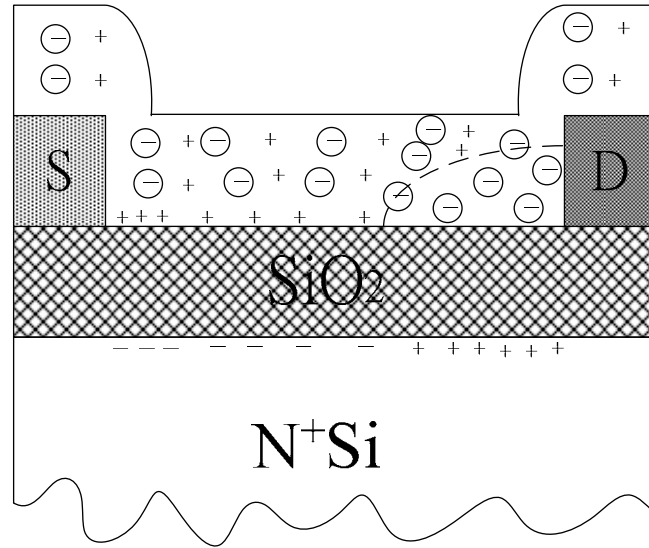


(d)

**Figure1-2:** Schematic of operation of organic thin film transistor, showing a lightly p-doped semiconductor: + indicates a positive charge in semiconductor ; (-) indicates a negatively charge counterion (a) no-bias (b) accumulation mode (c) depletion mode (d) non-uniform charge density (e) channel pinch-off [3] (continue)



$$V_S=0, V_D < V_G < 0$$



(e)

**Figure1-2:** Schematic of operation of organic thin film transistor, showing a lightly p-doped semiconductor: + indicates a positive charge in semiconductor ; (-) indicates a negatively charged counterion (a) no-bias (b) accumulation mode (c) depletion mode (d) non-uniform charge density (e) channel pinch-off [3]

Year	Mobility (cm <sup>2</sup> V <sup>-1</sup> s <sup>-1</sup> )	Material (deposition method) (v) = vacuum deposition (s) = from solution	$I_{on}/I_{off}^{10}$	W/L	Reference
1983	Minimal, not reported (NR)	Polyacetylene (s) (demonstration of field effect in an OTFT)	NR	200	[16]
1986	10 <sup>-7</sup>	Polythiophene (s)	10 <sup>3</sup>	NR	[17]
1988	10 <sup>-4</sup>	Polyacetylene (s)	10 <sup>3</sup>	350	[18]
	10 <sup>-3</sup>	Phthalocyanine (s)	NR	3	[19]
	10 <sup>-1</sup>	Poly(5-benzothio(phenyl)) (s)	NR	NR	[20]
1989	10 <sup>-1</sup>	Poly(3-alkylthiophene) (s)	NR	NR	[21]
	10 <sup>-3</sup>	<i>n</i> - <i>o</i> -hexathiophene (s)	NR	NR	[22]
1992	0.02 <sup>†</sup>	<i>n</i> - <i>o</i> -hexathiophene (s)	NR	100	[23]
	2 × 10 <sup>-2</sup>	Pentacene (v)	NR	NR	ibid.
1993	0.08	<i>n</i> - <i>o</i> -di- <i>n</i> -hexyl-hexathiophene (v)	NR	100–200	[24]
	0.22 <sup>†</sup>	Polythienylenevinylene (s)	NR	1000	[25]
1994	0.06	<i>n</i> - <i>o</i> -dihexyl-hexathiophene (s)	NR	50	[26]
1995	0.03	<i>n</i> - <i>o</i> -hexathiophene (s)	~10 <sup>3</sup>	21	[27]
	0.018	Pentacene (v)	140	1000	[28]
	0.3	C <sub>60</sub> (s)	NR	25	[29]
1996	0.02	Phthalocyanine (v)	2 × 10 <sup>3</sup>	NR	[30]
	0.045	Poly(3-hexylthiophene) (s)	340	20.8	[31]
	0.13	<i>n</i> - <i>o</i> -dihexyl-hexathiophene (s)	>10 <sup>3</sup>	2.5	[15]
	0.62	Pentacene (s)	10 <sup>3</sup>	11	[32]
1997	1.5	Pentacene (s)	10 <sup>4</sup>	2.5	[33]
	0.05	Hexyl(benzo)thiophene (s)	10 <sup>3</sup>	500	[34]
1998	0.1	Poly(3-hexylthiophene) (s)	>10 <sup>3</sup>	20	[35]
	0.23	<i>n</i> - <i>o</i> -dihexyl-quaterthiophene (v)	NR	1.5	[26]
	0.15	Dihexyl-orthodithiophene	NR	1.5	[37]
2000	0.1	<i>n</i> -decapentafluoroheptyl-methyl- naphthalene-1,4,5,8-tetracarboxylic diimide (v)	10 <sup>5</sup>	1.5	[38]
	0.1	<i>n</i> - <i>o</i> -dihexyl-quaterthiophene (s)	NR	NR	[36]

<sup>†</sup>Values for  $I_{on}/I_{off}$  correspond to different gate voltage ranges and thus are not directly comparable to one another. The reader is encouraged to read the details of the experiments in the cited references.

<sup>‡</sup>This result has not yet been reproduced.

**Table1-1:**Highest field-effect mobility( $\mu$ ) values measured from OTFTs as reported in the literature annually from 1986 through 2000.[1]

## **Chapter 2**

# **OTFTs Fabricated by Different Solvents and Weight Percentages of P3HT**

### **2.1 Introduction**

Lately, organic materials such as pentacene and poly (3-alkylthiophene) have attracted considerable attention due to their potentials for semiconductor electronics. In particular, the characteristics of P3AT thin film transistors (TFTs) have made such devices feasible for applications requiring large-area coverage, mechanical flexibility, and low overall cost.

There are four methods to form organic semiconductor film: (a) solution-processed deposition, (b) vacuum evaporation, (c) electro-polymerization, (d) Langmuir-Blodgett Technique [4]. Recently, many researchers extensively use solution-processed deposition to fabricate organic semiconductor film. For solution-deposited organic semiconductor film, one kind of the organic semiconductor material such as poly (3-alkylthiophene) are dissolved in solvent such as chloroform, and then the dissolved organic material are deposited onto the surface of substrate using spin-coating, dip-coating or drop-casting method. Among these three methods of casting P3HT thin film, the best way is dip-coating and it has been shown that the field-effect mobility is as high as  $0.2 \text{ cm}^2/\text{Vs}$  [5]. Nevertheless, devices made by dip-coating technique have a good mobility, but the dip-coating method can not be applied for coverage of a large area. Therefore, in all of our experiments, we used spin-coating technique as a key process of organic layer deposition.

Among a lot of organic semiconductor materials, we use poly (3-hexylthiophene) or P3HT

as the semiconducting layer. P3HT has many potential advantages to serve as the active layer of field-effect transistors. First, P3HT is a well-known organic semiconducting polymer and has shown the field-effect mobility from  $10^{-4}$  cm<sup>2</sup>/Vs in 1988 to 0.2 cm<sup>2</sup>/Vs in 2003[1], [4], [6]. Second, P3HT has high solvent selectiveness, which can dissolve in toluene, xylene chloroform and so on. Third, P3HT is solution processed; therefore it can be processed by spin coating. However, the performance of P3HT thin film transistors can be affected by: (1) the regioregularity of the P3HT, (2) solvents, (3) P3HT weight % in solvents, and (4) different deposition methods, such as spin-coating, dip-coating, or drop-casting [7].

In this chapter, we used different solvents, xylene and chloroform, to dissolve P3HT, and then used spin-coating technique to deposit organic semiconductor layer. Afterwards, we measured the electrical characteristics of P3HT OTFTs formed by different solvents, such as mobility, threshold voltage and on/off ratio. In addition to study different solvents, we also prepared different weight percentages of P3HT in chloroform, i.e. 0.1%, 0.3%, 0.8% and 2.0%. Afterwards, we investigated the electrical characteristics of P3HT OTFTs including mobility, threshold voltage and on/off ration etc., with different weight percentages of P3HT.

## 2.2 The Molecular Structure of P3HT

The structure of the polymer chain of P3HT is shown in **Fig 2-1**. The 3-alkyl substituents can be incorporated into a polymer chain with two different regioregularities: head to tail (HT) and head to head (HH) [7], [8].

R represents the alkyl side chain (C<sub>6</sub>H<sub>13</sub>, for hexylthiophene), which allows them to be dissolved in solvents, such as xylene or chloroform. This solution processability enables simple film deposition, one of the major attractions of conjugated polymers. A regiorandom P3HT

consists of both HH and HT 3-hexylthiophenes in a random pattern while a regioregular P3HT has only one kind of 3-alkylthiophene, either HH or HT. The position and direction of the side chain in the diagram shows a very highly ordered system. This type of order is known as regioregularity and has been shown to give much higher field-effect mobility values over regiorandom (disordered side chains) material [9]. Most interestingly, these polymers have been shown to have very different properties from their corresponding regiorandom polymers, such as smaller band gaps, better ordering and crystallinity in their solid states, and substantially improved electroconductivities. When regioregular P3HT consisting of 98.5% or more head-to-tail (HT) linkages was used to fabricate FETs, a dramatic increase in mobility was observed relative to regiorandom poly-3-alkylthiophenes [10]. In our experiments, regioregular P3HT (HT regioregularity of 98.5%) and high grade solvents, xylene and chloroform, were purchased from Aldrich Chemical Company. We did not perform further purification or sublimation to these chemicals.



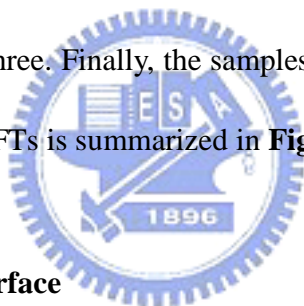
## 2.3 Fabrication of Organic Thin Film transistors

### 2.3.1 Process Flow of P3HT OTFTs Fabrication

The P3HT TFTs use a bottom-contact structure fabricated on silicon substrate as shown in **Fig 2-2**. The process flow of P3HT device is as following.

At first, an n-type bare silicon wafer was cleaned by the standard RCA cleaning process. After that, phosphorus atoms were diffused into an n-type silicon wafer by  $\text{POCl}_3$  to form a common gate electrode. After diffusing, we used dilute HF to remove  $\text{SiO}_2$  and measured its sheet resistance ( $3\sim 4\ \Omega/\square$ ). Before the insulating layer of silicon dioxide was deposited, the n+ silicon wafer must be cleaned again by the standard RCA cleaning process. Then a silicon

dioxide layer is deposited by PECVD using TEOS source and O<sub>2</sub> gas at 350°C. Afterwards, source and drain regions were defined through the photo lithography process followed by thermal evaporation steps of 20-nm thick Ti as an adhesion layer and 100-nm thick Pt as a contact material. Later, the wafer was then immersed in acetone to lift-off the photo resist/metals and to form the source/drain regions. The samples after S/D patterning were treated with 3 minute IPA cleaning, 5 minute D.I water cleaning. Next, oxide surfaces were treated with hexamethyldisilazane (HMDS) to improve the adhesion between the polymer chain and oxide surfaces. Then we prepared different solvents, xylene or chloroform, to dissolve P3HT. P3HT solution was filtered by a 0.2-μm pore-size PTFE filter and then spun onto the wafer surface. The detailed spin-coating parameters is 200 RPM for 10S as step one, 500 RPM for 25S as step two and 2000 RPM for 25S as step three. Finally, the samples were cured at 120°C for 3 minute. The process flow of P3HT based OTFTs is summarized in **Fig2-3**.



### 2.3.2 Modification of Oxide Surface

Oxide surfaces were treated with hexamethyldisilazane (HMDS) to improve the adhesion between polymer chain and oxide surfaces. Modification of the substrate surface prior to deposition of regioregular P3HT has also been found to influence the film morphology. For example, treatment of SiO<sub>2</sub> with hexamethyldisilazane (HMDS) replaces the hydroxyl groups at the SiO<sub>2</sub> surface with methyl or alkyl groups. The apolar nature of these groups apparently attracts the hexyl side chains of P3HT, favoring lamellae with an edge-on orientation (**Fig2-4**) [11]. According to the reference [11], the mobility of OTFTs with an edge-on orientation P3HT film is higher than that with a face-on orientation.

### 2.3.3 The Layout of Bottom-Contact OTFT

We used two kinds of layout in the fabrication of OTFTs, i.e. linear type and finger type as shown in **Fig2-5**. An interdigitated geometry as shown in Fig2-5 (b) for the source/drain contacts is chosen to minimize the device area and the associated gate to source/drain leakage current. The channel length (L) of the linear type layout is in a range of 10~50  $\mu\text{m}$  and the channel width (W) is in a range of 300~500  $\mu\text{m}$ . The channel length of the finger type is in a range of 10~50  $\mu\text{m}$  and the channel width is in a range of 1000~10000  $\mu\text{m}$ .

## 2.4 Electrical Characteristics of P3HT OTFTs

### 2.4.1 Measurement

Current-voltage characteristics of OTFT were measured in the air with a semiconductor parameter analyzer HP4156. All measurements were carried out in an electrically shielded box. The drain-source current  $I_{\text{DS}}$  was measured as a function of the drain-source voltage  $V_{\text{DS}}$  to observe the FET-like characteristics. And  $I_{\text{DS}}$  was measured as a function of the gate voltage  $V_{\text{G}}$  at a small drain-source voltage, which was constructed to determine the gate bias modulation of the FET conductive channel.

Three parameters were extracted from the experimental I-V curves and are: (1) the transistor threshold voltage ( $V_{\text{T}}$ ), (2) the current modulation (the ratio of the current in the accumulation mode over the current in the depletion mode, also referred to ON-OFF current ratio), and (3) the field effect mobility ( $\mu_{\text{FE}}$ ). The detailed extraction method will be discussed in the following section.

### 2.4.2 Threshold Voltage and OFF Current Definition

Inorganic semiconductors, such as Si or Ge, can be operated in three modes: depletion mode, accumulation mode and inversion mode. With regards to organic semiconductors, such as P3HT OTFTs, they can not be operated in the inversion mode. Therefore, P3HT OTFTs were turned ON in the accumulation mode ( $V_G < 0$ , see Fig1-2(b)) and were turned OFF in the depletion mode ( $V_G > 0$ , see Fig1-2(c)).

Because P3HT OTFTs are normally on devices, we define a so-called OFF current when the current is smaller than a certain value, and the gate voltage ( $V_G$ ) corresponding to this current is called threshold voltage ( $V_{th}$ ). **Fig2-6** shows a plot of normalized drain-source current vs. gate voltage. Based on this figure, we defined the normalized OFF current is  $10^{-12}$  Amp and thus the OFF current of a specified transistor is  $10^{-12} * W/L$ . The magnitude of OFF current with different channel length and different channel width are listed **Table2-1**

#### 2.4.3 The Extraction method of Mobility

P3HT OTFT is like a p-channel FET. Therefore, the linear regime field effect mobility can be obtained by the calculation described below. At low drain voltage ( $V_D$ ), source-drain current ( $I_{DS}$ ) increases linearly with  $V_D$  (linear regime) and is approximately determined from the following equation (2-1):

$$I_{DS} = \frac{W}{L} \mu C_i (V_G - V_{th} - V_D / 2) V_D \quad \text{as } V_D \ll V_G - V_{th} \quad [\text{Equation 2-1}]$$

where  $L$  is the channel length,  $W$  is the channel width,  $C_i$  is the capacitance per unit area of the insulating layer,  $V_{th}$  is the threshold voltage, and  $\mu$  is the field effect mobility, which can be calculated in the linear regime from the transconductance,

$$g_m = \left. \frac{\partial I_D}{\partial V_G} \right|_{V_D = \text{const}} = \frac{WC_i}{L} \mu V_D \quad [\text{Equation 2-2}]$$



by plotting  $I_{DS}$  versus  $V_G$  at a constant low  $V_D$ , with  $-V_D \ll -(V_G - V_T)$ , and equating the value of the slope of this plot to  $g_m$ . We can compute the linear regime mobility from equation 2-2

## 2.5 OTFTs Fabrication by Different Solvents

### 2.5.1 Experiment Detail

The detailed process flow of P3HT OTFTs fabrication was described in section 2.3.1. The different portion is that we prepared different solvents including xylene and chloroform to dissolve P3HT material. Specifically, the P3HT films were deposited from a solution of 0.3% P3HT in xylene or 0.3% P3HT in chloroform. And then the P3HT solution was filtered by a 0.2- $\mu\text{m}$  pore-size PTFE filter and spun onto the wafer surface.

### 2.5.2 Result and Discussion

#### 2.5.2.1 Physical properties of spin-on P3HT film

We used atomic force microscope to observe the surface morphology and topography of the deposited P3HT film. **Fig2-7** exhibits the surface morphology of the deposited P3HT film with different solvents. **Fig2-7(a)** shows that many clusters of undissolved P3HT powder, despite being filtered, still can be observed, implying that xylene is not a good solvent for P3HT. But from **Fig2-7(b)**, we can not find apparent clusters of undissolved P3HT powder. It follows that chloroform is a good solvent to dissolve P3HT material. Additionally, no apparent grain or grain-boundary structure was found in the AFM photograph because the P3HT thin film is a long-chain polymer.

#### 2.5.2.2 The anomalous gate leakage current effect from xylene solution

Current-voltage characteristics of OTFTs were measured in the air with a semiconductor parameter analyzer HP4156. **Fig2-8** illustrates source current ( $I_S$ ) and gate leakage current ( $I_G$ ) versus gate voltage where the P3HT OTFT was fabricated by 0.3% xylene solution. The OTFT was turned ON, and the “ON-current” was larger than the gate leakage current by one order. The gate leakage current was comparable to the source current when the device is nearly turned OFF, and finally the gate leakage current dominated the drain current. Due to anomalous gate leakage effect, we cannot measure the ideal I-V characteristics. As a result, the ON-OFF ratio would be affected by anomalous gate leakage current.

**Fig2-9(a)** shows source current versus drain voltage, where the P3HT OTFT was fabricated by 0.3% xylene solution. **Fig2-9(b)** shows source current versus drain voltage, where the P3HT OTFT was fabricated by 0.3% chloroform solution. Because of anomalous gate leakage current, the source current at zero bias was above  $10^{-7}$  Amp as shown in **Fig2-9(a)**. If the solvent was changed from xylene to chloroform, we could not observe apparent anomalous gate leakage current. From **Fig2-9(b)**, the source current at zero bias was below  $10^{-8}$  Amp. Therefore, the anomalous gate leakage current was suppressed by chloroform solution.

Because the anomalous leakage current is comparable to the source current of the OTFT with small W/L ratio, the result would be incorrect. Therefore, as the P3HT OTFT was fabricated by 0.3% xylene solution, the anomalous gate leakage current not only influenced the magnitude of source current at zero drain bias, but also the ON-OFF ratio with small W/L. From **Fig2-10**, if the P3HT OTFT was fabricated by 0.3% xylene solution, ON-OFF ratio was dependent on W/L ratio. But the solvent was changed from xylene to chloroform, the anomalous gate leakage current was suppressed. From **Fig2-10**, if the P3HT OTFT was fabricated by 0.3% chloroform solution, ON-OFF ratio was independent on W/L ratio.

### 2.5.2.3 The correlation between field-effect mobility of P3HT OTFT and solvent

The choice of solvents has a very significant impact on the field-effect mobility of P3HT OTFTs. In a recent publication, Bao *et al.* [12] observed that chloroform was used as a solvent and P3HT organic semiconductor layer was deposited by spin-coating, the field-effect mobility of P3HT OTFT is about  $10^{-3} \text{ cm}^2/\text{Vs}$ . Xylene was used as a solvent and P3HT organic semiconductor layer was deposited by spin-coating, the field-effect mobility of P3HT OTFT is about  $10^{-4} \text{ cm}^2/\text{Vs}$ , as shown in Table2-2. From **Fig2-11**, the field-effect mobility of P3HT OTFT which was fabricated by xylene is about  $10^{-3} \text{ cm}^2/\text{Vs}$  and the field-effect mobility of P3HT OTFT which was fabricated by chloroform solution is about  $10^{-4} \text{ cm}^2/\text{Vs}$ . The conclusion was in consistent with the publication [12].

## 2.6 OTFTs Fabrication by Different Weight Percentages of P3HT

### 2.6.1 Experiment Detail

In this section, we prepared 0.1%, 0.3%, 0.8%, and 2.0% of P3HT in chloroform. And then the P3HT solution was filtered by a 0.2- $\mu\text{m}$  pore-size PTFE filter and then spun onto the wafer surface. Next, we investigated the electrical characteristics of P3HT OTFTs, such as mobility, threshold voltage and on/off ratio, with different weight percentages of P3HT. Besides, we compared the performance of P3HT OTFTs which were fabricated by new and old P3HT material. New P3HT material, specifically “fresh” P3HT material, means that we purchased it from Aldrich chemical company and were used at once. Old P3HT, although purchased from the same company, had been opened and the remaining chemicals had been storing in air for a year.

### 2.6.2 Result and Discussion

### 2.6.2.1 Physical properties of spin-on P3HT film

We used atomic force microscope to observe the surface morphology and topography of deposited P3HT film. **Fig2-12~Fig2-15** exhibits the surface morphology of the deposited P3HT film with different weight percentage of 0.1%, 0.3%, 0.8% and 2.0% of P3HT in chloroform. It was found that the deposited films by the low weight percentage of P3HT, such as 0.1% and 0.3%, were very smooth, but the deposited films by high weight percentage of P3HT, such as 0.8% and 2.0%, were very rough. When the weight percentage of P3HT as high as 2.0%, there were apparent pinholes in the deposited film. **Table2-3** summarized the surface roughness of P3HT film with respect to weight percentage of P3HT in chloroform. The surface root-mean-square roughness of organic thin film deposited by 0.3% of P3HT is 8.24Å. That is much smoother than RMS roughness of organic thin film deposited in other weight percentages.

### 2.6.2.2 The bulk current effect from high weight percentage of P3HT

There are two current paths in organic semiconductor layer[13]. One is the channel current ( $I_{ch}$ ), it comes from source electrode (Pt) and goes through the accumulation holes and into drain electrode (Pt). Using established metal-oxide-field effect transistor (MOSFET) current-voltage relationships, the channel current can be written as:

$$I_{ch} = \frac{W}{L} \mu C_i (V_G - V_{th} - V_D / 2) V_D \quad \text{as } V_D \ll V_G - V_{th} \quad [\text{Equation 2-3}]$$

for the linear regime, where L is the channel length, W is the channel width,  $C_i$  is the capacitance per unit area of the insulating layer,  $V_{th}$  is the threshold voltage, and  $\mu$  is the field effect mobility. Another leakage path is the bulk current ( $I_{bk}$ ). It comes from source electrode (Pt) and goes through conductive layer which is above the accumulation holes and into drain electrode. The bulk current ( $I_{bk}$ ) can be represented as

$$I_{bk} = \mu \times \frac{W}{L} \times l \times V_{DS} \quad [\text{Equation 2-4}]$$

, where  $l$  is the organic semiconductor layer thickness [13].

The P3HT OTFTs were turned ON in the accumulation mode ( $V_G < 0$ , see Fig1-2(b)) and were turned OFF in the depletion mode ( $V_G > 0$ , see Fig1-2(c)). **Fig2-16** shows a typical source current versus drain voltage plot at various gate voltages in both accumulation [Fig.2-16(a)] and depletion [Fig.2-16(b)] modes. **Fig2-17** is the same. As the positive voltage increases, the source current decreases. It was shown that the device could be turned OFF. But from **Fig2-18**,  $I_S$  versus  $V_D$  curve in the depletion mode as a function of weight concentration of P3HT in chloroform, the devices which were fabricated by 0.8%, 2.0 % of P3HT can not be turned OFF. From two aspects of observation, it can be shown that the current is the bulk current. (1) As the organic semiconductor layer thickness increases, the source current increases. (2) As the drain voltage increases, the source current increases. These conclusions are consistent with Equation 2-4.

Either new or old P3HT material, the OTFTs fabricated by high weight percentage of P3HT such as 0.8% and 2.0% can not be observed the ideal  $I_S$ - $V_G$  characteristics as shown in **Fig2-19~Fig2-20** due to the bulk current effect. As a result, threshold voltage and ON-OFF ratio would be affected by the bulk current. **Fig2-21** and **Fig2-22** shows that threshold voltage as a function of weight concentration of P3HT in chloroform. Because of the bulk current effect there is a dramatic increase as weight concentration of P3HT is above 0.3%.

### ***2.6.2.3 The correlation between the performances of P3HT OTFT and weight percentage of P3HT***

For OTFTs fabricated by fresh P3HT material, the following phenomenon can be observed:  
(1) **Fig2-22** illustrates the dependence of threshold voltage and various weight percentages of

P3HT. The most appropriate wt% of P3HT is 0.1%-0.3%. (2) **Fig2-23** illustrates that the field-effect mobility (weight %) dependence shows a maximum at 0.3%-0.8%. (3) **Fig2-24** illustrates that ON-OFF ratio (weight %) dependence show a maximum at 0.1%-0.3%. OTFTs fabricated by 0.8 % of P3HT had a better mobility than the others, such as 0.1%, 0.3%, 2.0%, but they can not have an ideal  $I_S-V_G$  characteristic. Therefore, in order to acquire an OTFT with good mobility, high ON-OFF ratio as well as appropriate threshold voltage, the optimal weight percentage of P3HT would be 0.3%. For OTFTs fabricated by old P3HT material, the foregoing phenomenon could not be observed, except threshold voltage, as shown in **Fig2-21**, **Fig2-25** and **Fig2-26**. Although similar trends of field-effect mobility and ON-OFF current ratio could not be observed in these figures, the OTFTs fabricated by high weight percentage of P3HT such as 0.8% and 2.0% can not be observed the ideal  $I_S-V_G$  characteristics, which is the same with fresh material.



## 2.7 Summary

It was found that chloroform is a good solvent to dissolve P3HT, the anomalous gate leakage current was suppressed by chloroform solution, and the high ON-OFF ratio of about four orders of magnitude and the field-effect mobility of  $10^{-3} \text{ cm}^2/\text{Vs}$  were attributed to chloroform solution.

The surface root-mean-square roughness of organic thin film deposited by 0.3% of P3HT is  $8.24 \text{ \AA}$ . That is much smoother than RMS roughness of organic thin film deposited by others, 0.1%, 0.8% and 2.0%. As weight percentage of P3HT in chloroform is above 0.3%, the bulk current effect would affect  $I_S-V_G$  curves and  $I_S-V_D$  curves. Therefore, in order to acquire an OTFT with good mobility, high ON-OFF current, appropriate threshold voltage, the optimal weight

percentage of P3HT would be 0.3%.



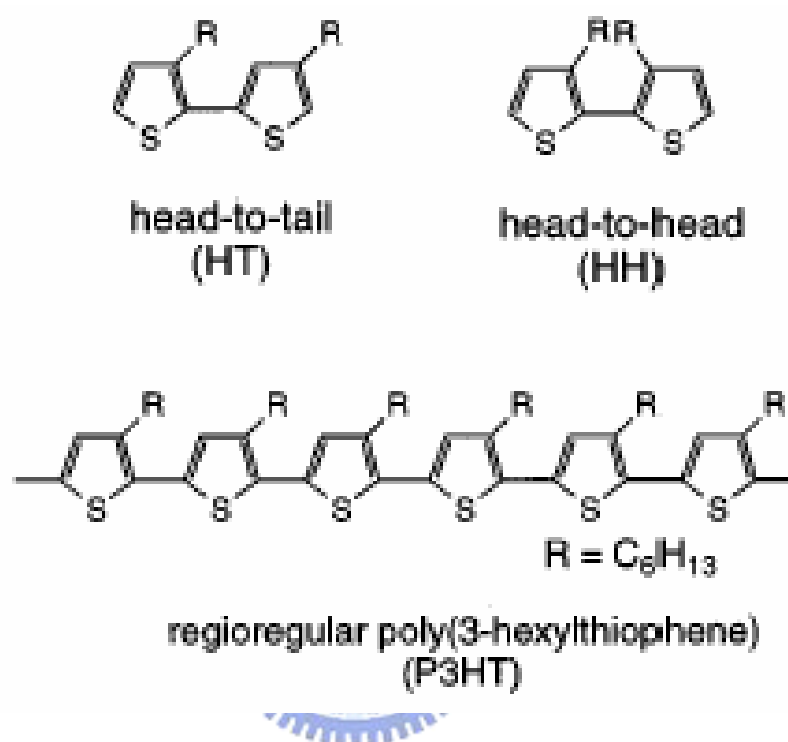


Figure 2-1: Chemical diagram of the polymer poly (3-hexylthiophene).R represents the alkyl chain



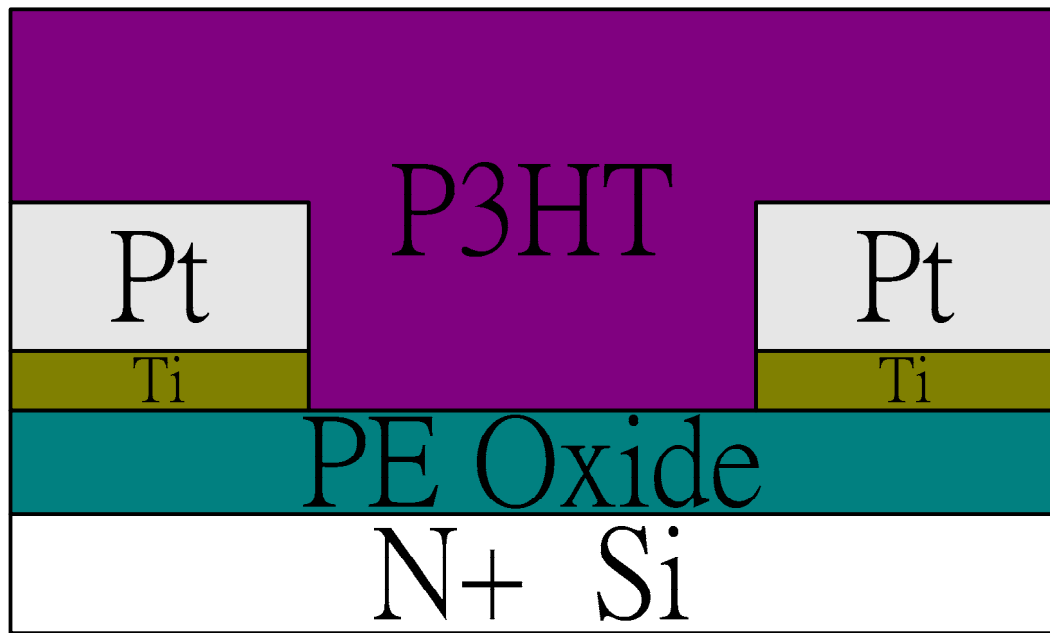


Figure2-2:Bottom-contact structure of P3HT OTFTs

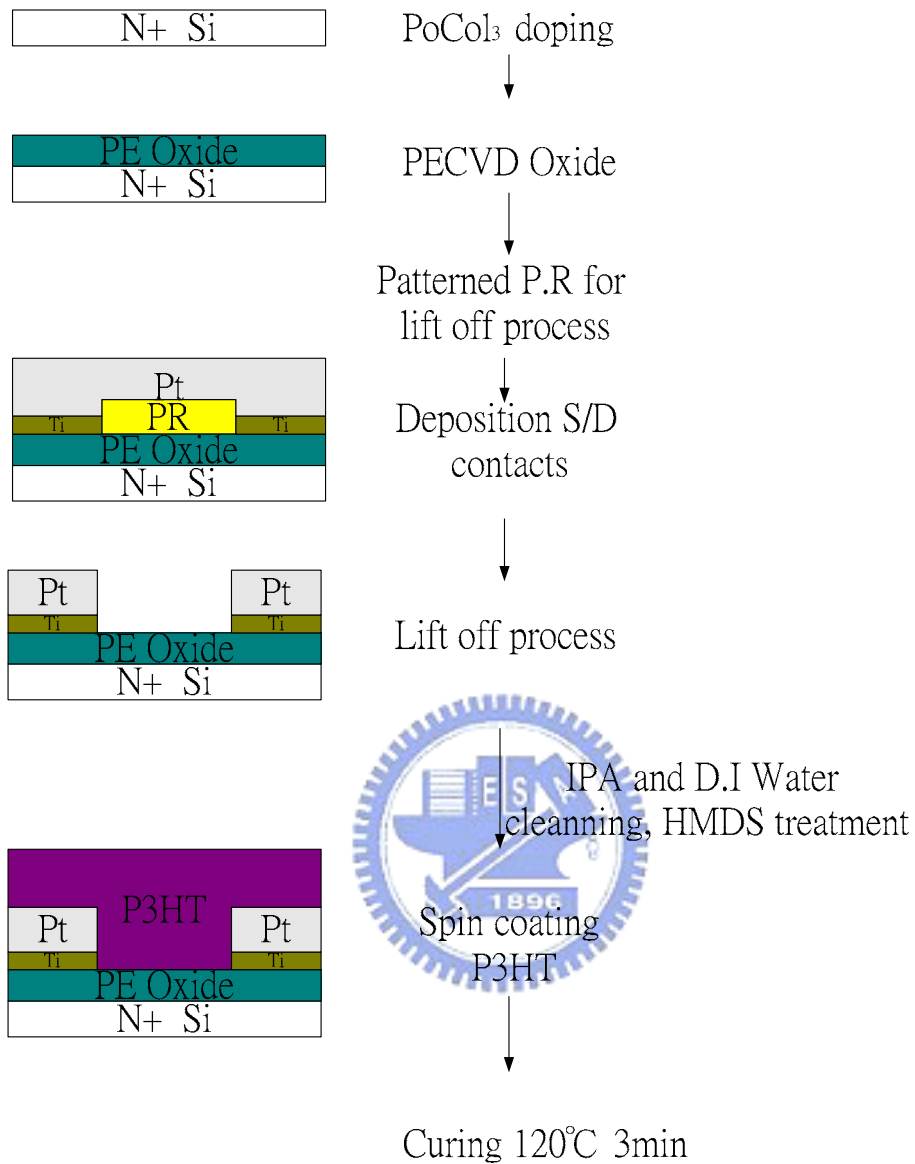
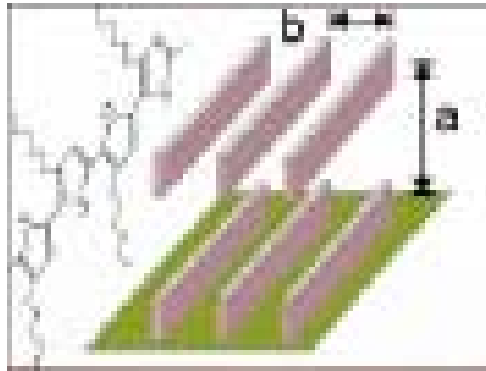
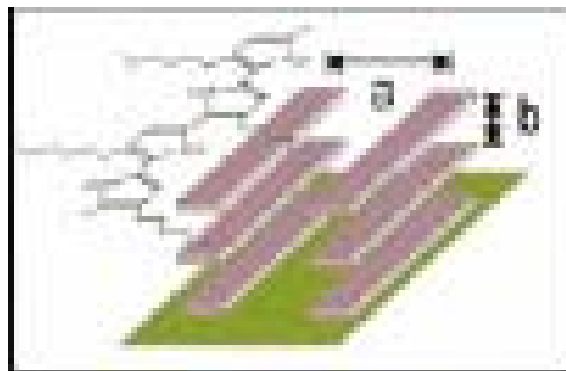


Figure2-3:Process flow of bottom-contact OTFTs

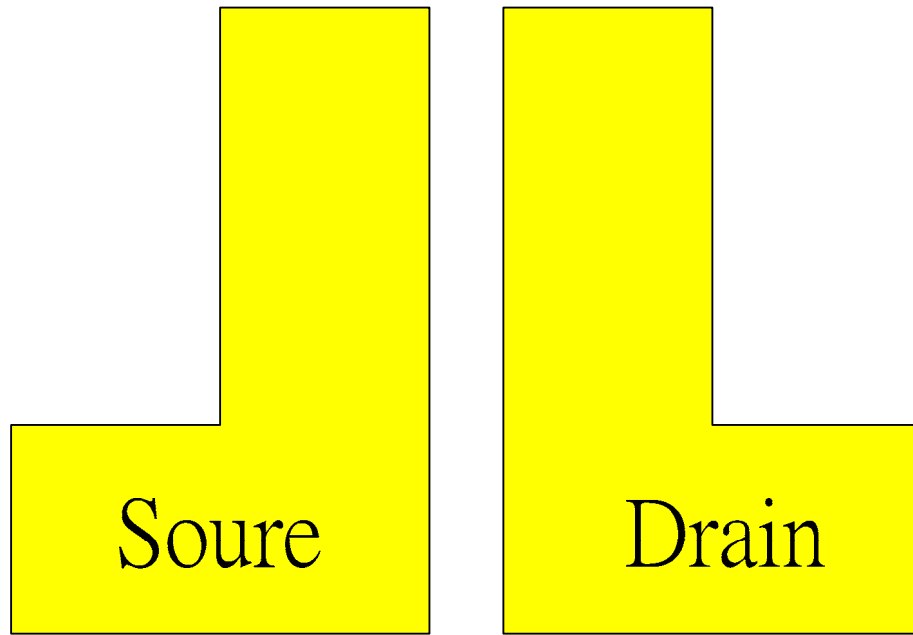


Edge-on orientation

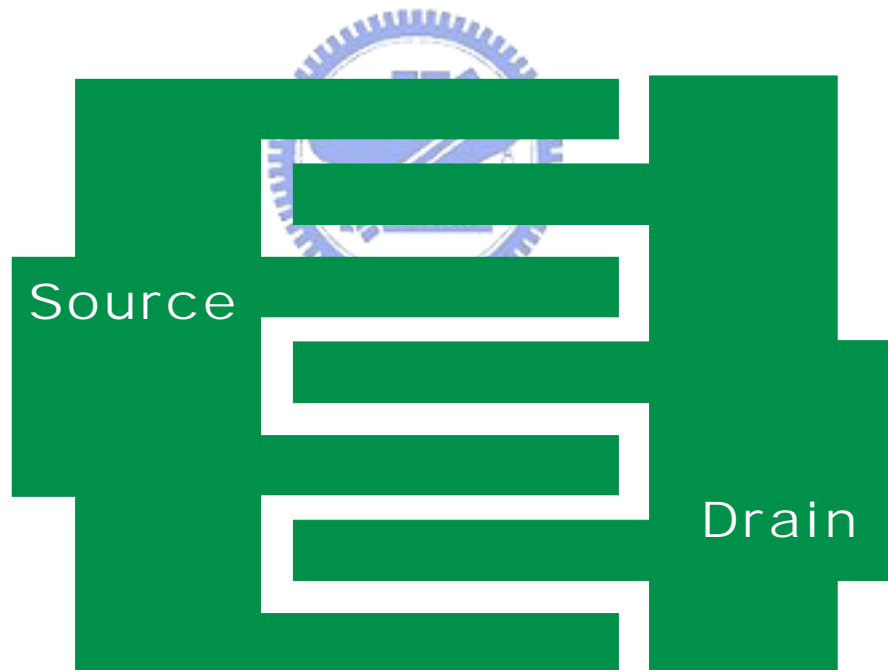


Face-on orientation

Figure2-4: Two different orientations of ordered P3HT domains with respect to the FET substrate [9]



(a)



(b)

Figure2-5: Layouts of bottom-contact OTFTs (a) linear type (b) finger type

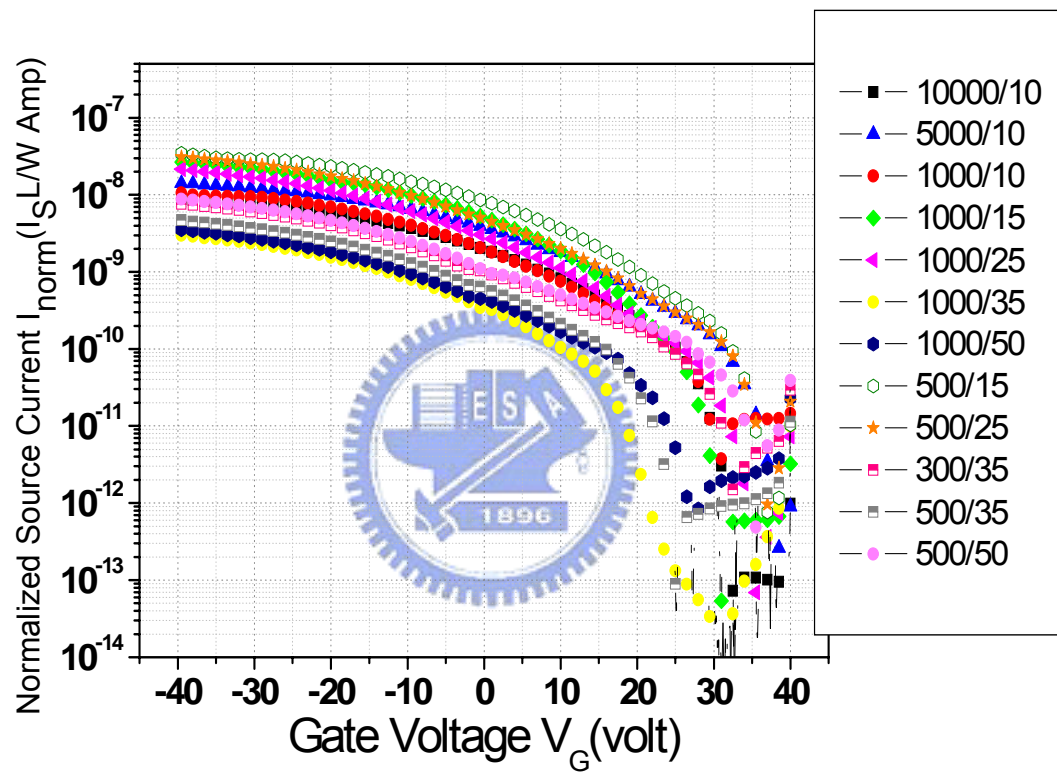
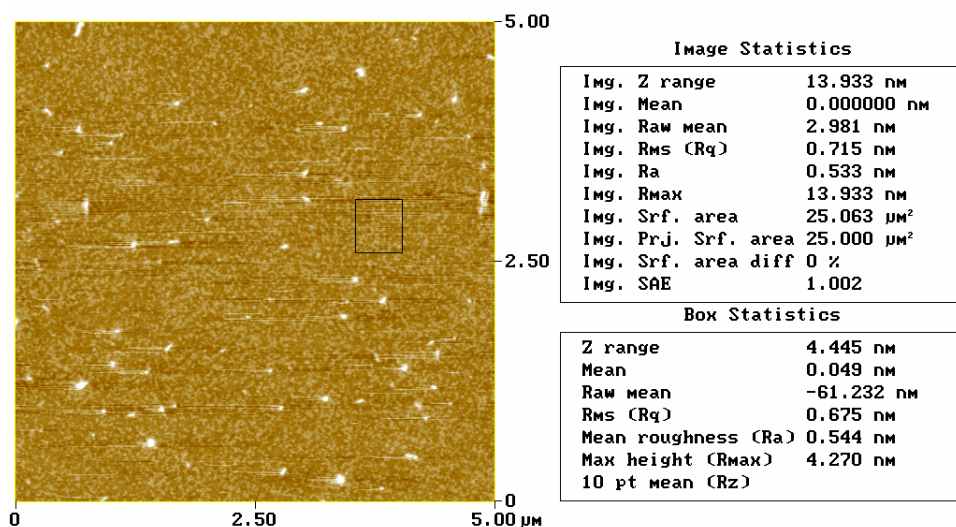


Fig2-6: Normalized drain-source current vs gate voltage

Peak Surface Area Summit Zero Crossing Stopband Execute Cursor

## Roughness Analysis

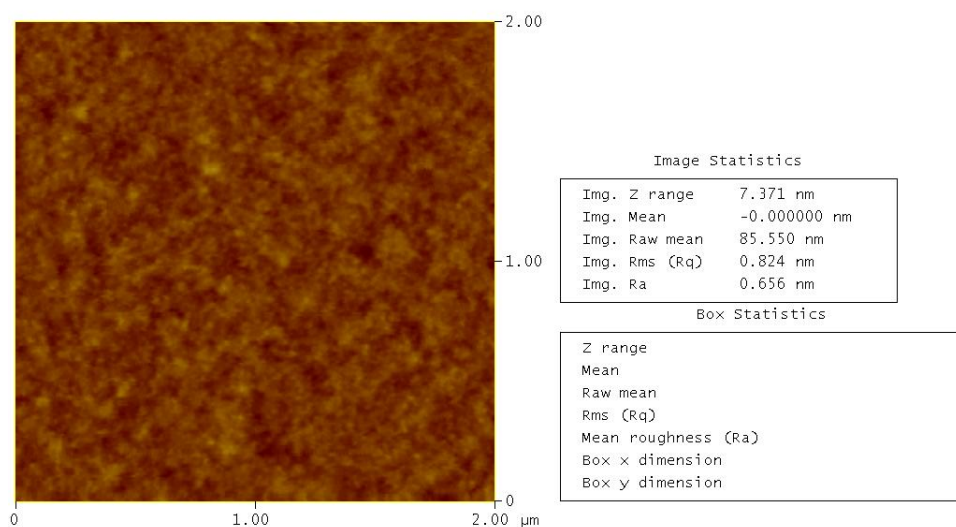


Peak Off Summit On Zero Cross. On Box Cursor

(a)

Peak Surface Area Summit Zero Crossing Stopband Execute Cursor

## Roughness Analysis



Peak Off Summit Off Zero Cross. Off Box Cursor

(b)

Figure2-7:AFM micrograph of P3HT 0.3% in (a) xylene (b) chloroform

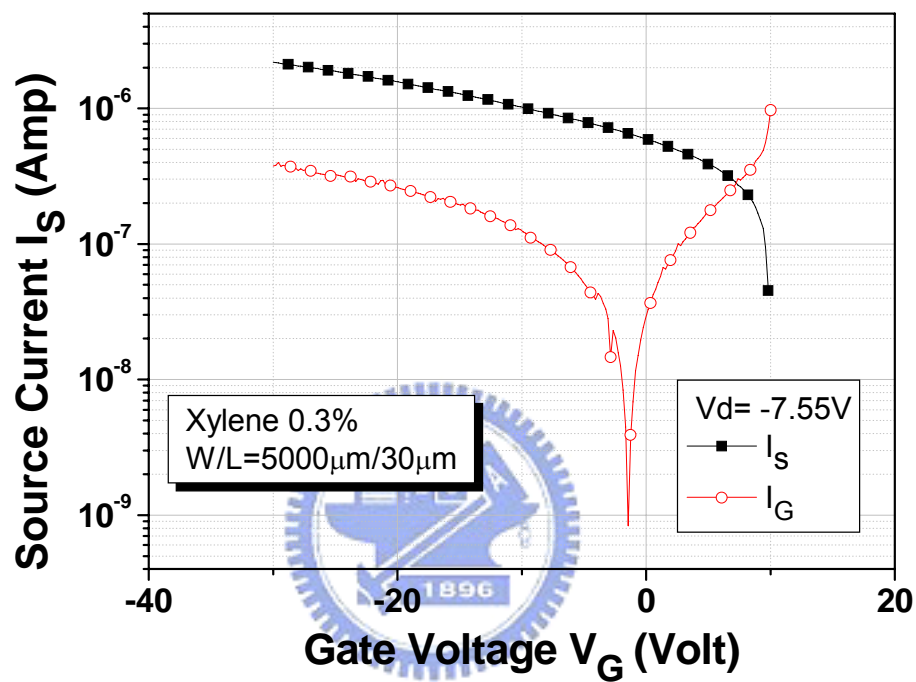
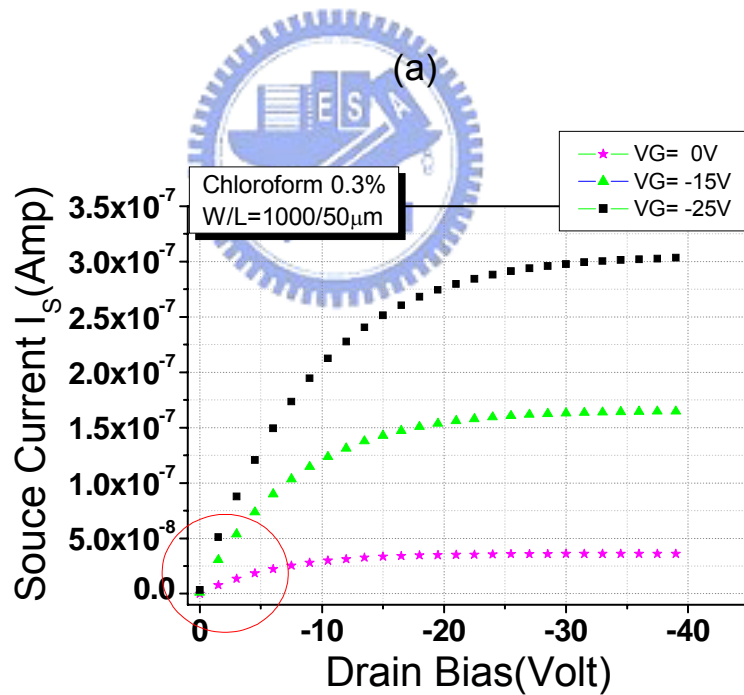
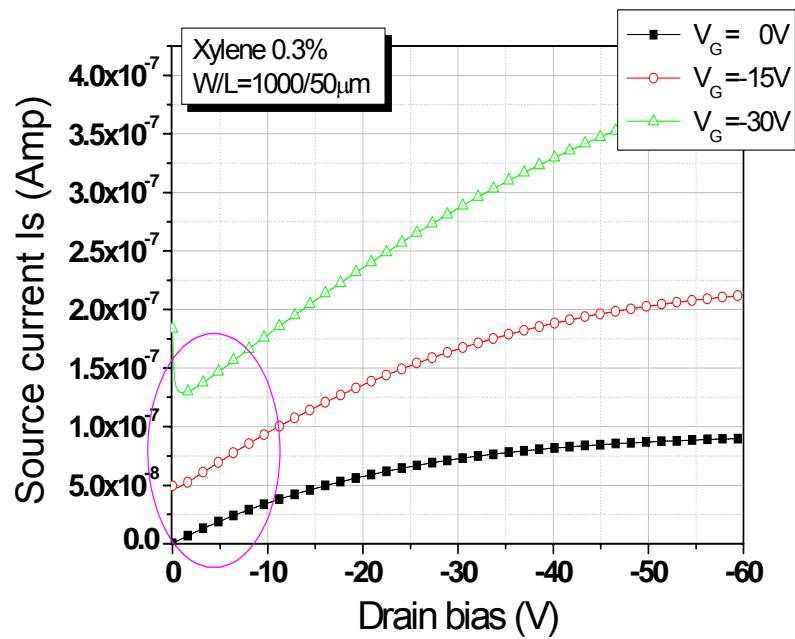


Figure 2-8: Source and gate leakage current versus gate bias



(b)  
Figure 2-9: Influence of gate leakage current on output characteristics  $I_s$  vs  $V_D$ : (a) xylene 0.3% (b) chloroform 0.3%



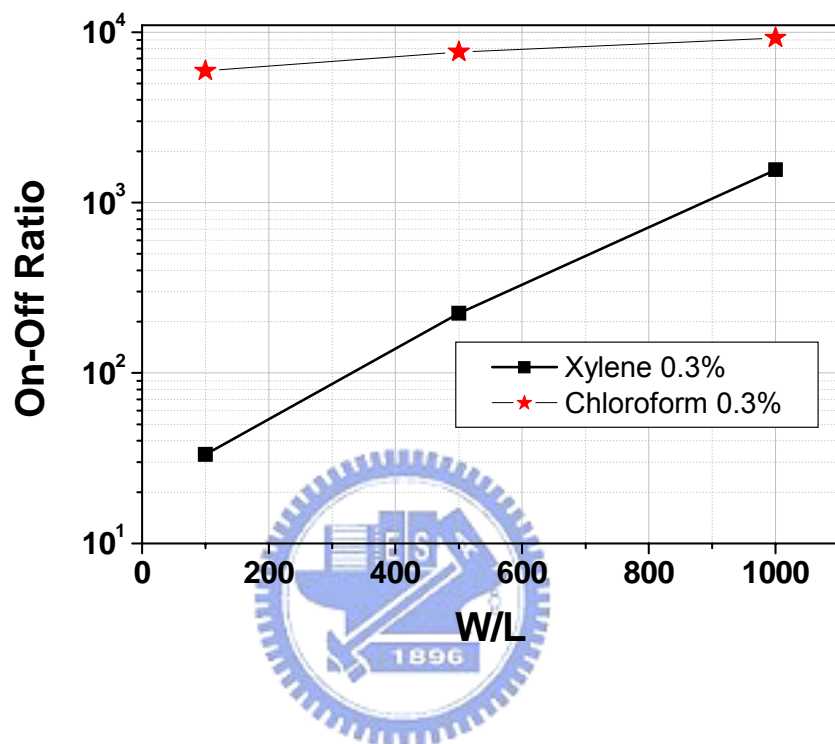
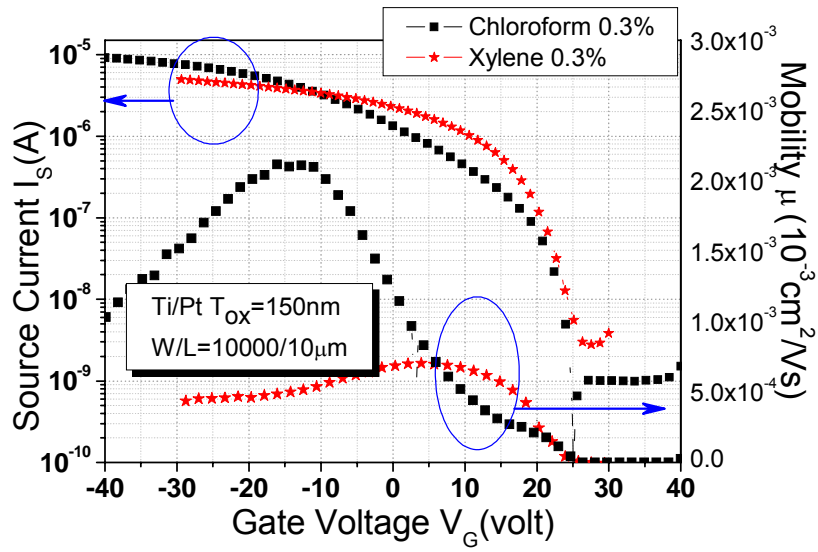
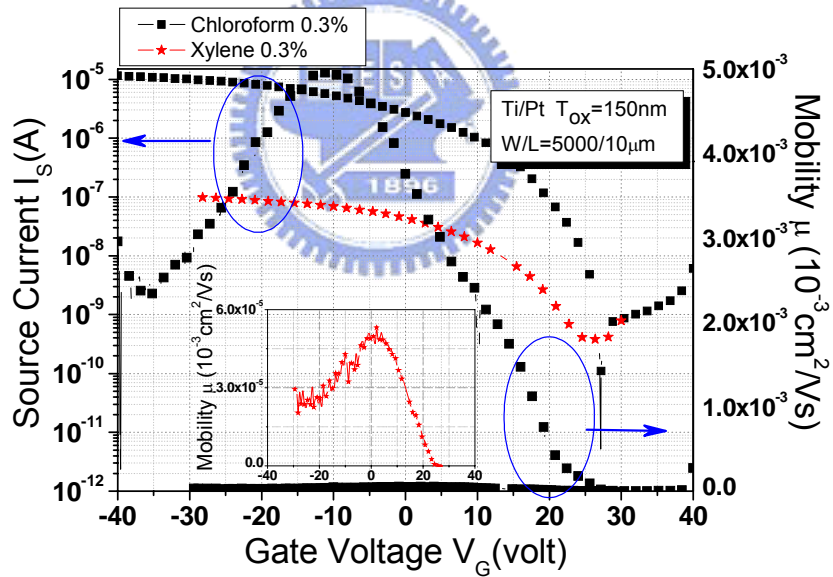


Figure2-10: On-Off ratio versus W/L

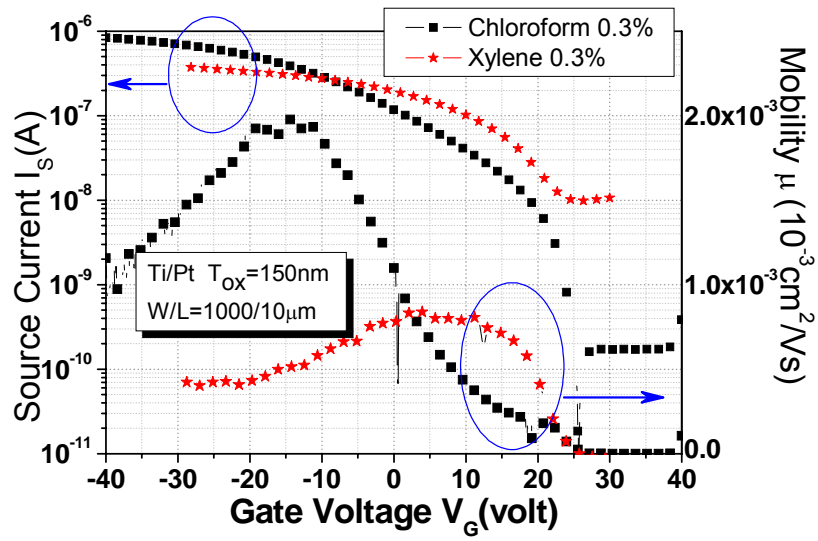


(a)

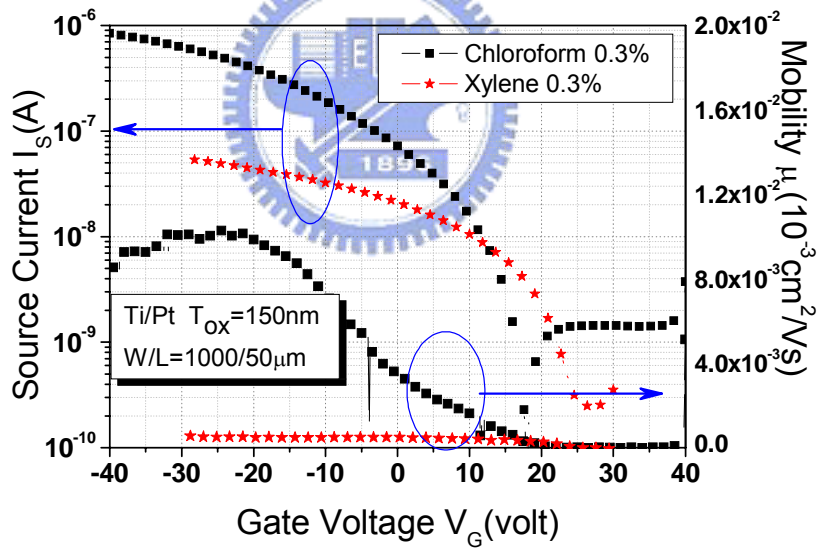


(b)

Figure2-11: Transfer characteristics  $I_S$  vs  $V_G$  and field-effect mobility of samples prepared from different solvrnt  
(a)  $W/L=10000/10\ \mu\text{m}$  (b)  $W/L=5000/10\ \mu\text{m}$  (c)  $W/L=1000/10\ \mu\text{m}$  (d)  $W/L=1000/50\ \mu\text{m}$  (continue)

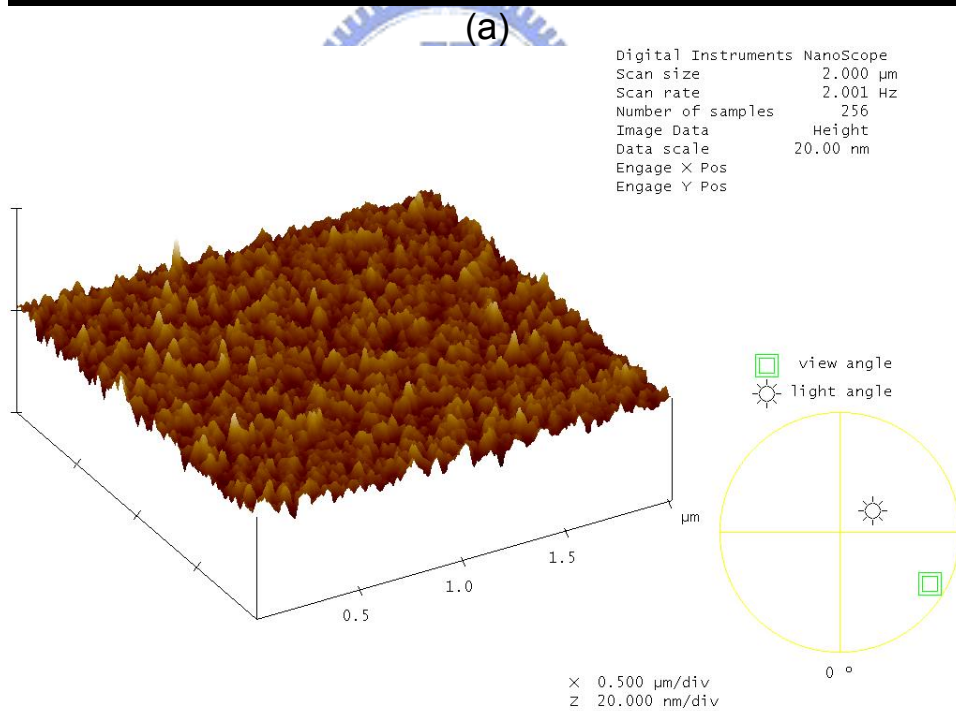
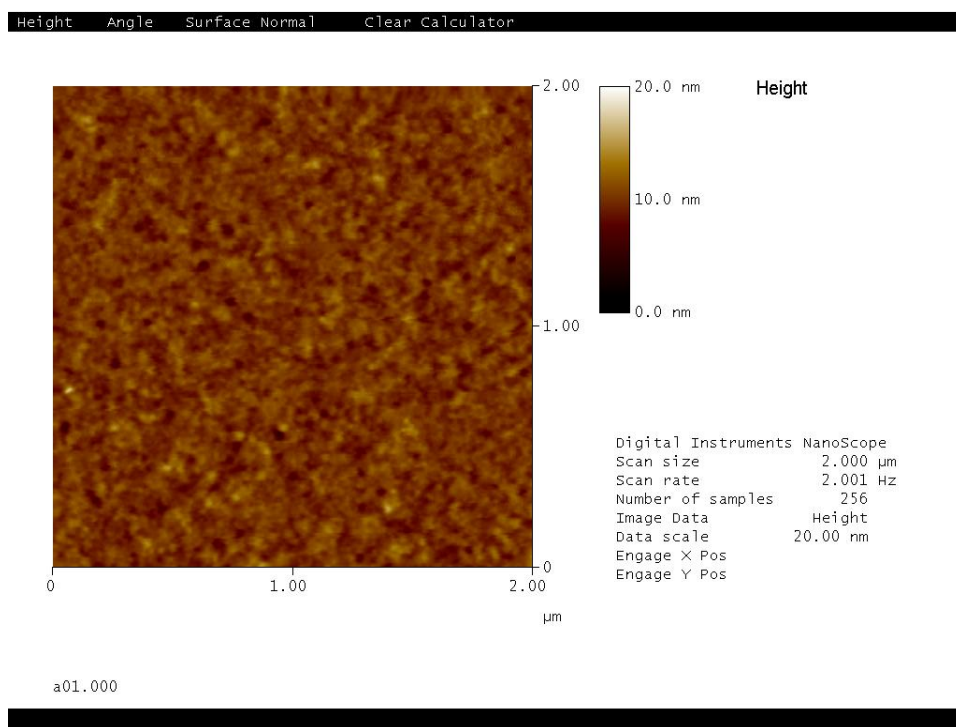


(c)



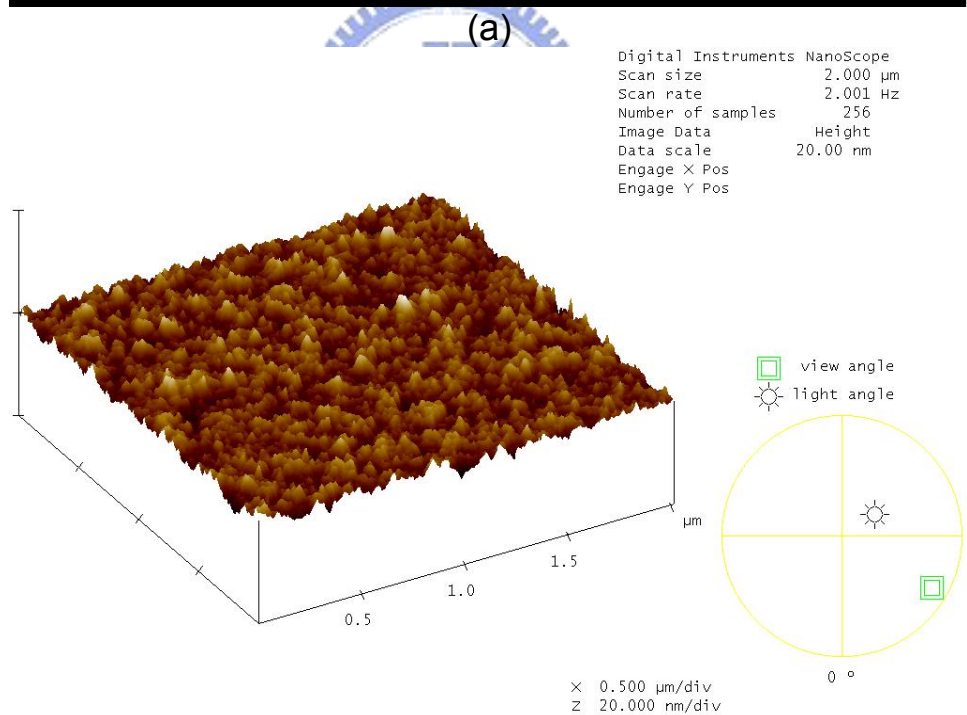
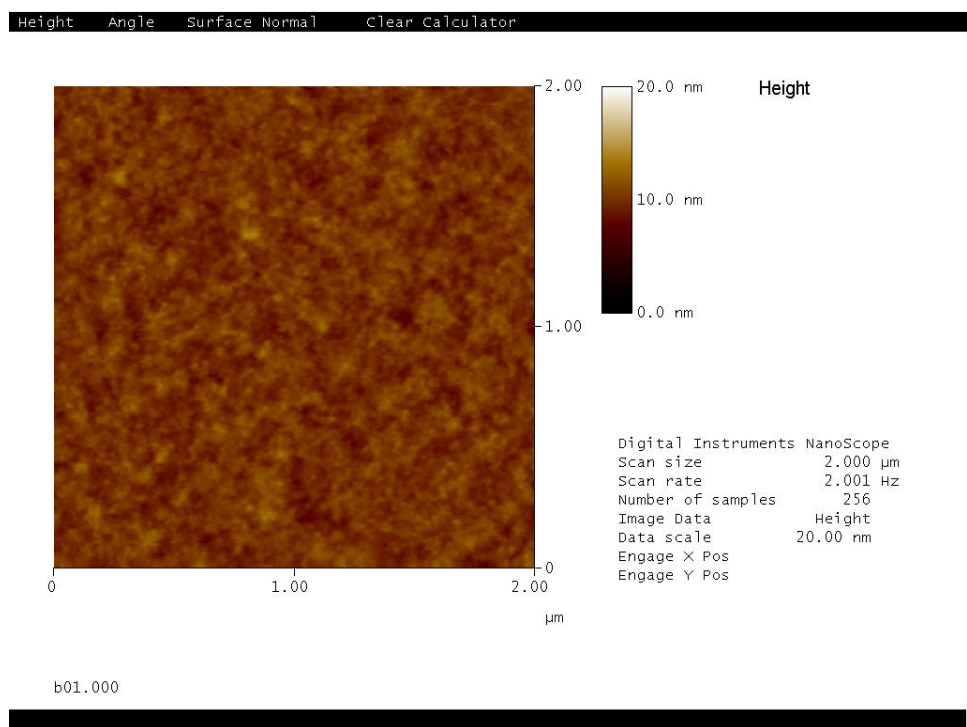
(d)

Figure2-11: Transfer characteristics  $I_s$  vs  $V_G$  and field-effect mobility of samples prepared from different solvent  
(a)  $W/L=10000/10\mu\text{m}$  (b)  $W/L=5000/10\mu\text{m}$  (c)  $W/L=1000/10\mu\text{m}$  (d)  $W/L=1000/50\mu\text{m}$



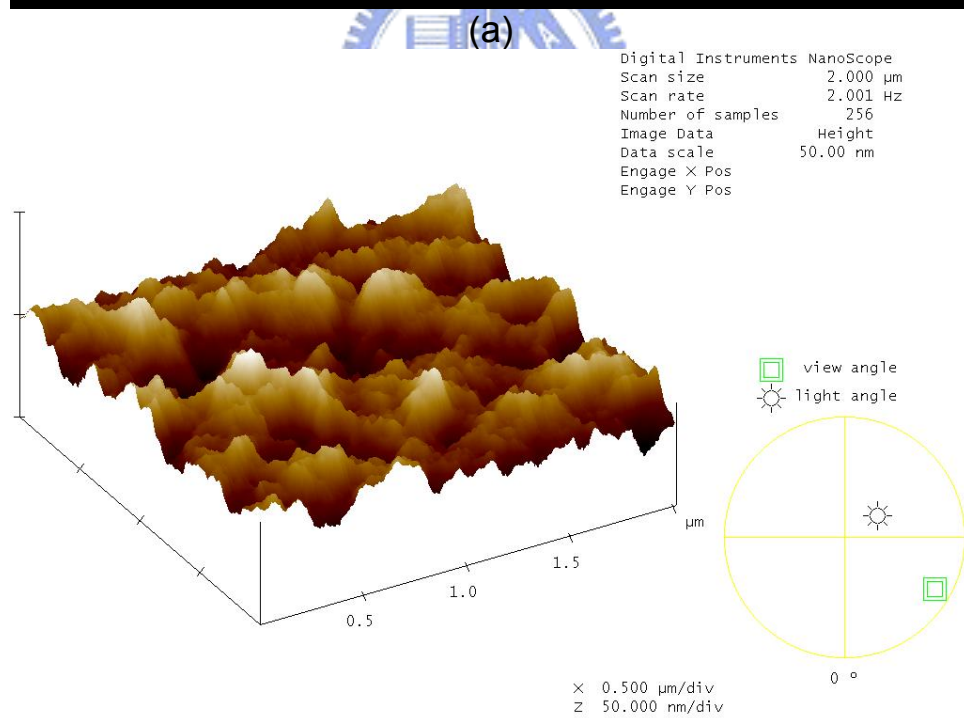
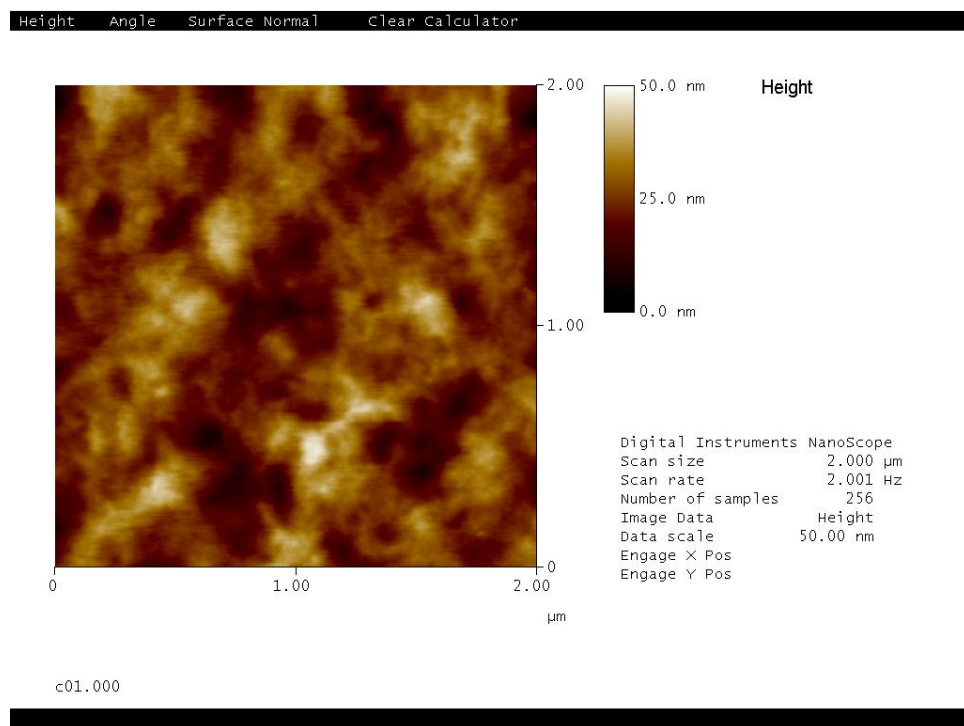
(b)

Figure 2-12: AFM micrograph of P3HT 0.1% in chloroform (a) top-view (b) high angle view

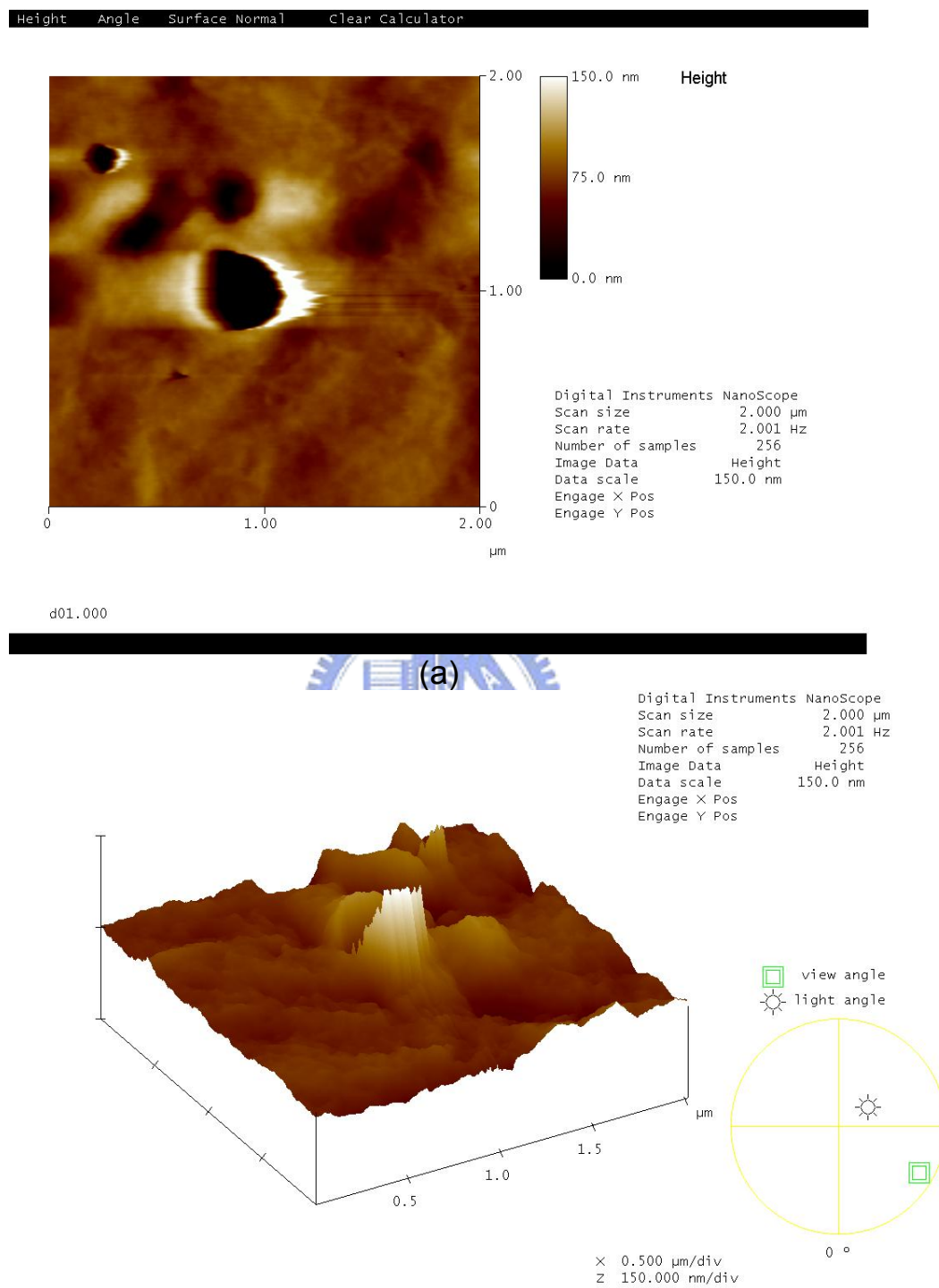


(b)

Figure 2-13: AFM micrograph of P3HT 0.3% in chloroform (a) top-view (b) high angle view

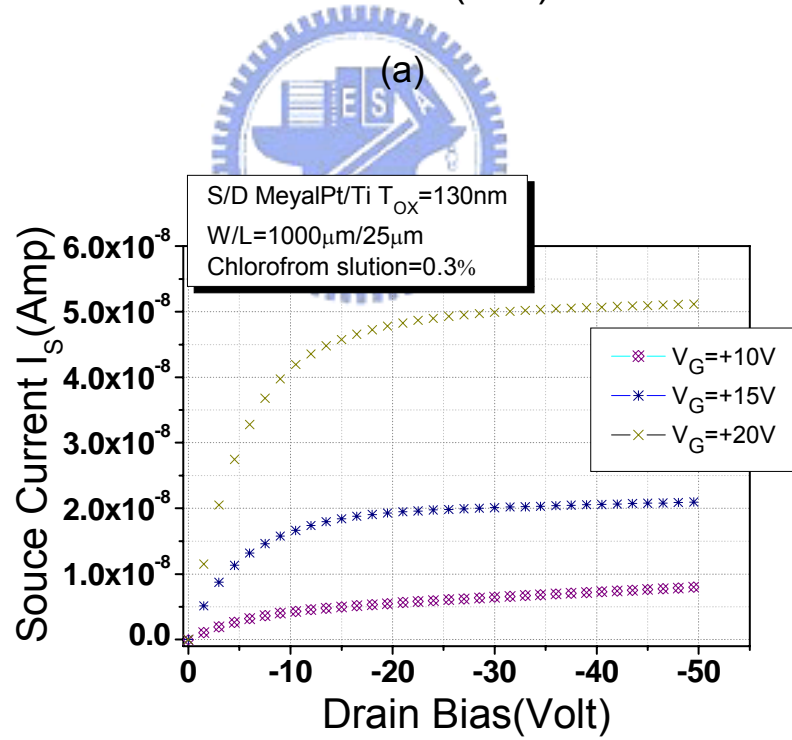
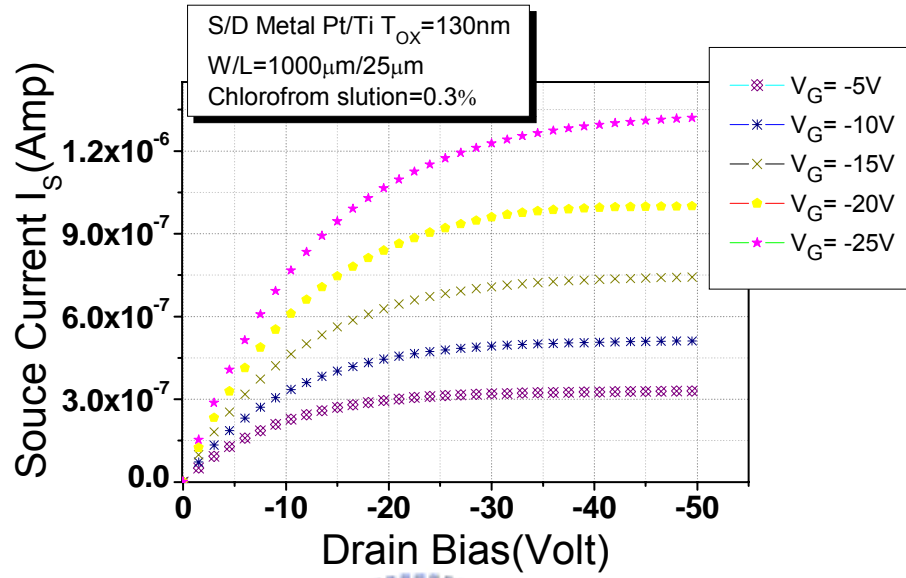


(b)  
 Figure 2-14: AFM micrograph of P3HT 0.8% in chloroform (a) top-view (b) high angle view



(b)  
 Figure 2-15: AFM micrograph of P3HT 2.0% in chloroform (a) top-view (b) high angle view

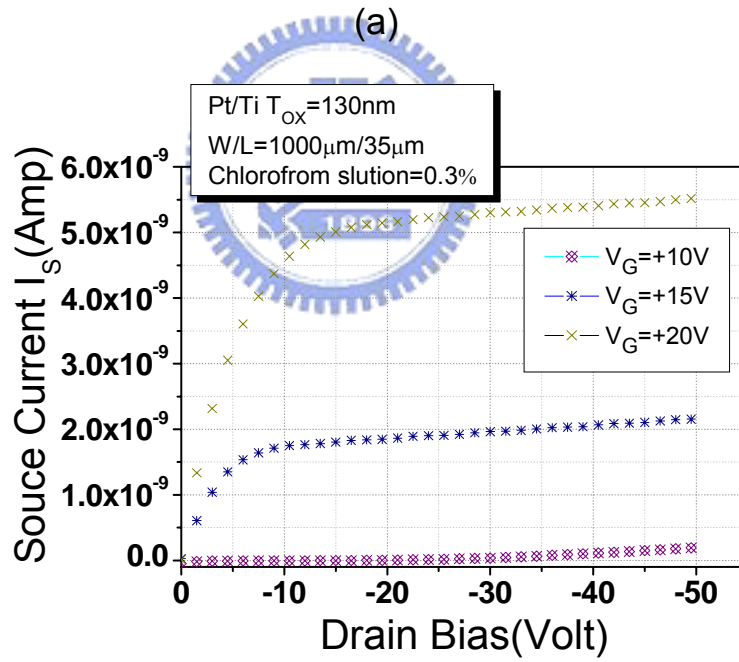
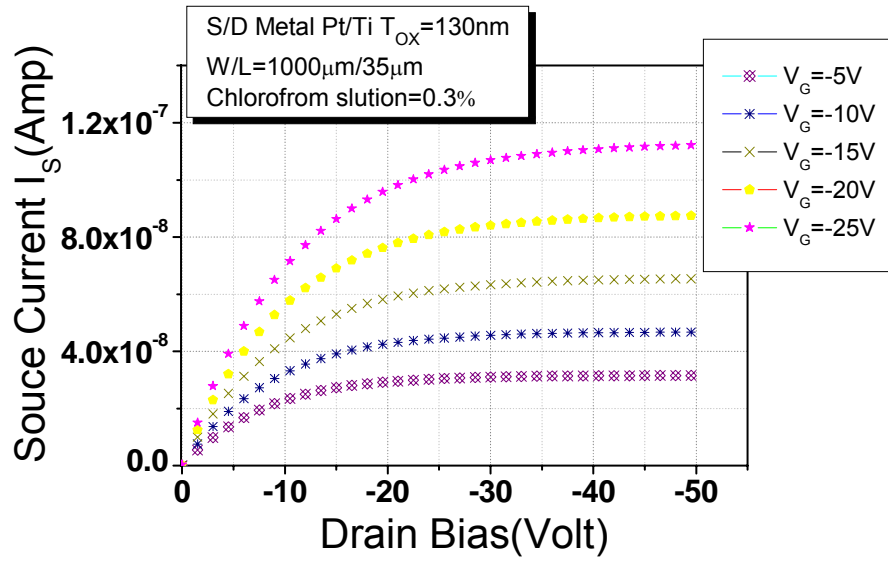




(b)

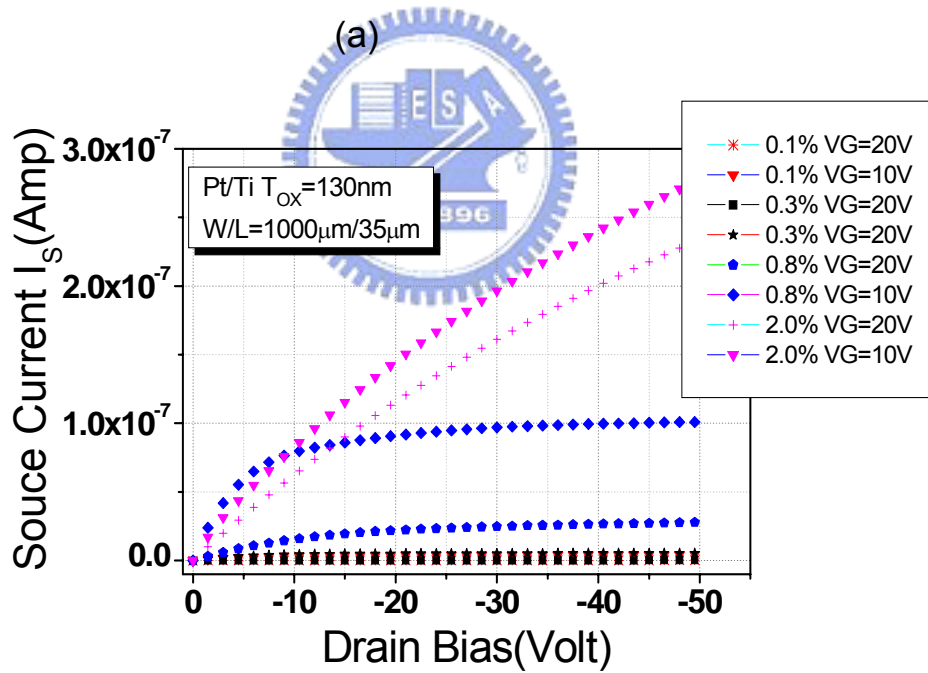
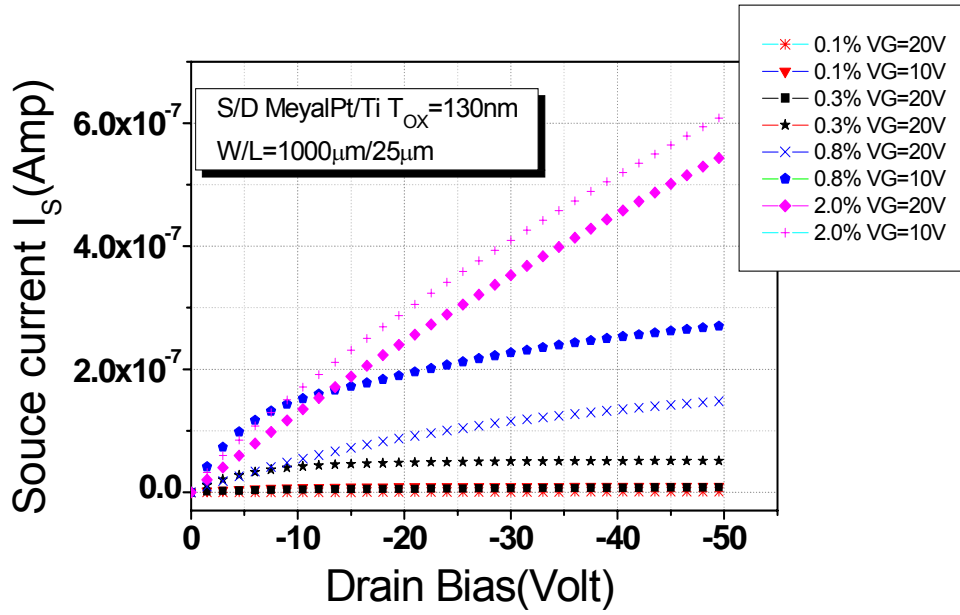
Figure 2-16:  $I_s$  versus  $V_D$  curve at different gate voltages (a) in the accumulation mode (b) in the depletion mode (W/L=1000/25 $\mu m$ )





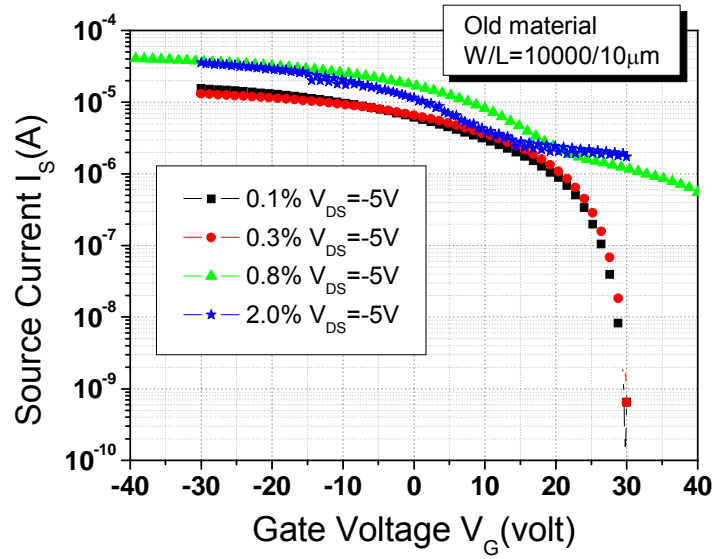
(b)

Figure2-17:  $I_s$  versus  $V_D$  curve at different gate voltages (a) in the accumulation mode (b) in the depletion mode ( $W/L=1000/35\mu\text{m}$ )

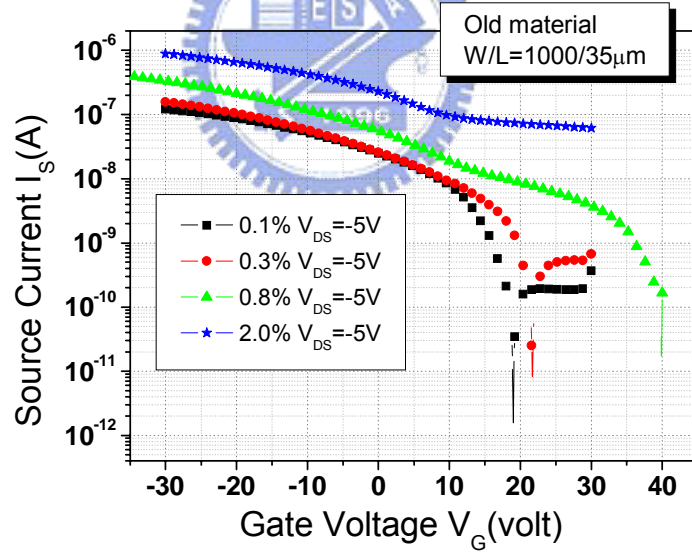


(b)

Figure 2-18:  $I_s$  versus  $V_D$  curve in the depletion mode as a function of weight concentration of P3HT in chloroform (a)  $W/L=1000/25\mu\text{m}$  (b)  $W/L=1000/35\mu\text{m}$



(a)



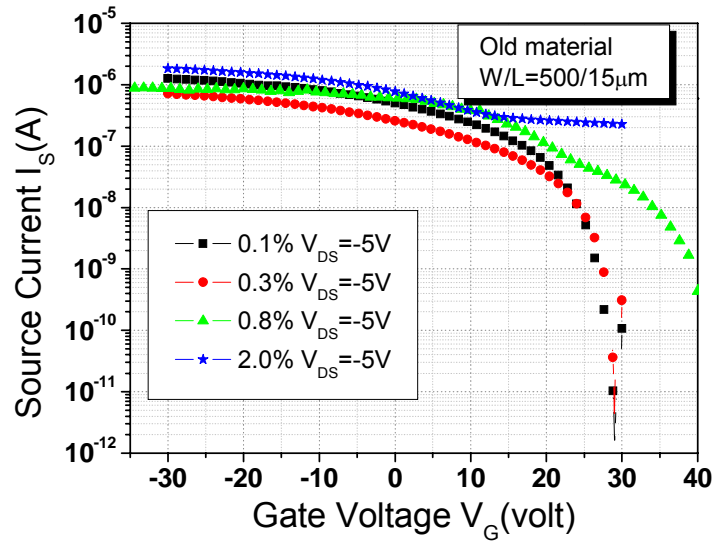
(b)

Figure2-19: Transfer characteristics  $I_s$  vs  $V_G$  as a function of weight concentration of P3HT in chloroform:

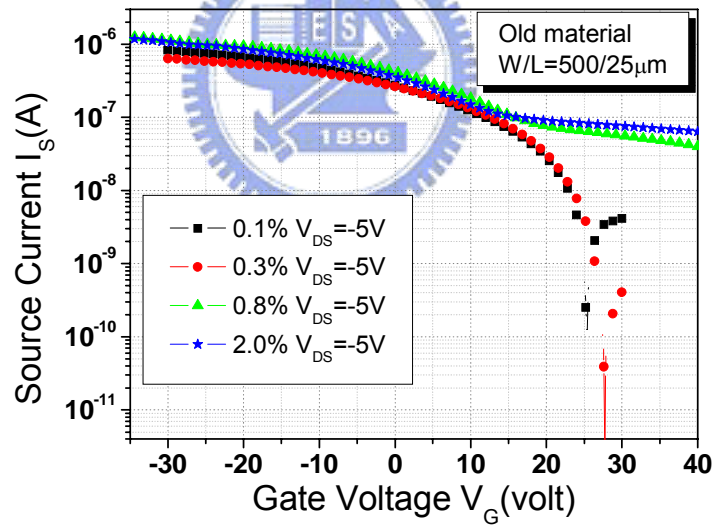
(a)W/L=10000/10 $\mu$ m (b)W/L=1000/35 $\mu$ m (c)W/L=500/15 $\mu$ m

(d)W/L=500/25 $\mu$ m

(continue)



(c)

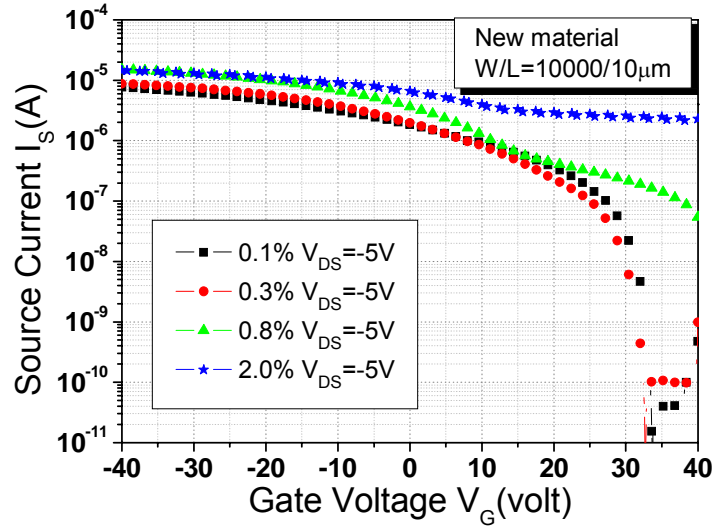


(d)

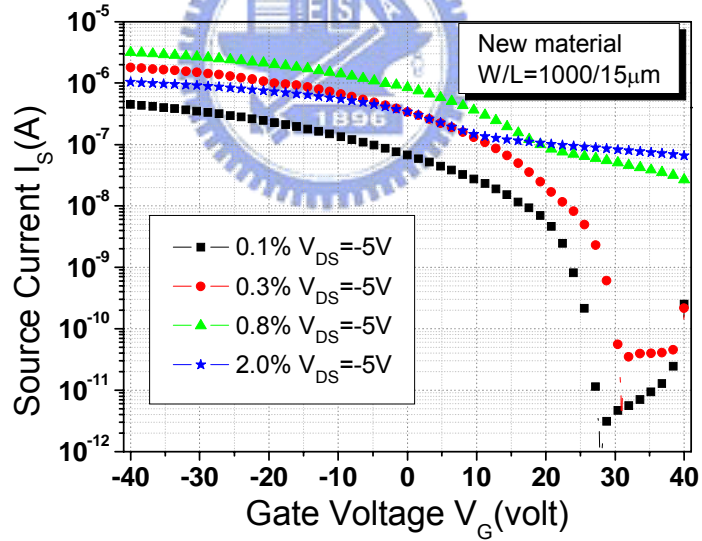
Figure2-19: Transfer characteristics  $I_s$  vs  $V_G$  as a function of weight concentration of P3HT in chloroform:

(a) W/L=10000/10 $\mu$ m (b) W/L=1000/35 $\mu$ m (c) W/L=500/15 $\mu$ m

(d) W/L=500/25 $\mu$ m



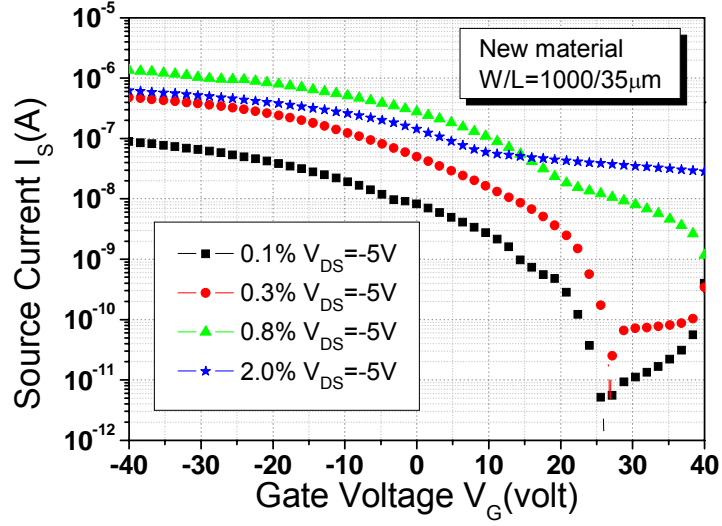
(a)



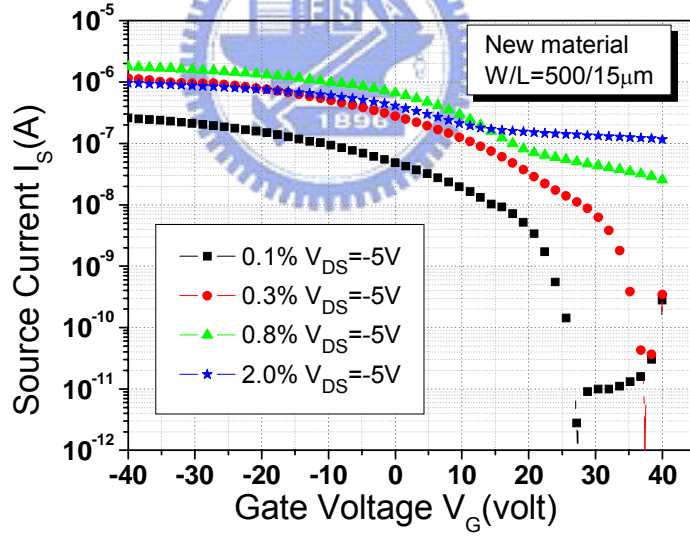
(b)

Figure2-20: Transfer characteristics  $I_s$  vs  $V_G$  as a function of weight concentration of P3HT in chloroform:

(a)  $W/L = 10000/10\mu\text{m}$  (b)  $W/L = 1000/15\mu\text{m}$  (c)  $W/L = 1000/35\mu\text{m}$   
(d)  $W/L = 500/15\mu\text{m}$  (e)  $W/L = 500/25\mu\text{m}$  (continue)



(c)



(d)

Figure2-20: Transfer characteristics  $I_S$  vs  $V_G$  as a function of weight concentration of P3HT in chloroform:

(a)  $W/L=10000/10\mu\text{m}$  (b)  $W/L=1000/15\mu\text{m}$  (c)  $W/L=1000/35\mu\text{m}$   
 (d)  $W/L=500/15\mu\text{m}$  (e)  $W/L=500/25\mu\text{m}$  (continue)

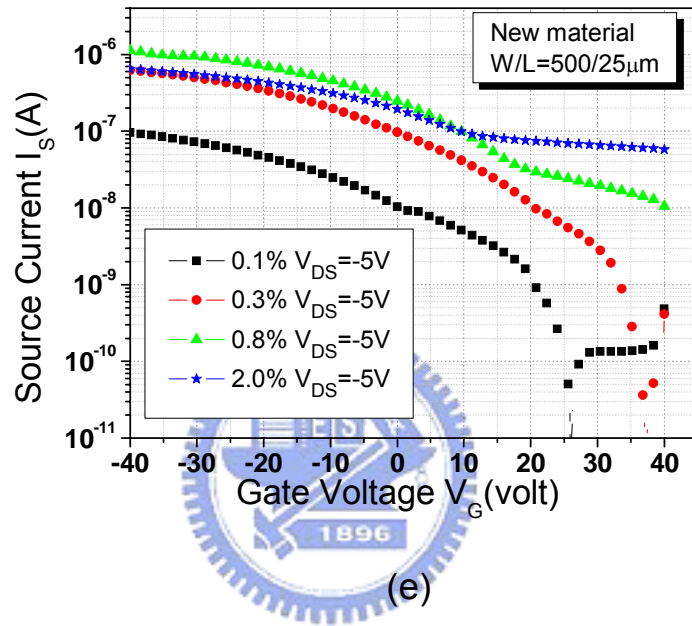


Figure2-20: Transfer characteristics  $I_s$  vs  $V_G$  as a function of weight concentration of P3HT in chloroform:  
 (a)  $W/L=10000/10\mu\text{m}$  (b)  $W/L=1000/15\mu\text{m}$  (c)  $W/L=1000/35\mu\text{m}$   
 (d)  $W/L=500/15\mu\text{m}$  (e)  $W/L=500/25\mu\text{m}$

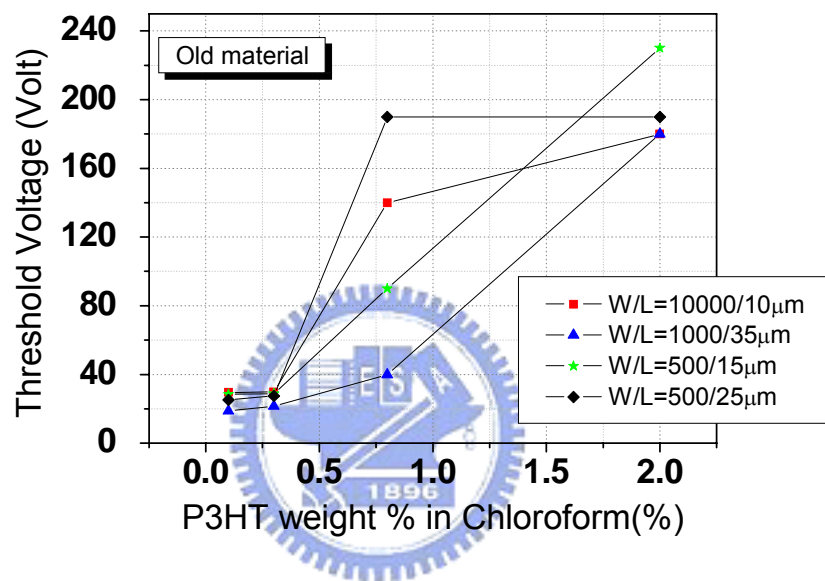
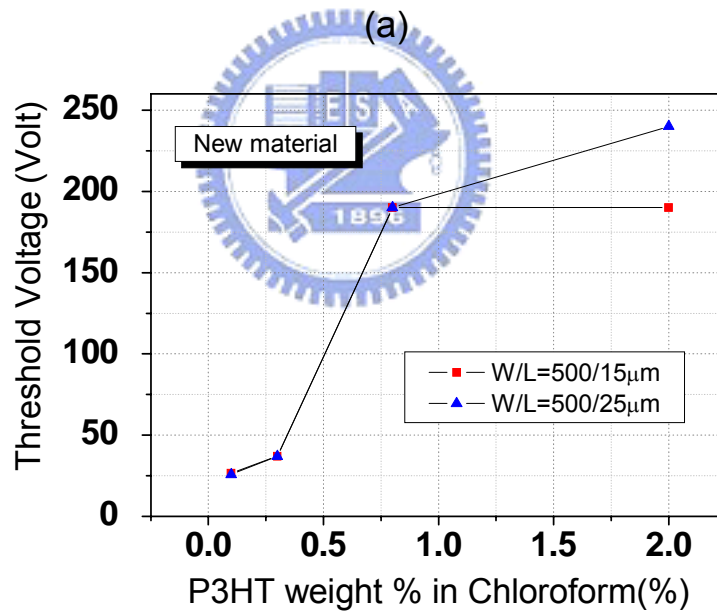
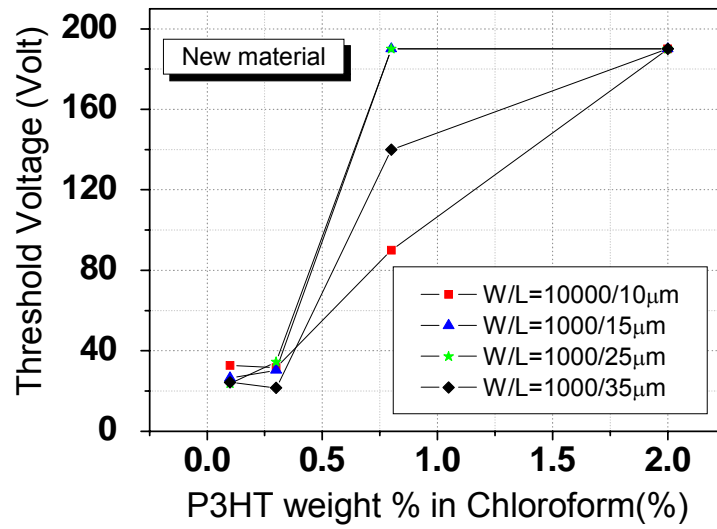


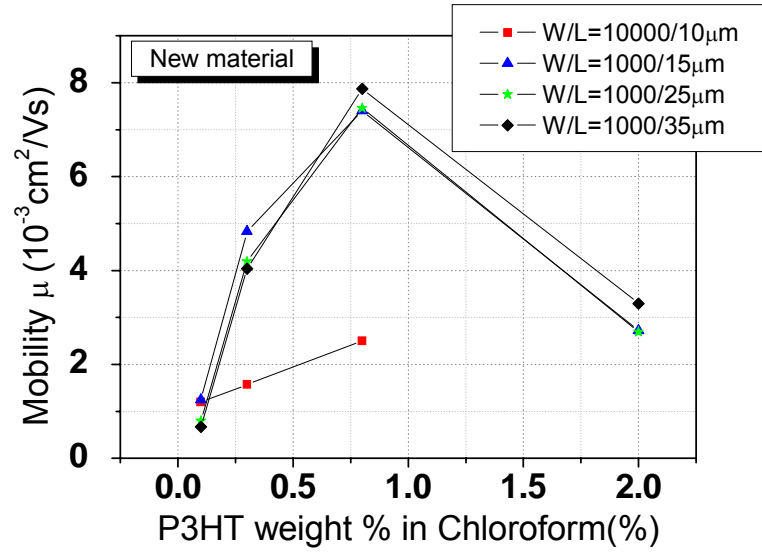
Figure2-21: Threshold voltage as a function of weight concentration of P3HT in chloroform



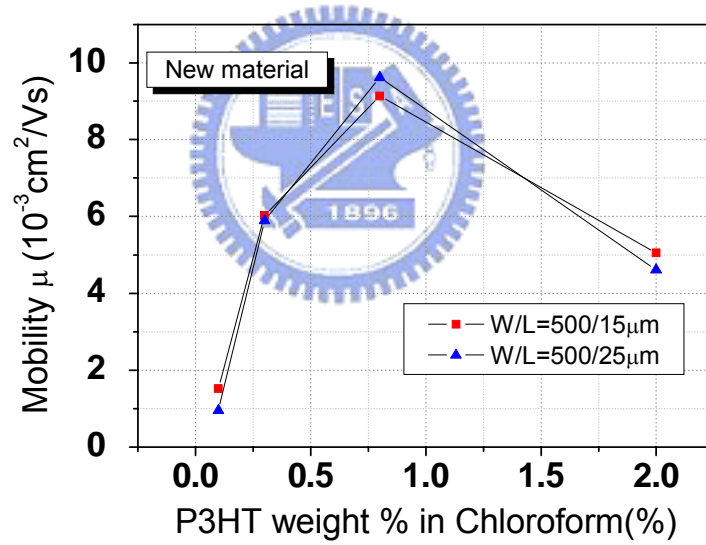


(b)

Figure2-22: Threshold voltage as a function of weight concentration of P3HT in chloroform: (a) inter-digital type (b) linear type

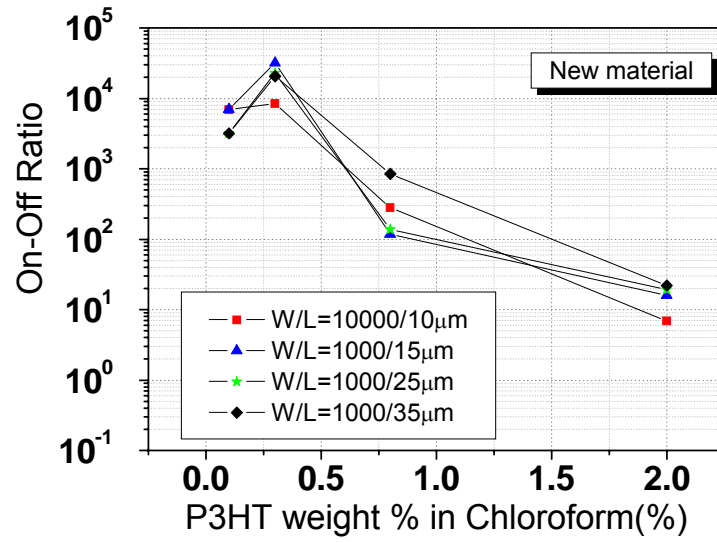


(a)

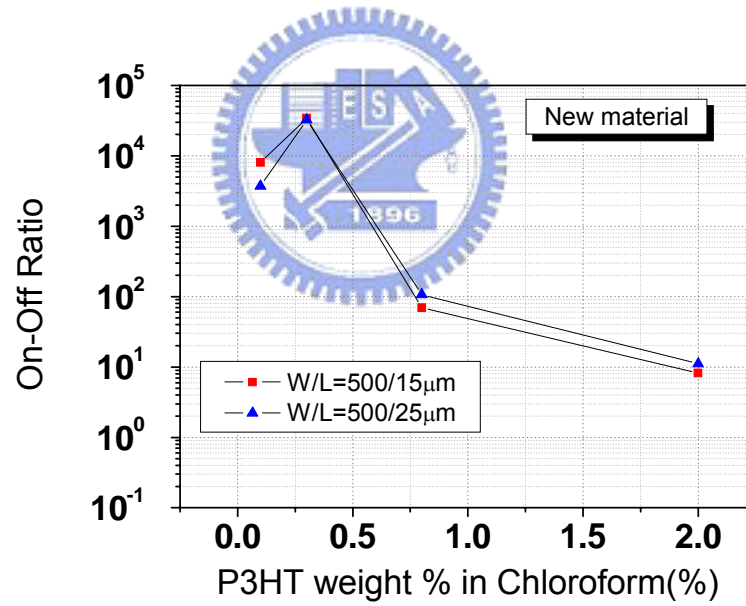


(b)

Figure2-23: Field-effect mobility in the linear regime as a function of weight concentration of P3HT in chloroform : (a) inter-digital type (b) linear type



(a)



(b)

Figure2-24: On-off ratio as a function of weight concentration of P3HT in chloroform : (a) inter-digital type (b) linear type

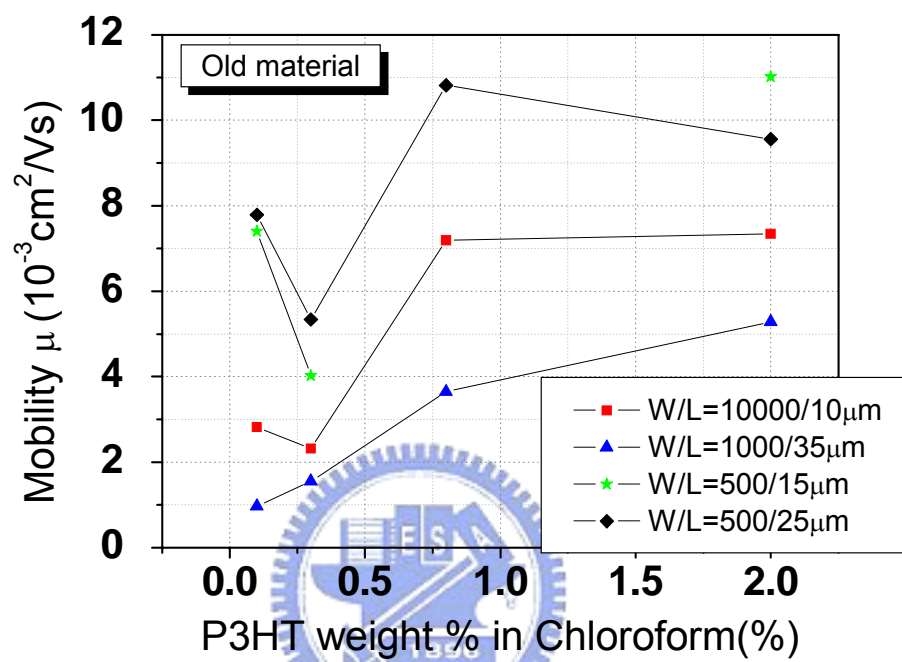


Figure2-25: Field-effect mobility in the linear regime as a function of weight concentration of P3HT in chloroform

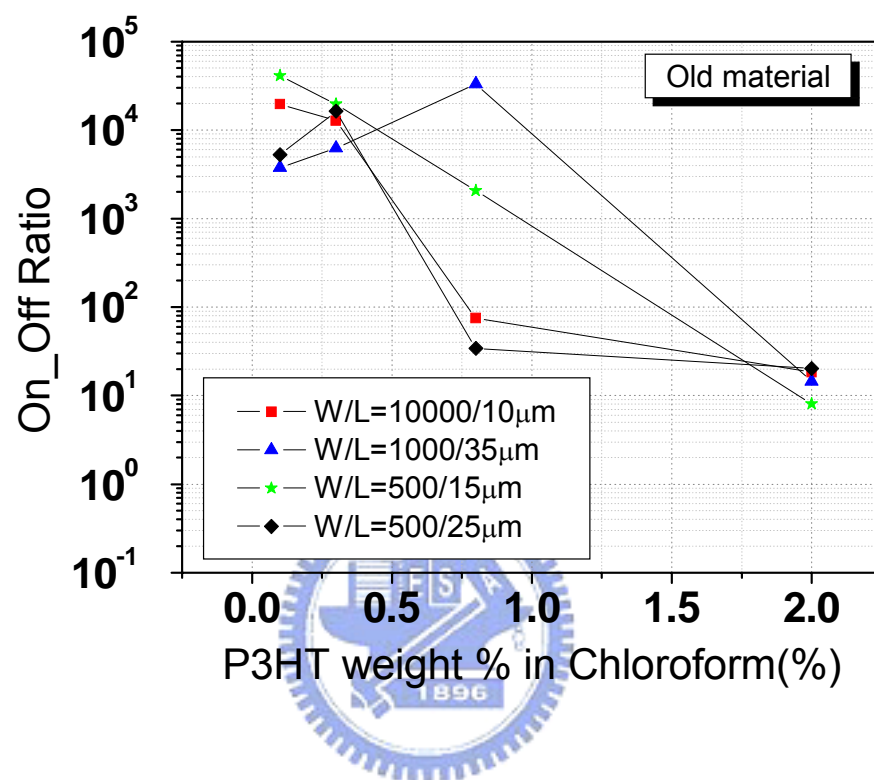


Figure2-26: On-off ratio as a function of weight concentration of P3HT in chloroform

W/L	$I_{NO}(\text{Amp})$	Off current(Amp)
W/L=10000/10 $\mu\text{m}$	1.00E-12	1.00E-09
W/L=5000/10 $\mu\text{m}$	1.00E-12	5.00E-10
W/L=1000/10 $\mu\text{m}$	1.00E-12	1.00E-10
W/L=1000/15 $\mu\text{m}$	1.00E-12	6.60E-11
W/L=1000/25 $\mu\text{m}$	1.00E-12	4.00E-11
W/L=1000/35 $\mu\text{m}$	1.00E-12	2.80E-11
W/L=1000/50 $\mu\text{m}$	1.00E-12	2.00E-11
W/L=500/10 $\mu\text{m}$	1.00E-12	5.00E-11
W/L=500/15 $\mu\text{m}$	1.00E-12	3.30E-11
W/L=500/25 $\mu\text{m}$	1.00E-12	2.00E-11
W/L=500/35 $\mu\text{m}$	1.00E-12	1.40E-11
W/L=500/50 $\mu\text{m}$	1.00E-12	1.00E-11
W/L=300/35 $\mu\text{m}$	1.00E-12	8.50E-12

Table2-1: The magnitude of off current with different channel length and different channel width

Entry	Solvent	Condition	Mobility (cm <sup>2</sup> /V s) <sup>a</sup>	On/off ratio <sup>b</sup>
1	THF	1	$6.2 \times 10^{-4}$	10
2	<i>p</i> -xylene	1	$1.9 \times 10^{-3}$	40
3		2	$1.9 \times 10^{-5}$	2
4	Toluene	1	$3.6 \times 10^{-3}$	10
5		2	$3.2 \times 10^{-3}$	25
6	Chlorobenzene	1	$4.7 \times 10^{-3}$	10
7		entry 6 condition 3	$4.7 \times 10^{-3}$	80
8		2	$6.9 \times 10^{-4}$	72
9	1,1,2,2-tetrachloroethylene	1	$6.8 \times 10^{-3}$	35
10	1,1,2,2-tetrachloroethane	1	$2.4 \times 10^{-2}$	6
11		entry 10 condition 4	$1.4 \times 10^{-2}$	35
12		entry 11 condition 5	$3.3 \times 10^{-3}$	15
13	Chloroform	2	$9.2 \times 10^{-3}$	80
14		1	$4.5 \times 10^{-2}$	340
15		entry 14 condition 3	$2.1 \times 10^{-2}$	9000

Table2-2: Field-effect mobility and ON/OFF ratios of samples prepared from different conditions Condition 1:cast, vacuum pumped for 24 h; condition 2: spin-coated; condition 3: treated with NH<sub>3</sub> for 10 h; condition 4:heated to 100 °C under N<sub>2</sub> for 5 min; condition 5: heated to 150 °C under N<sub>2</sub> for 35 min.

Weight concentration of P3HT in chloroform	Room mean square of P3HT film
0.1%	1.075nm
0.3%	0.824nm
0.8%	6.425nm
2.0%	23.927nm

Table 2-3: Room mean square of P3HT film as a function of weight concentration of P3HT in chloroform



## Chapter 3

# Reliability Characteristics of P3HT OTFTs

### 3.1 Introduction

Organic electronics has been a subject of increasing interest. One of the materials used for organic thin film transistors is poly (3-hexylthiophenes), P3HT. In the last few years, the main object on P3HT OTFTs is to improve the carrier mobility. Therefore, the performance of P3HT OTFTs has improved remarkably through optimization of process parameters and is comparable to amorphous silicon thin film transistors (a-TFTs) [5], [14]. Besides, OTFTs exhibit great potential for special applications such as flexible display, RF tags, and smart cards. However, comparing to inorganic transistors, organic devices show poor stability with time and different environmental ambient such as nitrogen, oxygen or moisture may affect the performance of organic devices [13], [15]. Therefore, stability issues of these organic devices are another challenge which should be kept in mind.

Several reports have indicated that P3HT OTFTs are sensitive to the presence of oxygen [13], [15]. Additionally, in our previous work we also observed obvious degradation of threshold voltage, mobility or ON/OFF current ratios of OTFTs after exposing devices in the air for several days. Thus, we treated OTFTs with O<sub>2</sub>, N<sub>2</sub> and H<sub>2</sub>O deliberately to clarify the correlation between electrical characteristics of P3HT OTFTs and the exposed ambient.

For organic devices, although there have been tremendous progress on prerequisites such as device fabrication and material optimization, studies of the operational lifetime have been scarce up to now [17]. Therefore, we investigate the behavior of P3HT OTFTs during stress

measurements.

## **3.2 The Effect of P3HT OTFTs Stored in Vacuum**

### **3.2.1 Experiment Detail**

As discussed in chapter 2, a good solvent to dissolve P3HT is chloroform and the optimal weight percentage of P3HT is 0.3%. Afterward, we used this condition to deposit organic semiconductor layer in the following experiments. The other detailed process flow of P3HT OTFTs fabrication was described in section 2.3.1. Notably, all of the processing steps were carried out under clean room conditions in the presence of ambient oxygen and relative humidity about 60%.

In this section, we prepared two samples. One was measured immediately in the air with semiconductor parameter analyzer HP4156 after the P3HT OTFTs were fabricated; the other one was stored in a high vacuum chamber with base pressure of  $1 \times 10^{-6}$  torr for 2 days after P3HT OTFT was fabricated, and then the sample was measured immediately in the air after being stored in vacuum.

### **3.2.2 Results and Discussion**

Several reports have indicated that P3HT polymer is sensitive to the presence of oxygen [18], [19]. It has been shown that oxygen is a kind of dopant for P3HT polymer. Moreover, if there are oxygen atoms in P3HT polymer, carriers scattering would occur and the field-effect mobility would decrease. Since our P3HT OTFTs were not fabricated in vacuo, the influence of oxygen to the characteristics of organic transistors is inevitable. Therefore, we employ vacuum storage to check the significance of oxygen auto-doping and whether the vacuum storage can

eliminate the effect of oxygen doping or not.

As can be seen from **Table3-1~Table3-3** and **Figure3-1**, the field-effect mobility of devices were further improved by storing the sample for 2days in high vacuum chamber before electrical measurements as the maximum field-effect mobility reaches  $10^{-2} \text{ cm}^2/\text{Vs}$ . Additionally, threshold voltage of devices were greatly decreased and ON-OFF ratios were improved by storing the sample for 2days in high vacuum chamber before electrical measurements. The above results are in consistent with those reported in literatures [20], [21] and verified that oxygen does affect the electrical characteristics of P3HT OTFTs.

Based on the above observation, our OTFT devices would be stored in high vacuum chamber for 2 days before electrical measurement in order to acquire a stable P3HT polymer film.

### 3.3 The Variation of Threshold Voltage and Field-Effect Mobility during the Electrical Measurement

#### 3.3.1 Experiment Detail

After the P3HT OTFTs had been fabricated, devices would be measured by Agilent 4156c within 60 minutes. In order to observe the variation of field-effect mobility and threshold voltage during the electrical measurement, we measured the same device repeatedly after 10sec, 30sec, 80sec, 180sec, 380sec, 880sec, 1880sec, 3880sec and 8880sec.

#### 3.3.2 Results and Discussion

**Fig3-2** indicates that the variation of field-effect mobility and threshold voltage within 120min of measurement. For first 60 min, the variation of field-effect mobility is insignificant,

which varies from  $1.79 \times 10^{-3} \text{cm}^2/\text{Vs}$  to  $1.90 \times 10^{-3} \text{cm}^2/\text{Vs}$ . After 60 min, the variation of field-effect mobility is still unapparent that ranges from  $1.90 \times 10^{-3} \text{cm}^2/\text{Vs}$  to  $2.07 \times 10^{-3} \text{cm}^2/\text{Vs}$ . The field-effect mobility slightly increases around 10%, because the traps at the polymer/insulator interface were filled after measurement. In contrast, for the first 60 min of measurement, the threshold voltage shifts obviously that varies from 24volt to 28volt. After 60 min, the threshold voltage shift becomes more significant that rises from 28volt to 35volt. Why would the threshold voltage drastically increase by an amount of 42% within just two hours? In order to investigate that which factor could lead to such a large threshold voltage shifts during measurement, we design some experiments and the detail will be described in section 3.4 and 3.5.

### **3.4 The Effect of P3HT OTFTs under O<sub>2</sub>, N<sub>2</sub>, and H<sub>2</sub>O Treatment**

#### **3.4.1 Experiment Detail**

There are two possible factors for resulting in drastic threshold voltage shifts. One is environmental influences such as nitrogen, oxygen or moisture. The other is applied biasing voltages during measurements. In this section, we will first discuss the environmental influences.

After the P3HT OTFTs had been fabricated following the process flow as described in section 2.3.1, they were treated with different conditions. Condition one: the samples were put in a furnace with oxygen flow rate of 5 liter/min at room temperature for 0 hour, 3 hours, 8hours before electrical measurement; condition two: the samples were put in a furnace with nitrogen flow rate of 5 liter/min at room temperature for 0 hour, 3 hours, 8hours before electrical measurement; condition three: the samples were immersed in water at room temperature for 0 hour, 3 hours, 8hours before electrical measurement. Next, the variation of electrical properties including field-effect mobility and threshold voltage were investigated.

### 3.4.2 Results and Discussion

**Fig3-3** delineates the threshold voltage shift and the variation of field-effect mobility under different treatment. Under  $H_2O$  treatment, the threshold voltage shift and the variation of field-effect mobility are weakly dependent on the treatment time. Therefore, it was proved that humidity will not affect the performance of P3HT OTFTs.

Several reports have indicated that P3HT polymer is sensitive to the presence of oxygen [18], [19]. It has been shown that oxygen is a kind of dopant for P3HT polymer. Therefore, there would be two effects on P3HT polymer. On one hand oxygen in the P3HT polymer would cause an increase to the conductivity of P3HT polymer and the bulk leakage current. On the other hand oxygen in the P3HT polymer would cause an increase to carrier scattering in channel. For electrical characteristics of P3HT OTFTs, the bulk leakage current increasing would lead to an overestimation of field-effect mobility but actually oxygen in P3HT polymer would lead to field-effect mobility decreasing.

Under  $N_2$  treatment, the field-effect mobility of devices was further improved and dependent on  $N_2$  treatment time; the threshold voltage shift is insignificant. Since the deposition process of the polymer semiconductor was carried out under ambient, easily oxidized segments in the polymer layer allow the oxygen to act as dopants increasing the channel conductance and to act as trap centers decreasing the carrier mobility. The  $N_2$  treatment was performed for the suppression of carrier scattering. It is well documented that oxidized and conductive polymer reverts to its neutral insulating states [22], [23]. As a result, the polymer semiconductor turns out so insulating that the unexpected factors may be constrained causing good electrical properties.

Under  $O_2$  treatment, the threshold voltage increased in the first 3 hours. Because the diffusion of oxygen into polymer bulk caused an increase to the conductivity of P3HT polymer

and the bulk leakage current, the device were hardly turned off. However, due to the bulk leakage current, the extraction of field-effect mobility was overestimated. Next, the threshold voltage still increased but the field-effect mobility decreased after 3 hours. Because diffusion of oxygen caused serious carriers scattering, the channel current drastically decreased. Therefore, the bulk current dominated the electrical characteristics of P3HT OTFTs and so the field-effect mobility decreased.

### 3.5 Stress Measurement of P3HT OTFTs

#### 3.5.1 Experiment Detail

Stress measurements were performed with an Agilent 4156c semiconductor parameter analyzer. The samples were kept in the air and in the dark at room temperature (25 °C). In order to obtain the insight into the stress behavior of P3HT OTFTs, we performed four different measurements: (1) a constant gate bias stress of -25 V was applied; the stress time was individually 10sec, 20sec, 50sec, 100sec, 200sec, 500sec, 1000sec, 2000sec and 5000sec. After each stress period, the  $I_D - V_G$  curves of OTFTs were measured. (2) a constant gate bias stress of +25 V was applied; the stress time was individually 10sec, 20sec, 50sec, 100sec, 200sec, 500sec, 1000sec, 2000sec and 5000sec. After each stress period, the  $I_D - V_G$  curves of OTFTs were measured. (3) no gate bias stress was applied, but the  $I_D - V_G$  characteristics of OTFTs were measured at 10sec, 20sec, 50sec, 100sec, 200sec, 500sec, 1000sec, 2000sec and 5000sec. (4) a negative gate bias of -25V was applied for 10sec and then the I-V characteristics of P3HT OTFTs were measured; next, a positive gate bias of +25V was applied for another 10sec and then the I-V characteristics of P3HT OTFTs were measured again. The same stress measurements were performed iteratively with various stress time for 20sec, 50sec, 100sec, 200sec, 500sec, 1000sec and 2000sec.

### 3.5.1 Results and Discussion

The experiment condition (3) is a control condition. For experiment condition (1), the field-effect mobility was  $1.03 \times 10^{-3} \text{ cm}^2/\text{Vs}$  before stress and was  $1.04 \times 10^{-3} \text{ cm}^2/\text{Vs}$  after stress with a negative gate bias of -25V. Therefore, the field-effect mobility was weakly dependent on the negative bias stress. Next, **Fig3-5** shows the transfer characteristics  $I_S$  vs.  $V_G$  of OTFT after a series of negative gate bias stress for various time. It was observed that the negative bias stress causes a negative threshold voltage shift. This effect was attributed to the polarization phenomenon in the P3HT polymer. When a negative bias was applied to the gate electrode, the electric field forces the dipoles to rearrange in the same direction, as shown in **Fig3-9(a)**. The well-arranged dipole moments induce a polarized electric field with a direction as shown in **Fig3-9(b)**. The polarized electric field prevents the free holes from accumulating at the P3HT/SiO<sub>2</sub> interface. Therefore, the device was easily turned off and the threshold voltage would decrease.

For experiment condition (2), the field-effect mobility was  $3.18 \times 10^{-3} \text{ cm}^2/\text{Vs}$  before stress and was  $3.28 \times 10^{-3} \text{ cm}^2/\text{Vs}$  after stress with a negative gate bias of +25V. Therefore, the field-effect mobility was weakly dependent on the positive bias stress. Next, **Fig3-6** shows the transfer characteristics  $I_S$  vs.  $V_G$  of OTFT after a series of positive gate bias stress for different time. It was observed that positive bias stress causes a positive threshold voltage shift. This effect was owing to the polarization effect in the P3HT polymer. When a positive bias was applied to the gate electrode, the electric field forces the dipoles to rearrange in the same direction, as shown in **Fig3-10(a)**. The well-arranged dipole moments induce a polarized electric field with a direction as shown in **Fig3-10(b)**. The polarized electric field enhances the free holes to

accumulate at the P3HT/SiO<sub>2</sub> interface. Therefore, the device was easily turned ON and the threshold voltage would increase. **Fig3-7** shows the results of experiment condition (2).

For the fourth series measurement, the polarization effect in the P3HT polymer was significant, as shown in **Fig3-8**.

### 3.6 Summary

Given the sensitivity of P3HT to oxygen absorbed during the fabrication process, it is expected that vacuum and N<sub>2</sub> treatments can be used to recover some of the lost performance through vacuum-induced expulsion of absorbed oxygen.

The threshold voltage shift of OTFTs with P3HHT as active material has been studied from our experiments. There are two elements for resulting in the threshold voltage shift. One is the diffusion of oxygen atoms into P3HT polymer; the other is the electric field of the polarization effect in the P3HT polymer.

Under O<sub>2</sub> treatment, since the diffusion of oxygen into P3HT polymer causes an increase to the conductivity of P3HT polymer and bulk leakage current, the device was hardly turned off. Therefore, the threshold voltage shift is dependent on O<sub>2</sub> treatment time. Nevertheless, the variation of field-effect mobility increases in the first 3 hours O<sub>2</sub> treatment, and then it decreases after 3 hours O<sub>2</sub> treatment. The phenomenon is owing to bulk leakage current. Due to the bulk leakage current, the extraction of field-effect mobility was overestimated in the first 3 hours. However, after 3 hours O<sub>2</sub> treatment oxygen continues diffusing into P3HT polymer, and it would degrade P3HT polymer characteristics and cause serious carriers scattering. Therefore, the field-effect mobility decreased after 3 hours O<sub>2</sub> treatment.

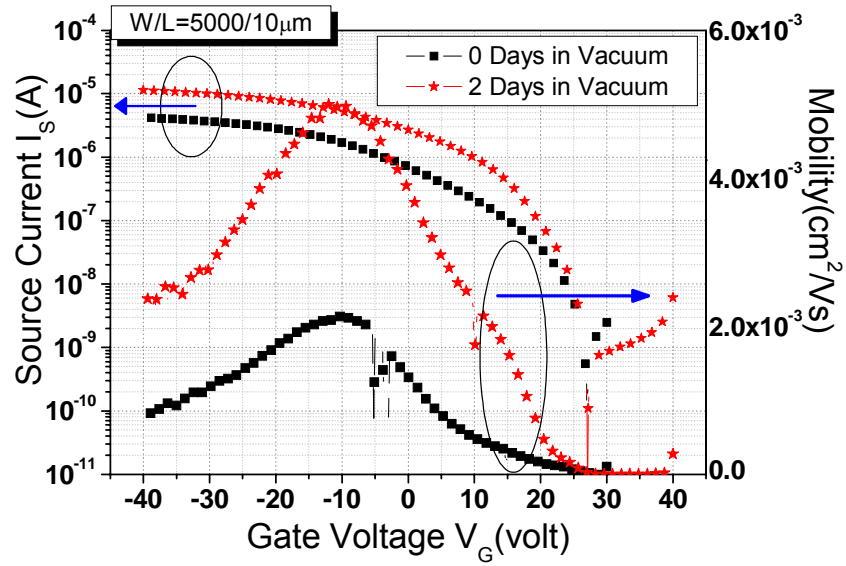
Under stress measurement, the threshold voltage shift is dependent on the polarity of gate bias. It was found that positive bias stress causes a positive threshold voltage shift and negative



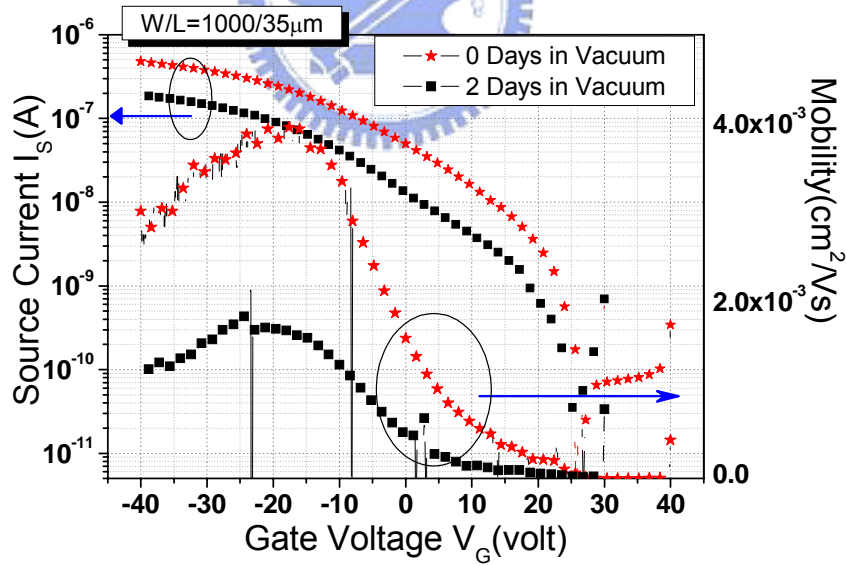
bias stress causes a negative threshold voltage shift. Nevertheless, the variation of field-effect mobility was independent on the polarity of gate bias.

Additionally, it was proved that humidity will not affect the performance of P3HT OTFTs.





(a)



(b)

Figure 3-1: Transfer characteristics  $I_S$  vs  $V_G$  and field-effect mobility of samples measured after 0 or 2 days in vacuum  
 (a) W/L=5000/10 $\mu$ m (b) W/L=1000/35 $\mu$ m (c) W/L=500/35 $\mu$ m (continue)

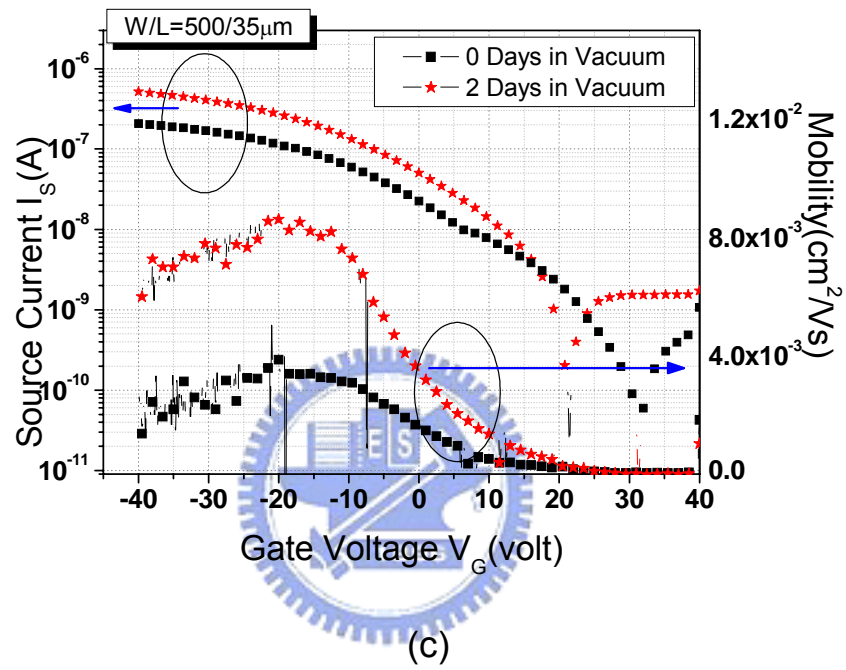


Figure3-1: Transfer characteristics  $I_S$  vs  $V_G$  and field-effect mobility of samples measured after 0 or 2 days in vacuum  
(a) W/L=5000/10 $\mu$ m (b) W/L=1000/35 $\mu$ m (c) W/L=500/35 $\mu$ m

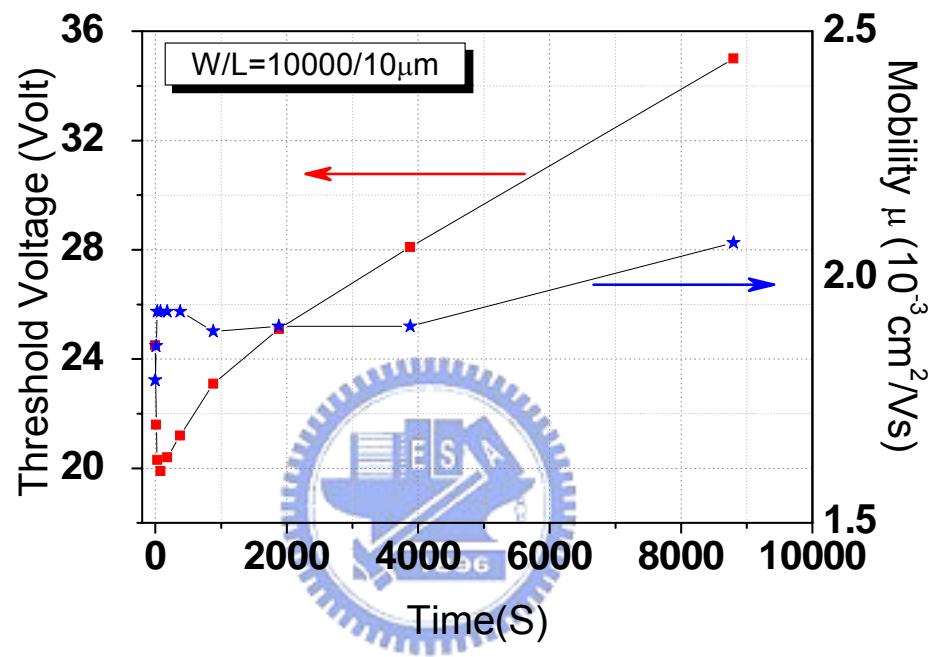
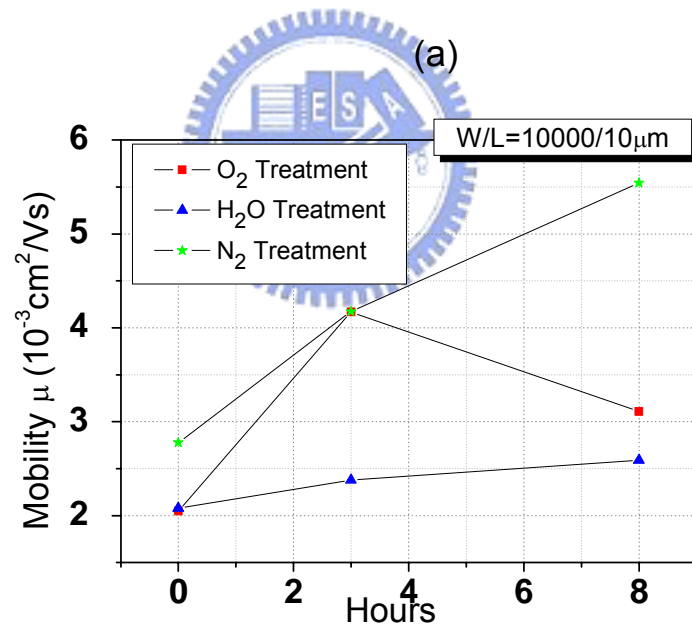
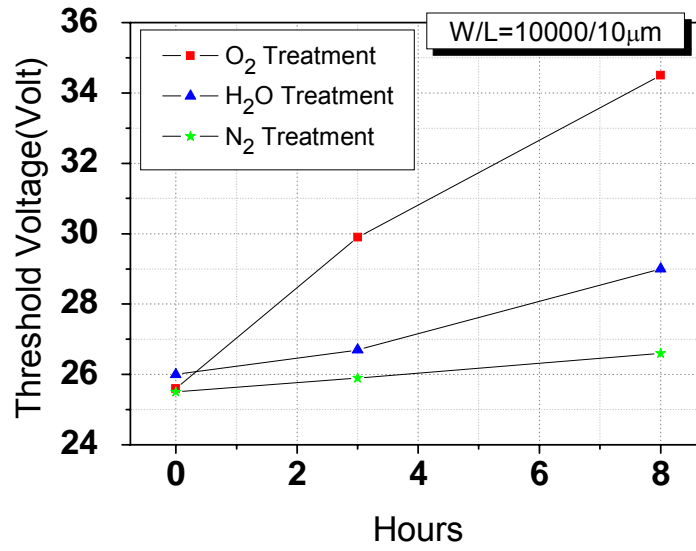


Figure3-2: The variation of field-effect mobility and threshold voltage within 120min of measurement



(b)

Figure3-3: (a) The threshold voltage shift and (b) the variation of field-effect mobility under different treatment.

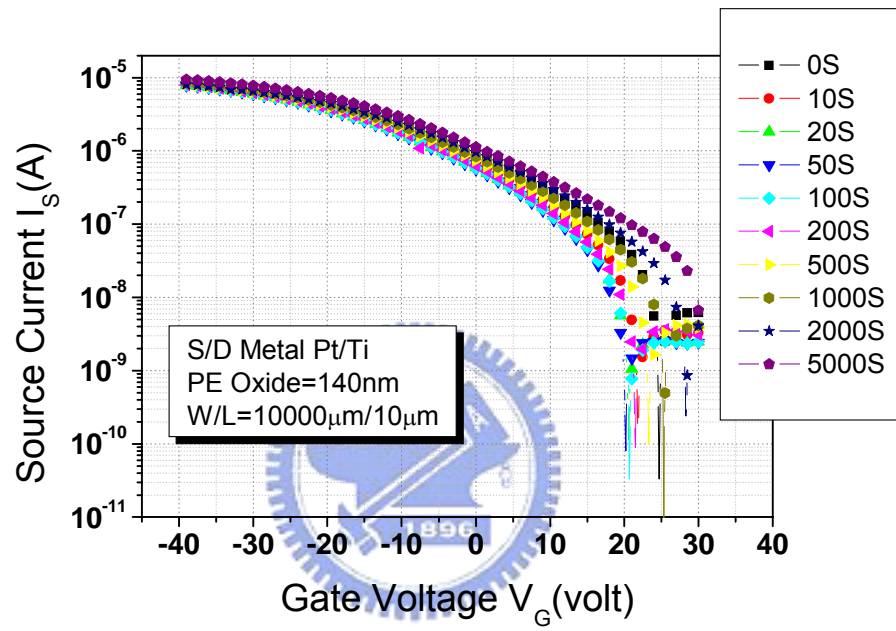


Figure3-4: Transfer characteristics  $I_s$  vs  $V_G$  of OTFT after 0sec, 10sec, 20sec, 50sec, 100sec, 200sec, 500sec, 1000sec, 2000sec and 5000sec

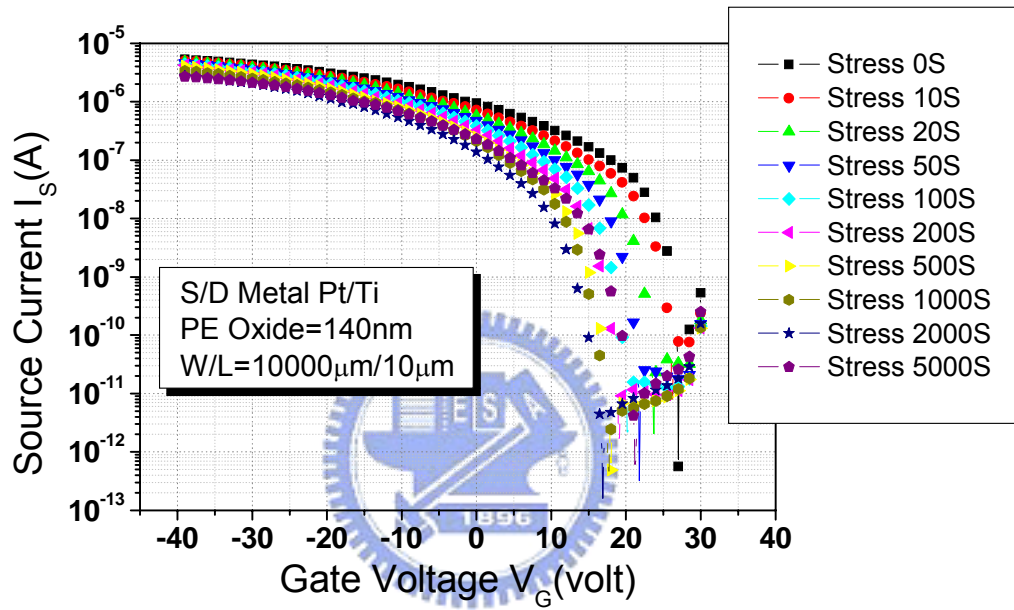


Figure3-5: Transfer characteristics  $I_s$  vs  $V_G$  of OTFT after 0sec, 10sec, 20sec, 50sec, 100sec, 200sec, 500sec, 1000sec, 2000sec and 5000sec -25V gate bias stress

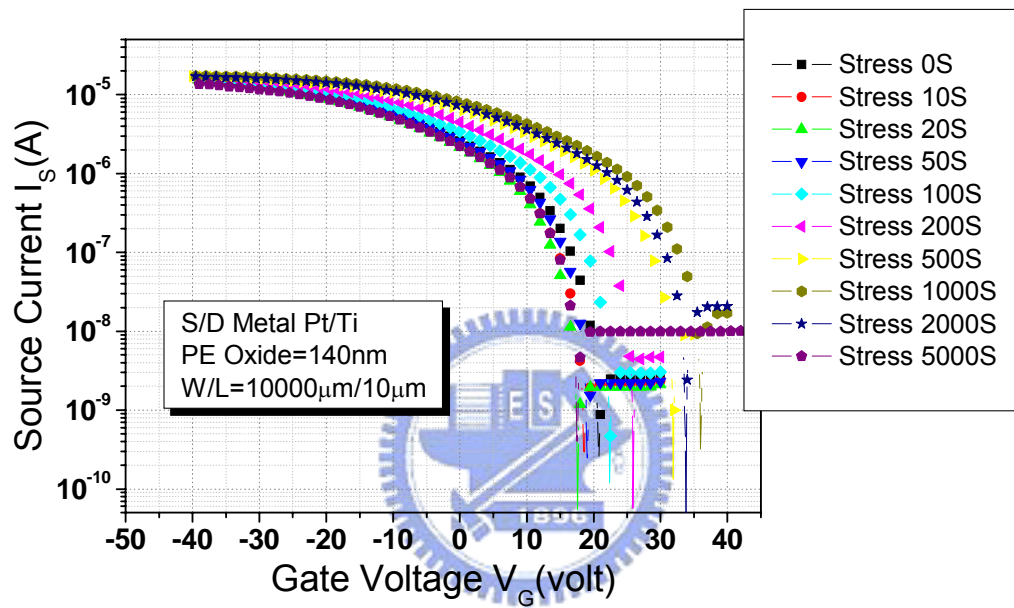


Figure3-6: Transfer characteristics  $I_S$  vs  $V_G$  of OTFT after 0sec, 10sec, 20sec, 50sec, 100sec, 200sec, 500sec, 1000sec, 2000sec and 5000sec +25V gate bias stress



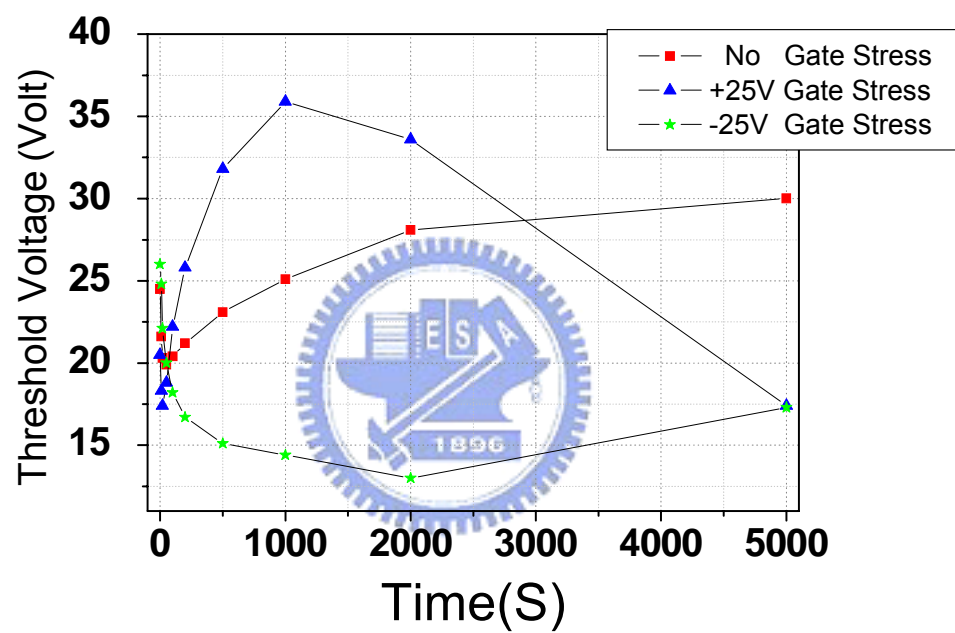


Figure3-7: The variation of threshold voltage under No gate stress,+25V gate stress and -25V gate stress

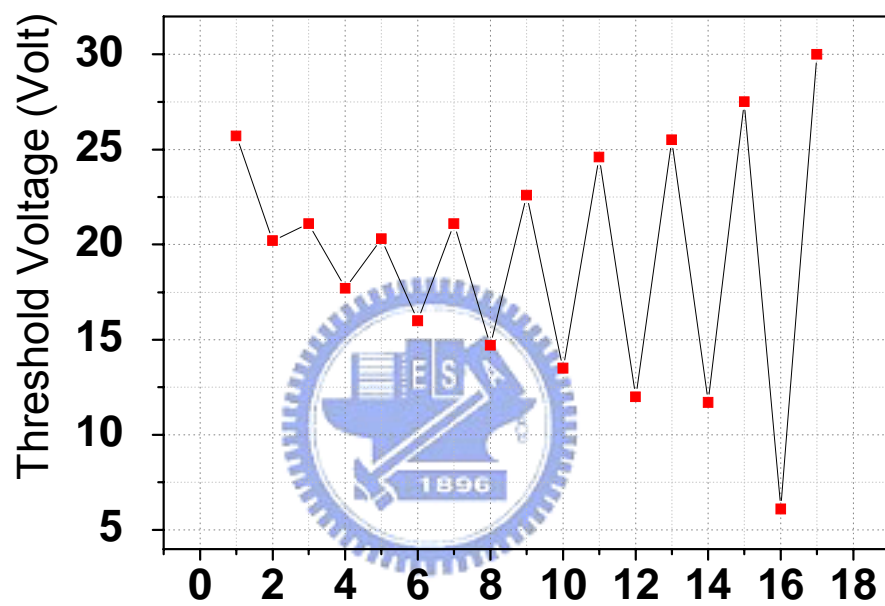


Figure3-8: Alternative gate bias stress (-25V/+25V) for 10sec, 20sec, 50sec, 100sec, 200sec, 500sec, 1000sec and 2000sec .The threshold voltage were measured at the end of each stress time.

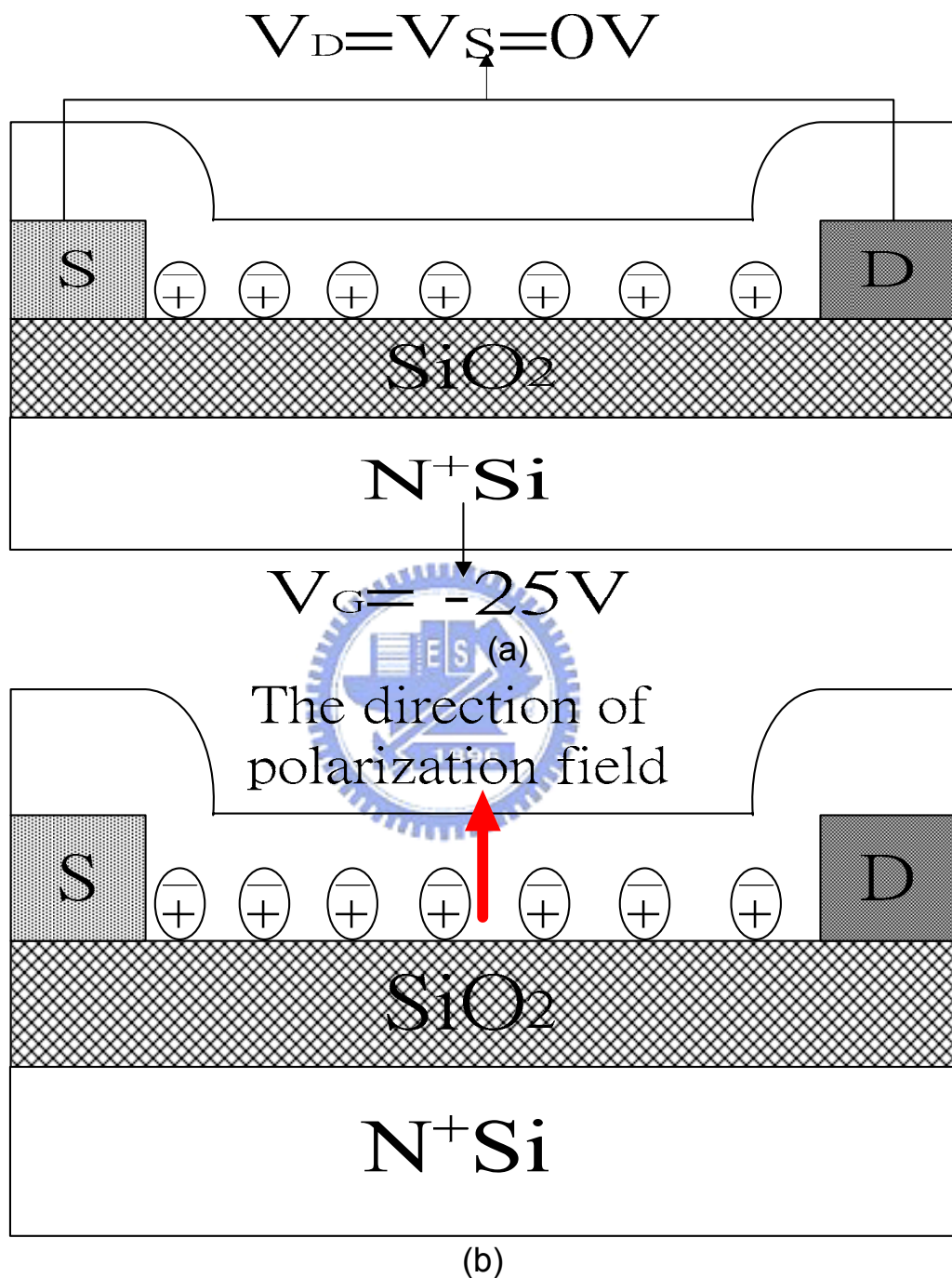


Figure3-9: The polarization effect in the P3HT polymer with negative gate bias.

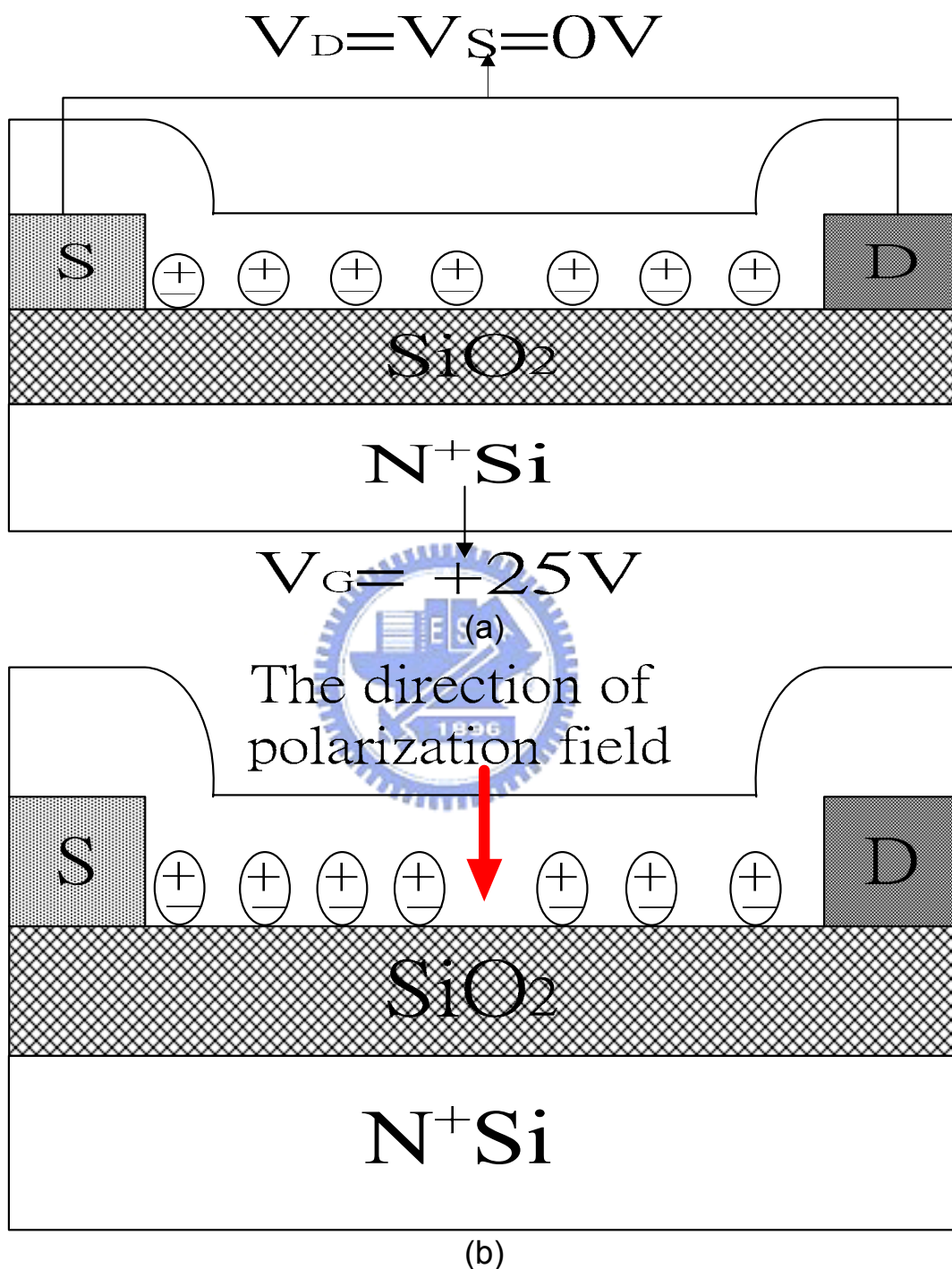


Figure3-10: The polarization effect in the P3HT polymer with positive gate bias.

	P3HT	New 0.3%	New 0.3%
	Store the samples in	vacuum	air
		2D	0D
W/L ratio	Mobility ( $\times 10^{-3} \text{cm}^2/\text{Vs}$ )		
	W/L=10000/10	2.11	2.32
	W/L=5000/10	4.99	2.12
	W/L=1000/10	4.03	1.72
	W/L=1000/15	4.33	1.59
	W/L=1000/25	2.15	2.05
	W/L=1000/35	4.04	1.65
	W/L=1000/50	10.16	3.04
	W/L=500/15	5.59	1.52
	W/L=500/25	7.73	2.46
	W/L=500/35	8.6	3.48
	W/L=500/50	5.58	2.71

Table3-1: Field-effect mobility of samples measured after 0 or 2 days in vacuum with different W/L ratio

	P3HT material	New 0.3%	New 0.3%
	Store the samples in	vacuum	air
		2D	0D
Threshold Voltage(Volt)			
W/L ratio			
W/L=10000/10		24.7	24.6
W/L=5000/10		26.8	26.8
W/L=1000/10		24.3	30
W/L=1000/15		25	29.9
W/L=1000/25		22.8	28.8
W/L=1000/35		26.6	25.3
W/L=1000/50		17.9	25.6
W/L=500/15		28.6	29.9
W/L=500/25		27.9	36.3
W/L=500/35		21.4	31.1
W/L=500/50		23.3	37.5

Table3-2: Threshold voltage of samples measured after 0 or 2 days in vacuum with different W/L ratio

	P3HT material	New 0.3%	New 0.3%
	Store the samples in	vacuum	air
		2D	0D
On/Off ratio			
W/L ratio			
W/L=10000/10		8.72E+03	9.27E+03
W/L=5000/10		2.52E+04	7.66E+03
W/L=1000/10		1.91E+04	5.94E+03
W/L=1000/15		2.04E+04	1.47E+04
W/L=1000/25		8.60E+03	8.76E+03
W/L=1000/35		2.05E+04	6.55E+03
W/L=1000/50		2.22E+04	1.25E+04
W/L=500/15		2.07E+04	5.82E+03
W/L=500/25		3.67E+04	9.78E+03
W/L=500/35		2.39E+04	9.26E+03
W/L=500/50		1.47E+04	9.02E+03

Table3-3: ON-OFF ratio of samples measured after 0 or 2 days in vacuum with different W/L ratio

# Chapter 4

## Contact Resistance of P3HT OTFTs

### 4.1 Introduction

Despite the considerable progress made in improving the performance of OTFTs in recent years, many aspects about the design, material, and process parameters which may impact the performances of organic thin film transistors are still poorly understood and controlled. One of such parameters is the contact resistance between the source/drain electrodes and the organic semiconductor [24], [25], [26]. The contact resistance between the source/drain electrodes and the semiconductor becomes increasingly important to device performance as the channel length decreases. In fact, when the channel length is small enough that the contact resistance dominates the overall device resistance, further reducing the device dimension should contribute to little benefits to the electrical performances. Understanding the electrical properties of the contacts and their dependence on electrode materials, organic semiconductors, and processing conditions is therefore quite important from engineering perspective of view.

Unlike the field-effect transistors based on single-crystalline silicon, polycrystalline silicon, or hydrogenated amorphous silicon, the source and drain contacts of OTFTs are not easily optimized by conventional processes, such as semiconductor doping or metal alloying. Therefore, the most straightforward method for improving the contact resistance is to find a suitable electrode material which can form ohmic contact between source/drain electrodes and the organic semiconductors.

In this chapter, we employed different electrode materials, such as Ti, Ni, Pt and Au, to



check whether it can form ohmic contact between source/drain electrodes and the organic semiconductor or not. Next, we adjust adhesion/contact thickness ratio to check its effect to the contact resistance.

## 4.2 Experiment Detail

First of all, we employed different electrode materials as contact metals, i.e. Ti, Ni, Pt and Au. In other words, after the photolithography process, four kinds of electrode materials were evaporated by e-gun evaporation with the thickness of 100nm. For Ni, Pt and Au, they must have an adhesion layer to prevent them from peeling from the SiO<sub>2</sub> surface. For this season, we used Ti as an adhesion layer with the thickness of 20nm.

Secondly, we adjusted the thickness ratio of adhesion/contact metals, such as Ti/Pt and Ti/Au. Specifically, after the photolithography process, we prepared four kinds of composition of adhesion/contact ratio: Ti/Pt = 20nm/100nm, Ti/Pt = 100nm/20nm Ti/Au = 20nm/100nm and Ti/Au = 100nm/20nm.

## 4.3 Results and Discussion

### 4.3.1 Channel Length Effect on OTFT Performance

While the contact resistance is independent on the channel length, the channel resistance is proportional to the channel length. Consequently, the relative influence of contact resistance increases as the channel length reduces. **Fig4-1** shows the variation of the threshold voltage and mobility in the linear regime as a function of the channel length. As expected, the field-effect generally increases with the channel length increasing since the influence of the contact resistance to the device mobility becomes weaker while the channel resistance turns into a

dominant factor as the channel length increases.

Under a constant W/L ratio, the effect of the contact resistance can be clearly observed from the output characteristics of OTFTs with different channel lengths. **Fig4-2** shows the output drain current at two gate voltages (-20V and -25V) for devices with channel lengths of 50, 25 and 15  $\mu$  m. At a drain voltage of -30V, a 50% reduction in drain current is observed as the channel length is decreased from 50 to 25  $\mu$  m. The drain current saturates at an increasingly higher drain voltage as the channel is 15  $\mu$  m. These observations can be attributed to either the lower field-effect mobility or a larger threshold voltage or both because of the increased percentage of the contact resistance to the channel resistance.

#### **4.3.2 Dependence between the Electrode Materials and the P3HT OTFT Performances**

As a p-type semiconductor, P3HT can form an ohmic contact with metal for its work function larger than 4.5eV. Therefore, Ni ( $\phi=4.84\text{eV}$ ), Pt ( $\phi=5.29\text{eV}$ ) and Au ( $\phi=4.58\text{eV}$ ) can form an ohmic contact with P3HT. Because work function of Ti ( $\phi=4.09\text{eV}$ ) is smaller than 4.5eV, Ti would form a Schottky barrier with P3HT so that it can not be observed the normal output characteristics  $I_S$  vs.  $I_D$  as shown in **Fig4-3(a)**.

From **Fig4-3(b)**, it was observed that the crowding effect was occurred at the small drain bias near the zero voltage. The crowding effect is caused by that the contact resistance between source/drain electrodes and the organic semiconductor is large enough to lead to Space-Charge Limited Current (SCLC) larger than ohmic current [27]. Nevertheless, the large contact resistance between Ni and P3HT is attributing to work function mismatch and chemical reactivity of Ni with P3HT or the interfacial layer formed at the Ni surface.

**Fig4-3(c)** and **Fig4-3(d)** illustrate that the crowding effect is vanished as the P3HT OTFTs

were fabricated by Pt or Au as electrode materials. Because Pt and Au are noble metal, comparing to Ni, they do not react to oxygen or P3HT and contribute to smaller contact resistance. In order to further clarify the contact resistance between Pt, Au and P3HT, we plot current-voltage characteristics of OTFT with (a) Ti/Au (b) Ti/Pt electrodes at small drain voltage, as shown in **Fig4-4**. Therefore, it was shown that the linear behavior is in consistent with ohmic contact.

**Fig4-5** shows the transfer characteristics ( $I_S$  vs.  $V_G$ ) of OTFTs in the linear regime with different S/D contact metals. According to the foregoing description, one can conclude that the OTFT with Au and Pt as contact has an ideal transfer characteristic; OTFT with Ni as contact metal results in low ON current due to large contact resistance and OTFT with Ti as contact metal does not have any normal transfer characteristics.



#### 4.3.3 The Effect of Adhesion/Contact Thickness Ratio on the P3HT Contact Resistance

For small drain bias  $V_D$  at a high gate drive, it is assumed that the ON resistance ( $R_{on}$ ) of OTFTs consists of the channel resistance  $R_{ch}$  and the contact resistance  $R_c$  [28], [29].

That is,

$$I_{DS} = \frac{W}{L} \mu C_i (V_G - V_{th} - V_D / 2) V_D \quad \text{as } V_D \ll V_G - V_{th} \quad [\text{Equation 4-1}]$$

$$R_{on} = \frac{\partial V_D}{\partial I_{DS}} \Big|_{V_G}^{V_D \rightarrow 0} = R_{ch} + R_c \quad [\text{Equation 4-2}]$$

and the channel resistance in the linear region is approximately given by

$$R_{ch} = \frac{L}{W \mu C_i (V_G - V_T)} \quad [\text{Equation 4-3}]$$

where L is the channel length, W is the channel width,  $C_i$  is the capacitance per unit area of the

insulating layer,  $V_{th}$  is the threshold voltage, and  $\mu$  is the field effect mobility. The contact resistance  $R_c$  can be extracted by measuring  $R_{on}$  of output characteristics of OTFT in the linear region and by plotting  $R_{on}W$  as a function of  $L$ . For each device with  $L$  ranging from 10 to 50  $\mu$  m, the drain current was measured at -1V and -5V with a gate voltage ranging from -5V to -30V. The resulting width-normalized ON resistance  $R_{on}W$  versus  $L$  is plotted in **Fig4-6~Fig4-9**. The contact resistance is a set of straight lines intersecting at a triangle area. The results are shown in **Table4-1**. It shows that the contact resistance is not dependent on composition of adhesion/contact materials at  $V_{DS} = -5V$ ; the contact resistance is dependent on adhesion/contact thickness ratio at  $V_{DS} = -1V$  and the contact resistance is smaller as the adhesion/contact thickness ratio is smaller.

Ideal non-rectifying contacts would exhibit no resistance to the flow of current in either direction through the contact, and their I-V characteristics would appear as shown in **Fig4-10(a)**. In general, however, when metal-to-semiconductor contacts are fabricated, they possess non-linear ohmic contact, as shown in **Fig4-10(b)**. Therefore, it was observed that the contact resistance at  $V_{DS} = -1V$  is larger than the contact resistance at  $V_{DS} = -5V$ .

The slope of  $R_{on}W$  versus  $L$  of **Fig4-7(b)** and **Fig4-9(b)**, i.e., the channel sheet conductance, contains only intrinsic device parameters independent of channel length, as predicted by [Equation4-3]. Therefore, by plotting the reciprocal of the slope or  $[(R_{on}W) / \Delta L]^{-1}$  versus gate voltage  $V_G$  as given in **Fig4-11** and **Fig4-12**, the slope of the linear least-square curve fit provides the field-effect mobility in the linear regime. The calculated field-effect mobility with Au as contact metals is  $2.12 \times 10^{-3} \text{ cm}^2/\text{Vs}$  and that with Pt as contact metals is  $2.22 \times 10^{-3} \text{ cm}^2/\text{Vs}$ . Both are in agreement on the values of mobility extracted from  $I_D - V_G$  curves in Chap.2 and Chap.3.

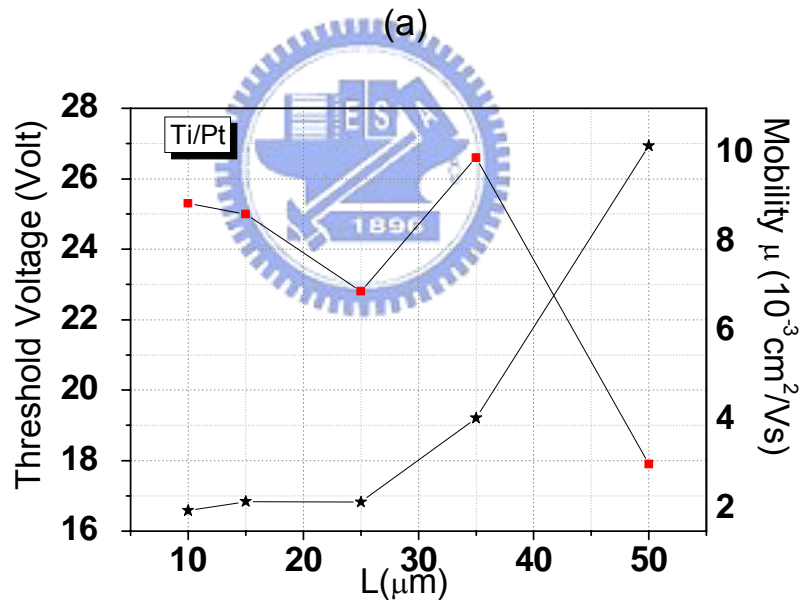
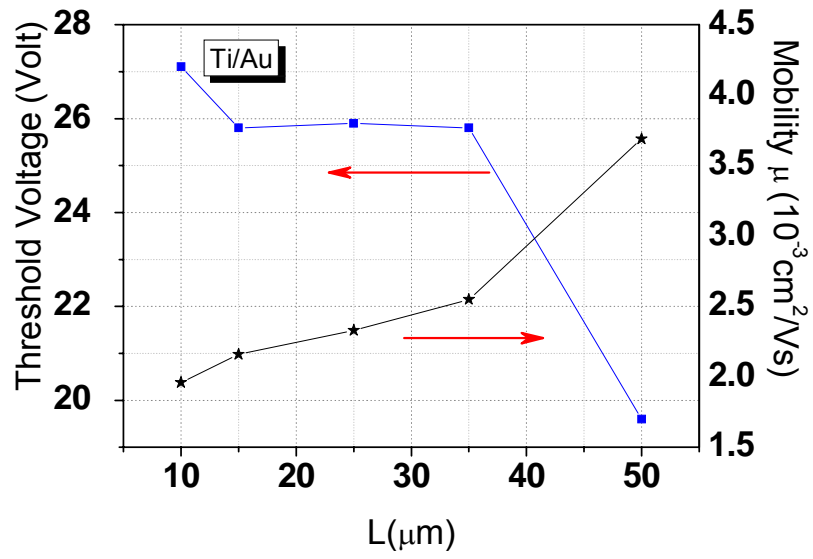
#### 4.4 Summary

The effect of contact resistance between source/drain electrodes and P3HT has been experimentally investigated for different channel length. Due to contact resistance effect, the field-effect mobility and the saturation current decreases with decreasing channel length.

Work function of metals higher than that of P3HT (e.g. Ni, Au and Pt) would form ohmic contact between S/D electrodes and P3HT OTFTs, a kind of p-channel device. On the contrary, metal work function lower than that of P3HT, such as Ti and Al, would form Schottky contact. The electrical characteristic of P3HT OTFT is not FET-like with a Schottky-type S/D contacts, because a high potential barrier at the interface between S/D electrodes and P3HT, causing carriers can not inject from S/D electrodes to P3HT.

Because interfacial layer formed at Ni surface leads to a large contact resistance, comparing to noble metal (Au and Pt), the crowding effect was occurred when the OTFTs were fabricated by Ni as contact electrodes. Therefore, using Pt or Au as S/D contact materials would result in better I-V characteristics.

Next, we applied a simple model to estimate the contact resistance between source/drain electrodes and P3HT and found that the contact resistance is typically greater than the contact resistance of inorganic transistors. Regardless of adhesion/contact thickness ratio, Pt and Au would form a good ohmic contact between S/D contact electrodes with a value of contact resistance of approximate  $0.3\text{M}\Omega\text{-cm}$ . Besides, the extracted field-effect mobility of OTFTs with Pt as contact electrodes is  $2.22\times 10^{-3}\text{ cm}^2/\text{Vs}$ , which is well agreement with those values described in Chap.2 and Chap.3.



(b)

Figure 4-1: The variation of threshold voltage and mobility in the linear regime as a function of the channel length (a) S/D metal is Ti/Au (b) S/D metal is Ti/Pt

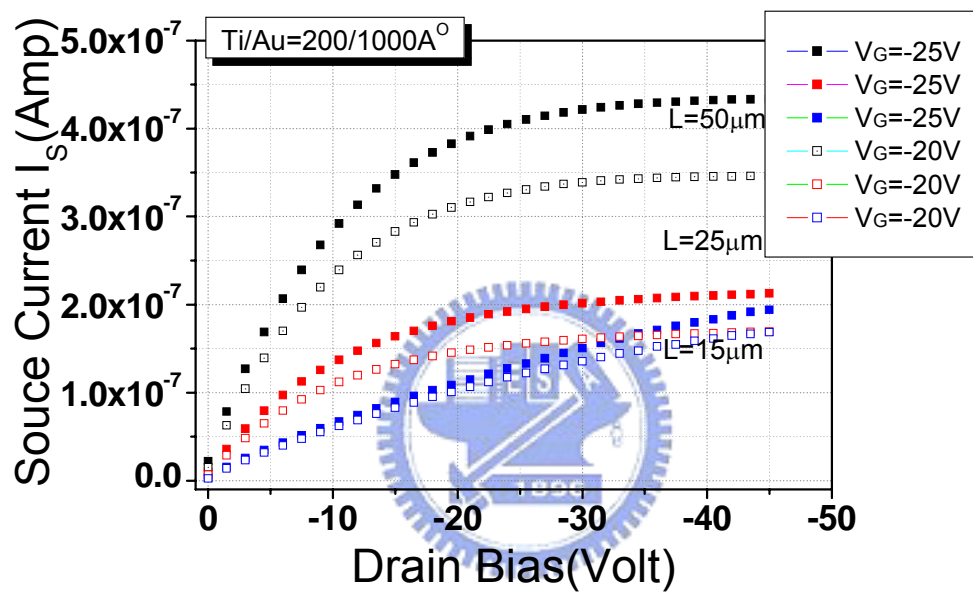
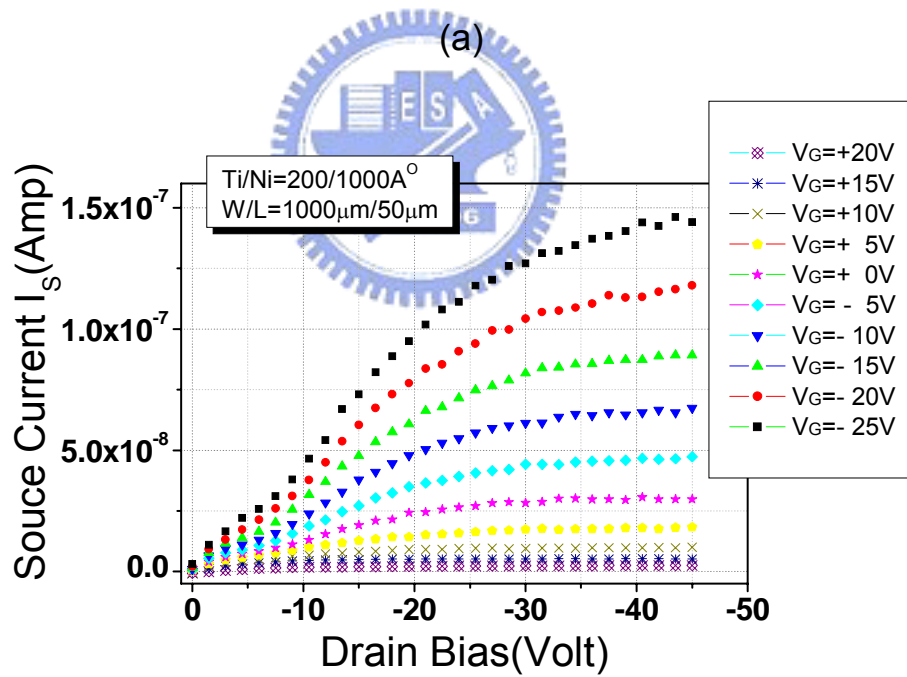
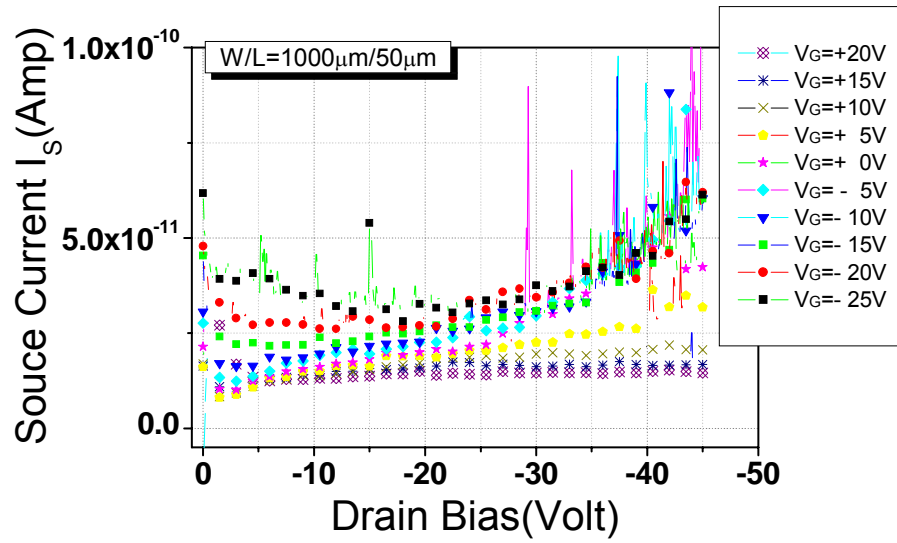


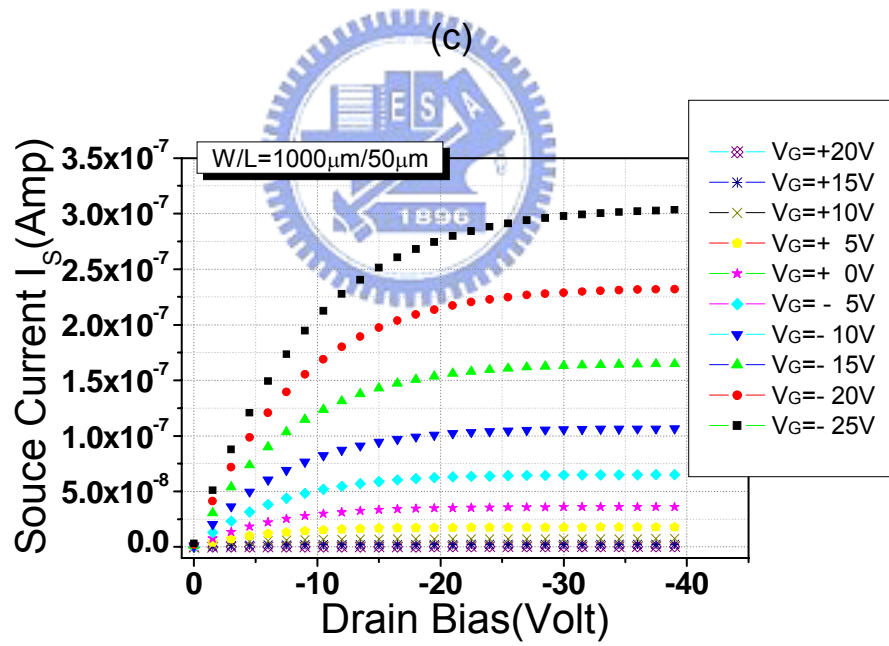
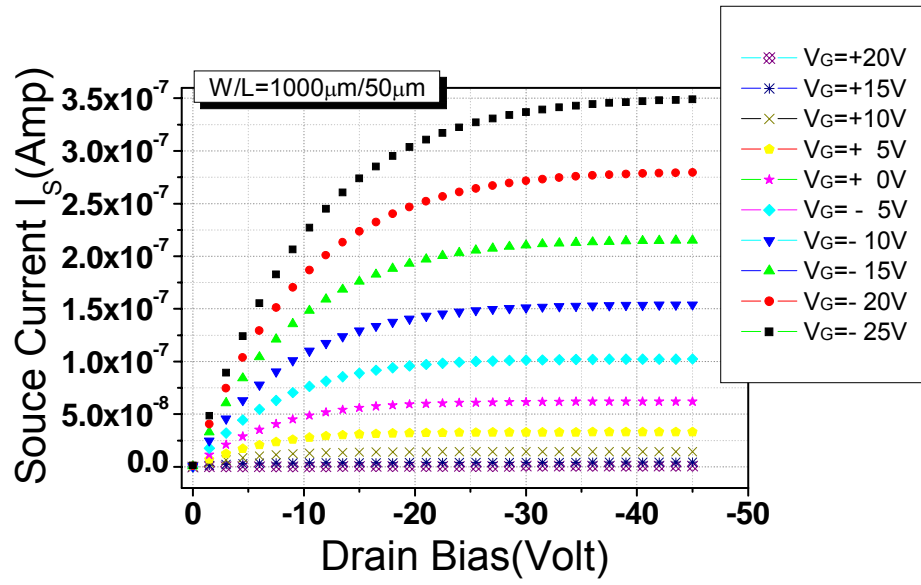
Figure 4-2: Output characteristics  $I_S$  vs  $V_D$  for OTFTs with different channel lengths of 50,25,15 $\mu m$ .  $W/L=20$



(b)

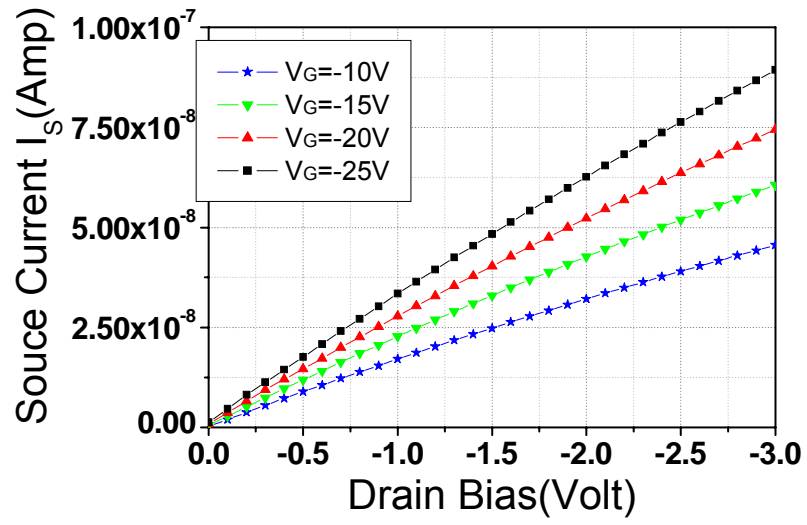
Figure 4-3: Output characteristics  $I_s$  vs  $V_D$  of OTFT with (a)Ti (b)Ti/Ni (c)Ti/Au (d)Ti/Pt Source and Drain contact (continue)



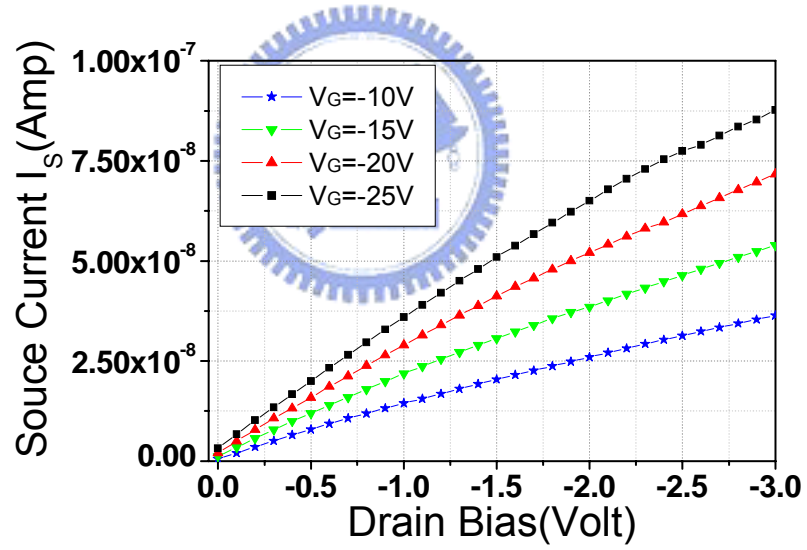


(d)

Figure 4-3: Output characteristics  $I_s$  vs  $V_D$  of OTFT with (a)Ti (b)Ti/Ni (c)Ti/Au (d)Ti/Pt Source and Drain contact



(a)



(b)

Figure 4-4: Current-voltage characteristics of OTFT with (a) Ti/Au (b)Ti/Pt electrodes at small drain voltage

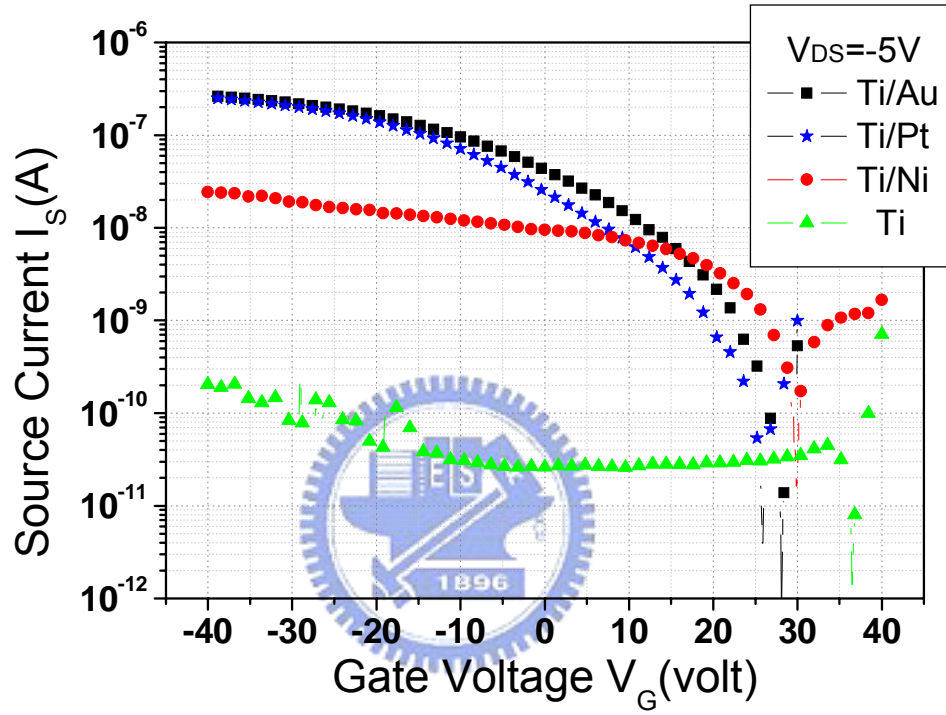
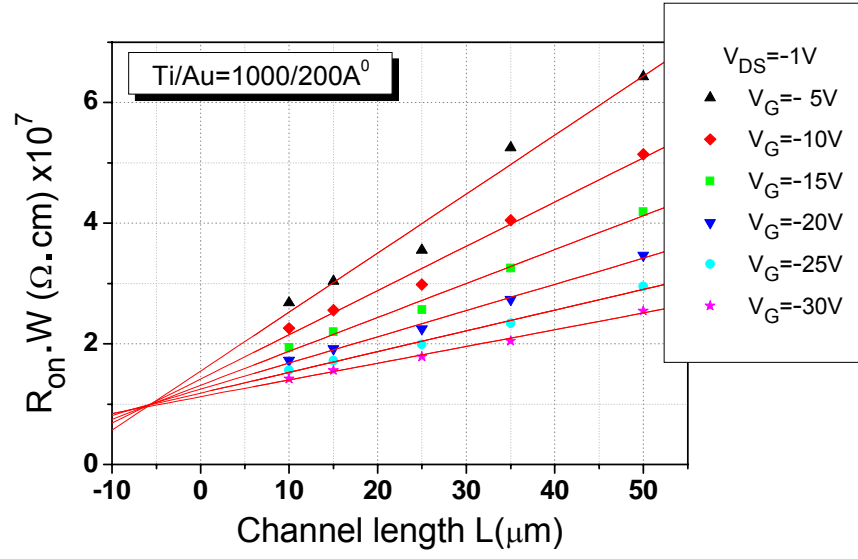
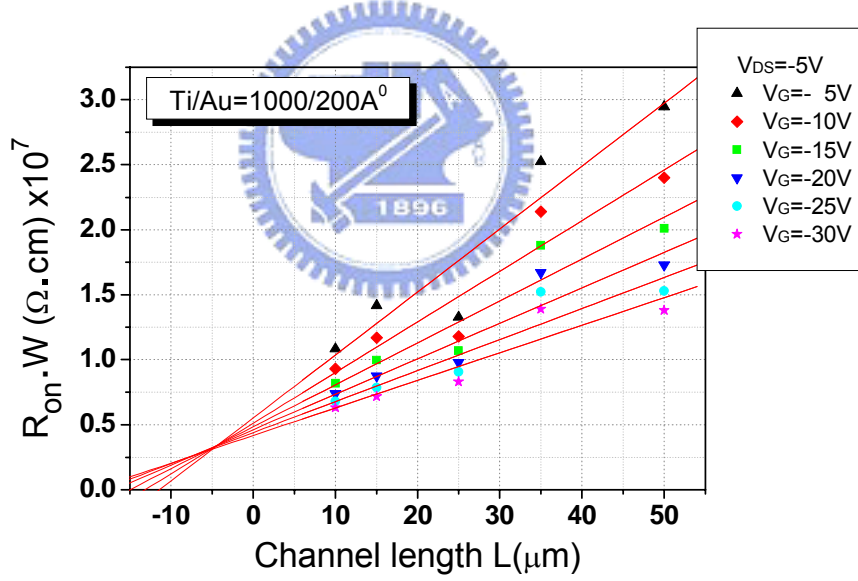


Figure 4-5: Transfer characteristics  $I_s$  vs  $V_G$  of OTFT in the linear regime with different S/D contact metal ( $W/L=1000/50\mu m$ )

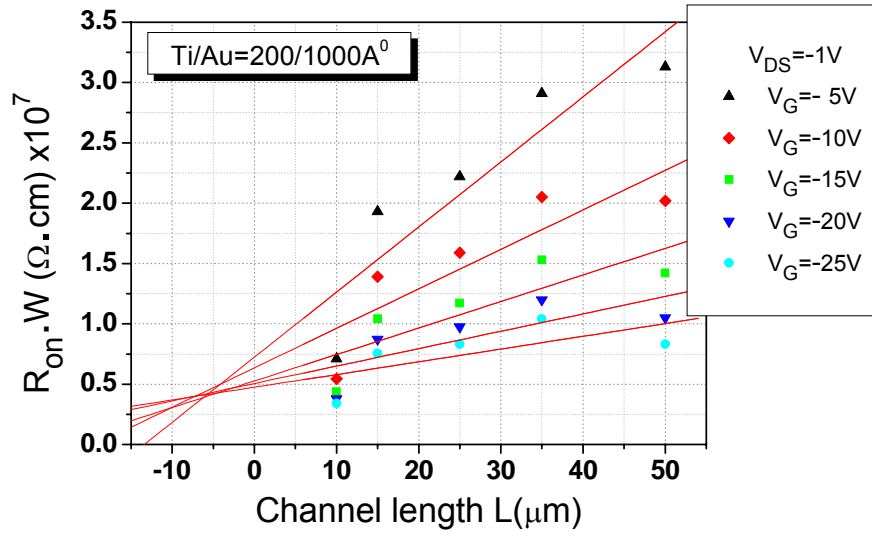


(a)

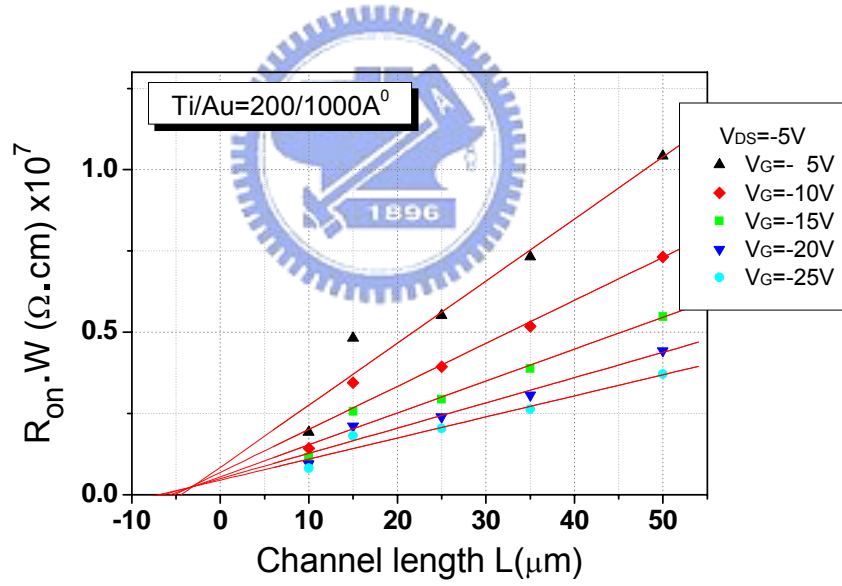


(b)

Figure 4-6: Width-normalized ON resistance as a function of channel length at different gate voltage and at (a)  $V_{DS} = -1\text{V}$  (b)  $V_{DS} = -5\text{V}$ . The solid lines represent the linear least square fit of the data. ( $\text{Ti}/\text{Au} = 1000/200\text{\AA}$ )

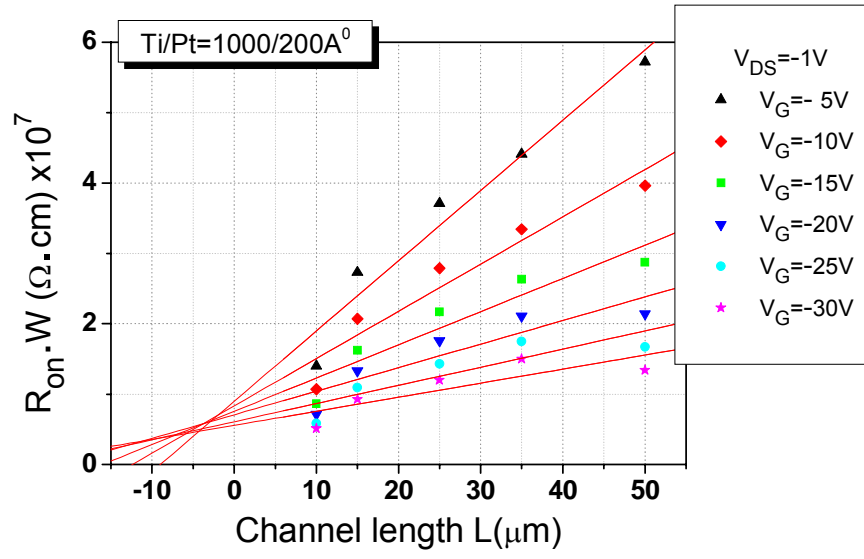


(a)

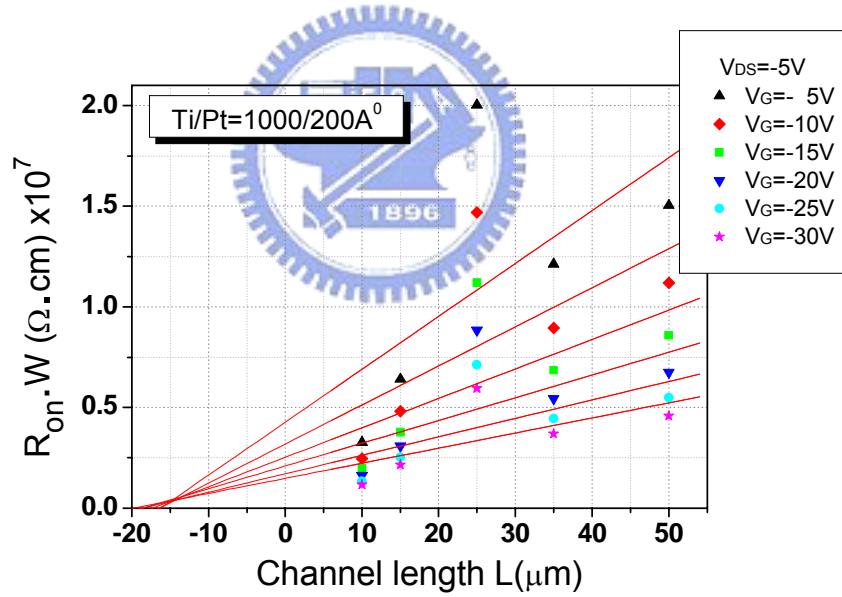


(b)

Figure 4-7: Width-normalized ON resistance as a function of channel length at different gate voltage and at (a)  $V_{DS} = -1\text{V}$  (b)  $V_{DS} = -5\text{V}$ . The solid lines represent the linear least square fit of the data. ( $\text{Ti}/\text{Au} = 200/1000\text{\AA}$ )

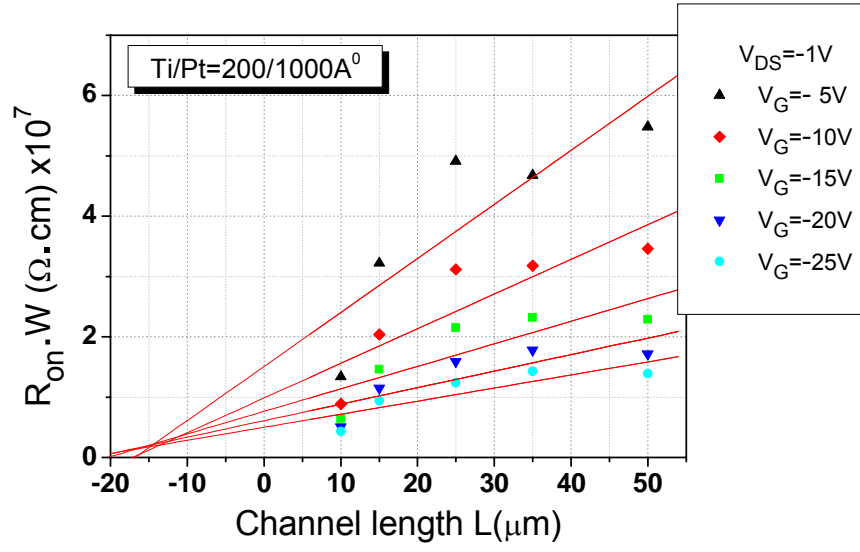


(a)

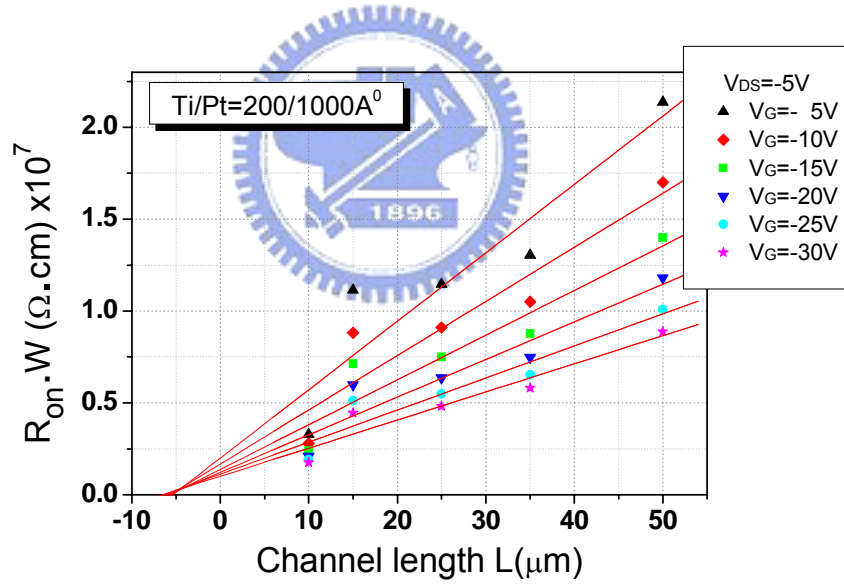


(b)

Figure 4-8: Width-normalized ON resistance as a function of channel length at different gate voltage and at (a)  $V_{DS} = -1\text{V}$  (b)  $V_{DS} = -5\text{V}$ . The solid lines represent the linear least square fit of the data. ( $\text{Ti/Pt} = 1000/200\text{\AA}$ )

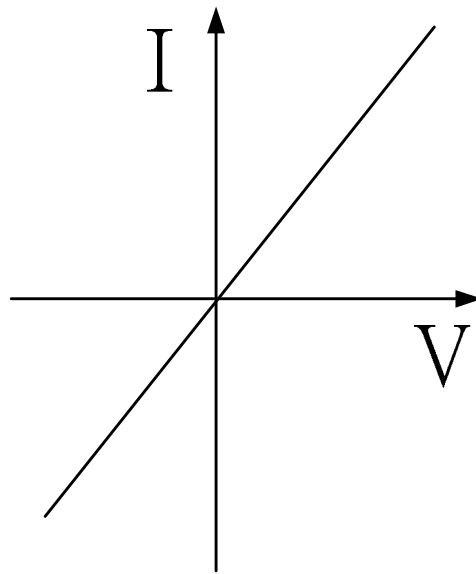


(a)

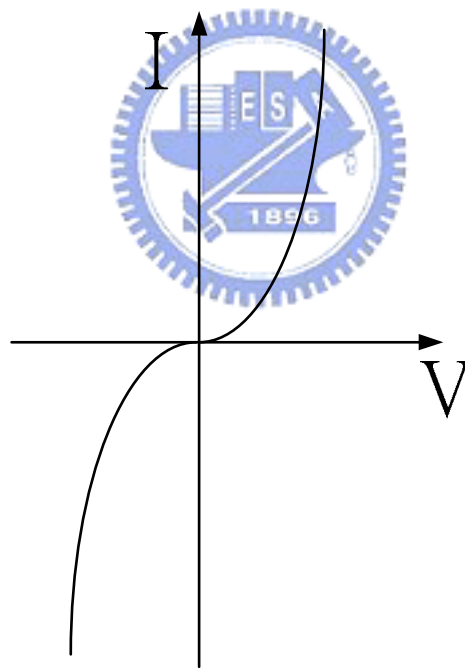


(b)

Figure 4-9: Width-normalized ON resistance as a function of channel length at different gate voltage and at (a)  $V_{DS} = -1\text{V}$  (b)  $V_{DS} = -5\text{V}$ . The solid lines represent the linear least square fit of the data. ( $\text{Ti/Pt} = 200/1000\text{\AA}$ )



(a)



(b)

Figure4-10: I-V characteristics of contacts between metal and semiconductor in integrated circuits (a) Ideal ohmic contact (b) nonlinear ohmic contact



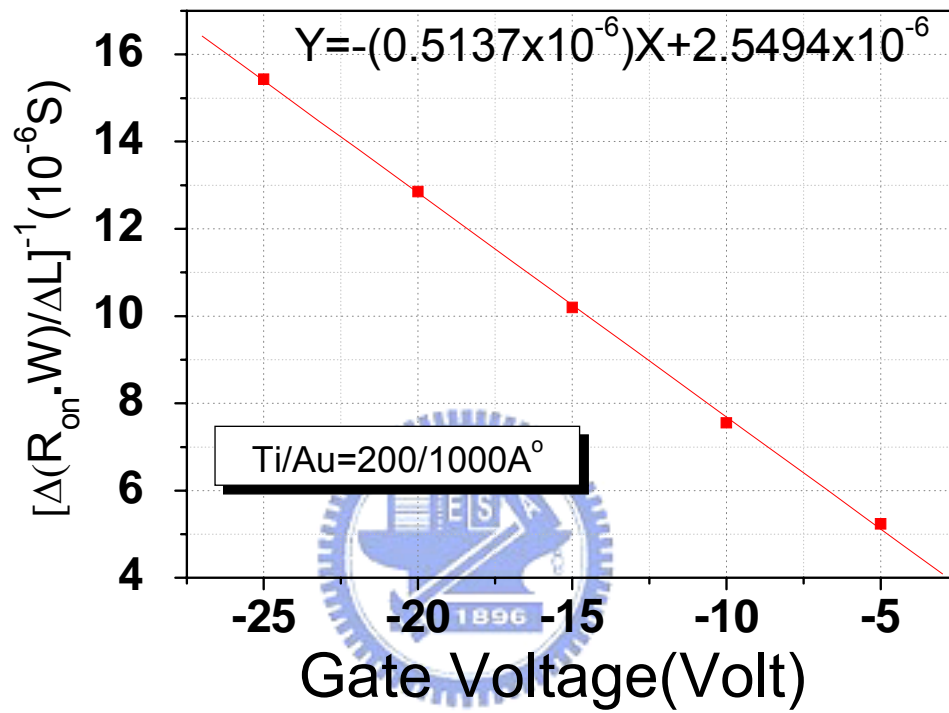


Figure 4-11: OTFT channel sheet conductance as a function of gate voltage (S/D contact metal is Ti/Au)

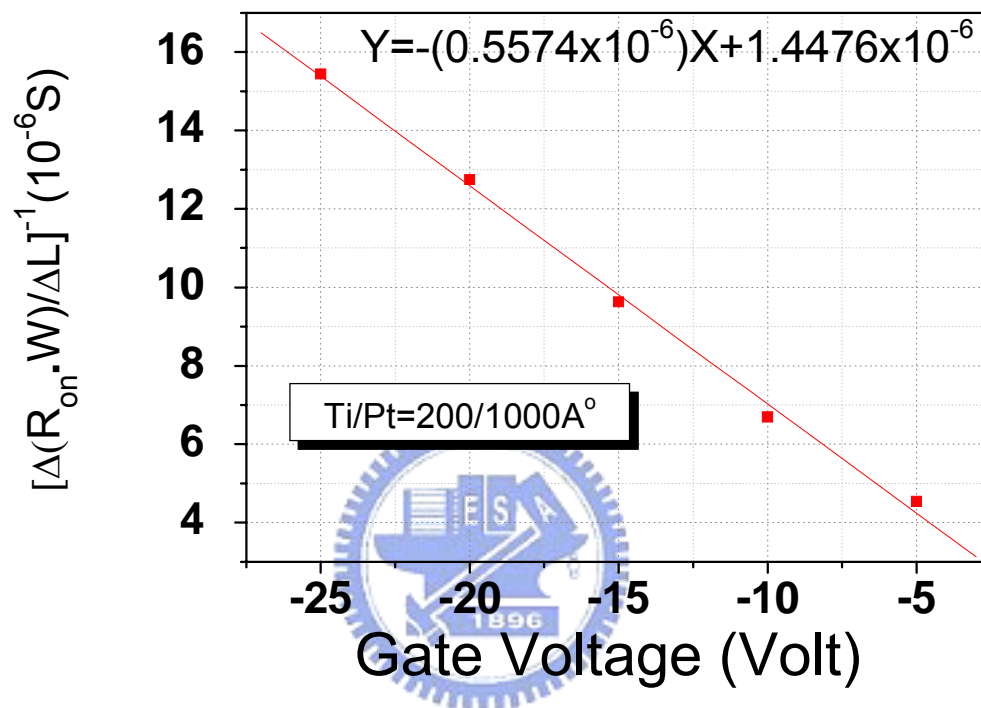


Figure 4-12: OTFT channel sheet conductance as a function of gate voltage (S/D contact metal is Ti/Pt)

Source /Drain Metal	$V_{DS}=-5V$	$V_{DS}=-1V$
	Contact Resistance ( $\times 10^6 \Omega \cdot \text{cm}$ )	Contact Resistance ( $\times 10^6 \Omega \cdot \text{cm}$ )
Ti/Pt=200/1000Å	0.3	1.0~2.5
Ti/Au=200/1000Å	0.25	0.4~0.5
Ti/Pt=1000/200 Å	0.3~0.4	4.5~6.0
Ti/Au=1000/200 Å	0.3~0.35	1.0

Table4-1: The contact resistance between source/drain electrodes and P3HT with different composition of adhesion/contact materials.

## Chapter 5

### Conclusion and Future work

#### 5.1 Conclusions

The feasibility study of Spin-Coating technique, physical and the electrical characteristics of P3HT OTFT are investigated. Here, we conclude our study into three parts: (1) OTFTs Fabricated by Different Solvents and Weight Percentages of P3HT (2) Reliability Characteristics of P3HT OTFTs (3) Contact Resistance of P3HT OTFTs

##### 5.1.1 OTFTs Fabricated by Different Solvents and Weight Percentages of P3HT

It was found that chloroform is a good solvent to dissolve P3HT, the anomalous gate leakage current was suppressed by chloroform solution, and the high ON-OFF ratio of about 4 order magnitudes and the field-effect mobility of  $10^{-3} \text{ cm}^2/\text{Vs}$  were attributed to chloroform solution. Next, we investigate the performance of P3HT OTFTs which was fabricated different weight percentage of P3HT in chloroform.

The surface root-mean-square roughness of organic thin film deposited by 0.3% of P3HT is  $8.24 \text{ \AA}$ . That is much smoother than RMS roughness of organic thin film deposited by others, 0.1%, 0.8% and 2.0%. As weight percentage of P3HT in chloroform is above 0.3%, the bulk current effect would affect  $I_S-V_G$  curves and  $I_S-V_D$  curves. Therefore, in order to acquire an OTFTs with good mobility, high ON-OFF current, appropriate threshold voltage, the optimal weight percentage of P3HT would be 0.3%.

##### 5.1.2 Reliability Characteristics of P3HT OTFTs

Given the sensitivity of P3HT to oxygen absorbed during the fabrication process, it is

expected that vacuum and N<sub>2</sub> treatments can be used to recover some of the lost performance through vacuum-induced expulsion of absorbed oxygen.

The threshold voltage shift of OTFTs with P3HT as active material has been studied from our experiments. There are two elements for resulting in the threshold voltage shift. One is the diffusion of oxygen atoms into P3HT polymer; the other is the electric field of the polarization effect in the P3HT polymer.

Under O<sub>2</sub> treatment, since the diffusion of oxygen into P3HT polymer causes an increase to the conductivity of P3HT polymer and bulk leakage current, the device was hardly turned off. Therefore, the threshold voltage shift is dependent on O<sub>2</sub> treatment time. Nevertheless, the variation of field-effect mobility increases in the first 3 hours O<sub>2</sub> treatment, and then it decreases after 3 hours O<sub>2</sub> treatment. The phenomenon is owing to bulk leakage current. Due to the bulk leakage current, the extraction of field-effect mobility was overestimated in the first 3 hours. However, after 3 hours O<sub>2</sub> treatment oxygen continues diffusing into P3HT polymer, and it would degrade P3HT polymer characteristics and cause serious carriers scattering. Therefore, the field-effect mobility decreased after 3 hours O<sub>2</sub> treatment.

Under stress measurement, the threshold voltage shift is dependent on the polarity of gate bias. It was found that positive bias stress causes a positive threshold voltage shift and negative bias stress causes a negative threshold voltage shift. Nevertheless, the variation of field-effect mobility was independent on the polarity of gate bias.

Additionally, it was proved that humidity will not affect the performance of P3HT OTFTs.

### **5.1.3 Contact Resistance of P3HT OTFTs**

The effect of contact resistance between source/drain electrodes and P3HT has been experimentally investigated for different channel length. Due to contact resistance effect, the

field-effect mobility and the saturation current decreases with decreasing channel length.

Work function of metals higher than that of P3HT would form ohmic contact between S/D electrodes and P3HT for p-type OTFTs, such as Ni, Au and Pt. On the contrary, work function of metals lower than that of P3HT, such as Ti, would form Schottky contact. The electrical characteristic of P3HT OTFT is not FET-like with a Schottky-type S/D contacts, because a high barrier at the interface between S/D electrodes and P3HT, causing the charges can not inject from S/D electrodes to P3HT.

Because interfacial layer formed at Ni surface leads to large contact resistance, comparing to noble metal (Au and Pt), the crowing effect was occurred as the OTFTs were fabricated by Ni as contact electrodes. Therefore, using Pt or Au as S/D contact materials would form a good ohmic contact.

Next, we applied a simple model to estimate the contact resistance between source/drain electrodes and P3HT and found that the contact resistance is typically greater than the contact resistance of inorganic transistors. Regardless of adhesion/contact thickness ratio, Pt and Au would form a good ohmic contact between S/D contact electrodes and P3HT and the contact resistance is approximate  $0.3\text{M}\Omega\text{-cm}$ . By this method, the field-effect mobility with Pt as contact electrodes is  $2.22\times 10^{-3}\text{ cm}^2/\text{Vs}$  and is very well in agreement with those values from chap2 and chap3.

## 5.2 Future work

### *An in-situ pacivation layer for protecting the P3HT film*

From our experimental results, P3HT OTFTs are sensitive to ambient conditions. Protection from the environment by encapsulation is critical to the stability of P3HT OTFTs. Therefore, using a suitable material as pacivation to protect P3HT film from environmental effect is another

important topic.

#### *A new method to deposit P3HT thin film*

There are three methods to deposit P3HT thin films: (1) spin-coating (2) dip-coating (3) drop-casting. In our experiment, we made use of spin-coating method to deposit P3HT thin films and attain an optimized deposition parameter for producing P3HT thin films. However, among the three methods to deposit P3HT thin films, the best method is drop-casting. Therefore, in the future we will make use of drop-casting to deposit P3HT thin films, and study the deposition parameters of drop-casting.

#### *Thermal stability of P3HT OTFTs*

In addition to studies of device lifetime and the stability of P3HT in different ambient, thermal stability is another topics .This is an important topic for various reasons. First, poly (3-hexylthiophenes) devices will be likely exposed to elevated temperatures during the fabrication process, due to the annealing requirements of other layers. Second, thermal cycling studies provide crucial insights into device lifetime and stability. [30]

#### *New gate insulator materials for P3HT OTFTs*

From the performance point of view, the most important parameters are charge carrier mobility, ON-OFF current ratio and the operational voltage range. However, the operating voltages of P3HT OTFT required to produce such performance were impractically high, around 50~60V. Although decreasing the thickness of SiO<sub>2</sub> could reduce the operating voltages of P3HT OTFT, the gate leakage current would increase with decreasing the thickness of SiO<sub>2</sub> and affect the performance of P3HT OTFT. Therefore, the use of high dielectric gate insulator materials is possible for reducing operating voltages of P3HT and gate leakage current. [31], [32], [33]

## References

- [1] Christos D. Dimitrakopoulos, D. J. Mascaro, **“Organic thin film transistors : A review of recent advances ”** IBM J. RES. & DEV. 45(1), 11, (2001)
- [2] P.W.M. Blom, M.C.J.M. Vissenberg; **“Charge transport in poly(p-phenylene vinylene)light-emitting diodes”** ; Materials Science and Engineering, 27 (2000) 53-94
- [3] A.R. Brown, C.P. Tarrett, D.M. de Leeuw, M. Matters; **“Field-effect transistor made from solution-processed organic semiconductors”** ; Synthetic Metals 88 (1997) 37-55
- [4] Christos D. Dimitrakopoulos, Parick R. Malenfant, **“Organic thin film transistors for large area electronics”** Adv. Mater. 2002, 14, No2, January 16
- [5] Guangming Wang, James Swensen, Daniel Moses, and Alan J. Heeger, **“Increased mobility from regioregular poly(3-hexylthiophene) field-effect transistors”** JOURNAL OF APPLIED PHYSICS VOLUME 93, NUMBER 10
- [6] A. Assadi, C. Svensson, M. Willander, O. Inganas, **“Field-effect mobility of poly(3-hexylthiophene)”** Appl. Phys. Lett. 53(3), 18 July 1988
- [7] Zhenan Bao,a) Ananth Dodabalapur, and Andrew J. Lovinger ; **“Soluble and processable regioregular poly(3-hexylthiophene) for thin film field-effect transistor applications with high mobility”** Appl. Phys. Lett., Vol. 69, No. 26, 23 December 1996
- [8] Bao, Z.; Lovinger, A. J, **“Soluble Regioregular Polythiophene Derivatives as Semiconducting Materials for Field-Effect Transistors”** Chem. Mater.(Article); 1999
- [9] Sirringhaus, Henning; Tessler, Nir; et al. ; **“Integrated optoelectronic devices based on conjugated polymers”**, Science, 06/12/98, Vol. 280 Issue 5370, p1741
- [10] Sirringhaus, H.; Brown, P.J.; Friend, R.H.; Nielsen, M.M.; Bechgaard, K.; Langeveld-Voss, B.M.W.; et. al. **”Microstructure–mobility correlation in self-organised, conjugated polymer field-effect transistors”** Synthetic Metals Volume: 111-112, June 1, 2000, pp. 129-132
- [11] H. Sirringhaus, P. J. Brown, R. H. Friend, M. M. Nielsen, K. Bechgaard, B. M. W. Langeveld-Voss, A. J. H. Spiering, R. A. J. Janssen, E. W. Meijer, P. Herwig & D. M. de Leeuw; **“Two-dimensional charge transport in self-organized, high-mobility conjugated polymers”** NATURE |VOL 401 | 14 OCTOBER 1999
- [12] Zhenan Bao,a) Ananth Dodabalapur, and Andrew J. Lovinger ; **“Soluble and processable regioregular poly(3-hexylthiophene) for thin film field-effect transistor applications with high mobility”** Appl. Phys. Lett., Vol. 69, No. 26, 23 December 1996



- [13] Mohamed S. A. Abdou, Francesco P. Orfino, Yongkeun Son, and Steven Holdcroft; **“Interaction of Oxygen with Conjugated Polymers: Charge Transfer Complex Formation with Poly(3-alkylthiophenes)”** ; J. Am. Chem. Soc. 1997, 119, 4518-4524
- [14] Sung Kyu Park, Yong Hoon Kim, Jeong In Han, Dae Gyu Moon, and Won Keun Kim; **“High-Performance Polymer TFTs Printed on a Plastic Substrate”** ; IEEE TRANSACTIONS ON ELECTRON DEVICES
- [15] A. Ullmann, W. Fix, H. Rost, and W. Clemens **“Stability of polythiophene-based transistors and circuits”** JOURNAL OF APPLIED PHYSICS VOLUME 94, NUMBER 4 15 AUGUST 2003
- [16] Y. Harima, T. Eguchi, K. Yamashita; **“Enhancement of carrier mobility in poly(3-menthythiophene) by an electrochemical doping”** ; Synthetic Metals 95 (1998) 69-74
- [17] A.R. Brown, C.P. Tarrett, D.M. de Leeuw, M. Matters; **“Field-effect transistor made from solution-processed organic semiconductors”** ; Synthetic Metals 88 (1997) 37-55
- [18] Taylor, D. M.; Gomes, H. L.; Underhill, A. E.; Edge, S.; Clemonson, P. I. *J. Phys. D, Appl. Phys.* **1991**, 24, 2032.
- [19] Abdou, M. S. A.; Orfino, F. P.; Xie, Z.; Deen, M. J.; Holdcroft, S. *AdV. Mater.* **1994**, 6, 838.
- [20] Sung Kyu Park, Yong Hoon Kim, Jeong In Han, Dae Gyu Moon, and Won Keun Kim **“High-Performance Polymer TFTs Printed on a Plastic Substrate”** 2002 IEEE TRANSACTIONS ON ELECTRON DEVICES
- [21] Aleshin, A.N.; Sandberg, H.; Stubb, H. **“Two-dimensional charge carrier mobility studies of regioregular P3HT”** Synthetic Metals Volume: 121, Issue: 1-3, March 15, 2001, pp. 1449-1450
- [22] C. Yang, F. P. Orfino, and S. Holdcroft, **“A phenomenological model for predicting thermochromism of regioregular and nonregioregular poly(3-alkylthiophenes),”** *Macromolecules*, vol. 29, p. 6510, 1996.
- [23] A. Tsumura, H. Koezuka, and T. Ando, **“Macromolecular electronic device: Field-effect transistor with a polythiophene thin film,”** *Appl. Phys. Lett.*, vol. 49, p. 1210, 1998.
- [24] Hagen Klauk, Gunter Schmid, Wolfgang Radlik, Werner Weber, Lisong Zhou, Chris D. Sheraw, Jonathan A. Nichols, Thomas N. Jackson; **“Contact resistance in organic thin .lm transistors”** ; Solid-State Electronics 47 (2003) 297–301

- [25] Graciela B. Blanchet, C. R. Fincher, and Michael Lefenfeld **“Contact resistance in organic thin film transistors”** APPLIED PHYSICS LETTERS VOLUME 84, NUMBER 2 12 JANUARY 2004
- [26] Giles Lloyd , Munira Raja , Ian Sellers , Naser Sedghi , Raffaella Di Lucrezia , Simon Higgins , Bill Eccleston ; **“The properties of MOS structures using conjugated polymers as the semiconductor”** ; Microelectronic Engineering 59 (2001) 323–328
- [27] Chung-Kun Song, Kang Dae Kim, Yong-Xian Xu, Myung-Won Lee, Kwang-Hyun Kim **“Performance Improvement of Pentacene OTFT for Display Application”** SID 03 DIGEST
- [28] P. V. Necliudov, M. S. Shur, D. J. Gundlach, T. N. Jackson; **“Modeling of organic thin film transistors of different designs”** ; J. Appl. Phys., Vol. 88, No. 11, 1 December 2000
- [29] Shengwen Luan and Gerold W. Neudeck **“An experimental study of source/drain parasitic resistance effects in amorphous silicon thin film transistors”** J. Appl. Phys., Vol. 72(2), 15, July 1992
- [30] Brian A. Mattis, Paul C. Chang, and Vivek Subramanian **“Effect of thermal cycling on performance of Poly(3-hexylthiophene) Transistors”** Mat. Res. Soc. Symp. Proc. Vol. 771 © 2003 Materials Research Society
- [31] C.D. Dimitrakopoulos, S. Purushothaman, J. Kymissis, A. Callegari, J.M. Shaw **“Low-Voltage Transistors on Plastic Comprising High-Dielectric Constant Gate Insulator”** 5 February 1999 VOL283
- [32] Carmen Bartic, Henri Jansen, Andrew Campitelli, Staf Borghs **“Ta<sub>2</sub>O<sub>5</sub> as Gate Dielectric Material for Low-Voltage Organic Thin-Film Transistors”** Organic Electronics 3(2002) 65-72
- [33] Guangming Wang, Daniel Moses, Alan J. Heeger **“Poly(3-hexylthiophene) field-effect transistors with high dielectric constant gate insulator”** Journal of Applied Physics Vol95, Number 1 January 2004

## 簡歷

姓名：林榮祥

性別：男

出生地：台灣省台南縣

出生日期：民國 68 年 01 月 11 日

住址：台南縣歸仁鄉辜厝村中正路 193 巷 102 弄 30 號

學歷：國立高雄師範大學物理系

(86 年 6 月至 90 年 6 月)

國立交通大學電子工程研究所碩士班

(91 年 6 月至 93 年 6 月)

### Publications

- [1] Shuo-Cheng WANG, Jen-Chung Lou, Bo-Lin Liou, *Ron-Xion Lin*, and Ching-Fa Yeh “Process Improvement and Reliability Characteristics of Spin-on Poly-3-hexylthiophene Thin-Film Transistor” Electron Devices and Materials Symposia, 2003